AD_____

GRANT NUMBER DAMD17-94-J-4228

TITLE: Estrogen Receptor Accessory Factors in Breast Cancer Cells

PRINCIPAL INVESTIGATOR: Geoffrey L. Greene, Ph.D.

CONTRACTING ORGANIZATION: University of Chicago
Chicago, Illinois 60637

REPORT DATE: August 1998

TYPE OF REPORT: Final

PREPARED FOR: Commanding General
U.S. Army Medical Research and Materiel Command
Fort Detrick, Maryland 21702-5012

REPORT DOCUMENTATION PAGE

Form Approved
OMB No. 0704-0188

1. AGENCY USE ONLY *(Leave blank)*	2. REPORT DATE	3. REPORT TYPE AND DATES COVERED
	August 1998	Final (25 Jul 94 - 24 Jul 98)

4. TITLE AND SUBTITLE
Estrogen Receptor Accessory Factors in Breast Cancer Cells

5. FUNDING NUMBERS
DAMD17-94-J-4228

6. AUTHOR(S)
Geoffrey L. Greene, Ph.D.

7. PERFORMING ORGANIZATION NAME(S) AND ADDRESS(ES)
University of Chicago
Chicago, Illinois 60637

8. PERFORMING ORGANIZATION REPORT NUMBER

9. SPONSORING / MONITORING AGENCY NAME(S) AND ADDRESS(ES)
U.S. Army Medical Research and Materiel Command
Fort Detrick, Maryland 21702-5012

10. SPONSORING / MONITORING AGENCY REPORT NUMBER

11. SUPPLEMENTARY NOTES

12a. DISTRIBUTION / AVAILABILITY STATEMENT
Approved for Public Release; Distribution Unlimited

12b. DISTRIBUTION CODE

13. ABSTRACT *(Maximum 200 words)*

The goal of this investigation was to identify proteins that associate with the ERα in a ligand-dependent manner and may therefore play a role in mediating the activity of the receptor. We have used the ligand binding domain of the ER (ERα-LBD) to capture proteins from mammalian cell extracts that associate with the ERα. One protein isolated by this technique is a kinase, able to bind and phosphorylate the ERα only in the presence of estrogen agonists such as estradiol. Using an array of chromatographic techniques and monitoring kinase activity, we have purified a stoichiometric complex of proteins to apparent homogeneity. Mass spectrometric sequencing has identified two of the protein components as Ca^{2+}/calmodulin-dependent protein kinase II γ and δ (CamKII). Coimmunoprecipitation experiments show *in vivo* association of CamKII with ER upon stimulation of cells with estradiol and recent transfection experments suggest CamKII activity plays a role in transcriptional activation through the ERα. Additionally, site directed mutagenesis has defined the kinase binding site on the ER-LBD as a hydrophobic cleft previously implicated in recruitment of nuclear receptor coactivator proteins. Taken together, our data suggest that CamKII can serve as a novel modulator of ERα action.

14. SUBJECT TERMS
Breast Cancer, estrogen receptor, accessory proteins, transcriptional regulation, estrogen versus estrogen antagonists, kinases

15. NUMBER OF PAGES
63

16. PRICE

17. SECURITY CLASSIFICATION OF REPORT	18. SECURITY CLASSIFICATION OF THIS PAGE	19. SECURITY CLASSIFICATION OF ABSTRACT	20. LIMITATION OF ABSTRACT
Unclassified	Unclassified	Unclassified	Unlimited

FOREWORD

Opinions, interpretations, conclusions and recommendations are those of the author and are not necessarily endorsed by the U.S. Army.

____ Where copyrighted material is quoted, permission has been obtained to use such material.

____ Where material from documents designated for limited distribution is quoted, permission has been obtained to use the material.

__X__ Citations of commercial organizations and trade names in this report do not constitute an official Department of Army endorsement or approval of the products or services of these organizations.

__X__ In conducting research using animals, the investigator(s) adhered to the "Guide for the Care and Use of Laboratory Animals," prepared by the Committee on Care and use of Laboratory Animals of the Institute of Laboratory Resources, national Research Council (NIH Publication No. 86-23, Revised 1985).

____ For the protection of human subjects, the investigator(s) adhered to policies of applicable Federal Law 45 CFR 46.

__X__ In conducting research utilizing recombinant DNA technology, the investigator(s) adhered to current guidelines promulgated by the National Institutes of Health.

__X__ In the conduct of research utilizing recombinant DNA, the investigator(s) adhered to the NIH Guidelines for Research Involving Recombinant DNA Molecules.

__X__ In the conduct of research involving hazardous organisms, the investigator(s) adhered to the CDC-NIH Guide for Biosafety in Microbiological and Biomedical Laboratories.

Geoffrey T Brune 8/24/98

PI - Signature Date

ANNUAL REPORT FOR GRANT NO. DAMD17-94-J-4228

TABLE OF CONTENTS

INTRODUCTION

The estrogen receptor alpha (ERα) is a member of the superfamily of nuclear receptors for small hydrophobic ligands, including steroid hormones, thyroid hormone, vitamin D, and retinoic acid (1). As a class, these receptors are transcription factors whose activity is regulated allosterically by ligand binding. Upon diffusion into the cell, estradiol binds to the ER initiating a series of events including receptor dimerization, release and recruitment of accessory proteins, and hyperphosphorylation, whereupon the receptor is activated for transcription. The ERα mediates estrogenic responses in target tissues including the brain, mammary gland, and tissues of the reproductive tract as well as hormone-sensitive cancers such as breast cancer.

Transcriptional activation is mediated by at least two activation domains in the ER, AF-1 in the N-terminus and AF-2 in the ligand binding domain (LBD). Mounting evidence suggest that the activity of AF-1 is modulated by growth factors acting through the MAP kinase pathway (2) while AF-2 activity is responsive to ligand binding (3). Crystal structure analyses of the ligand binding domains of retinoid X receptor α (RXRα) (4), retinoic acid receptor γ (RARγ) (5), thyroid hormone receptor ß (TRß) (6), and ERα (7, 8), demonstrate that a conformational change results from ligand binding, allowing realignment of a conserved helical region (Helix 12) essential for AF-2 activity.

Antiestrogens, such as the major adjuvant chemotherapeutic agent tamoxifen, antagonize the effects of estrogens by competing for receptor binding. Once bound to the receptor, the subsequenct steps by which these compounds alter the regulation of estrogen-dependent gene transcription remain largely undefined. Tamoxifen has partial agonistic activities in the uterus which complicate its therapeutic use. ICI 182, 780 (ICI) has been shown to be a complete antagonist and may interfere with receptor dimerization or promote receptor degradation. Clearly there are still a number of key aspects of ligand-mediated receptor activity that remain unresolved.

The results presented here represent our ongoing characterization of the process by which ERα is transformed from an inactive state in the absence of ligand to an activated state. The

major focus of our studies has been to identify proteins that act as adapters, coregulators, and/or effectors to modulate the transcriptional activity of the ERα. We specifically wish to test the hypothesis that estrogen agonists and antagonists promote differential transcriptional activity of the ER by altering accessory protein interactions. Consistent with this theory, biochemical and genetic approaches over the last several years have led to the identification of potential coactivator proteins that associate in a ligand-dependent manner with nuclear receptors (9). These include RIP160 (10), RIP140 (11), SRC-1/N-CoA1 (12), TIF2/GRIP1 (SRC-2) (13, 14), RAC3/ACTR/AIB1 (SRC-3) (15), and CBP/p300 (16). Many of these proteins enhance ligand-dependent transcriptional activation by several different nuclear receptors (17, 18). In addition. the recent report of partial hormone resistance in mice with a disrupted SRC-1 gene (19) provides convincing evidence for true coactivator function.

Many of these coactivator proteins, including SRC-1, GRIP1/TIF2 and CBP/p300 associate with nuclear receptors through a short signature motif (LxxLL) called a nuclear receptor box (NR box) (20). Both mutagenesis and peptide binding studies indicate that most of the binding affinity coactivators have for NRs can be attributed to this short peptide sequence. Binding preferences and specificity are presumed to be inherent in sequences flanking the NR box.

To identify novel ERα regulatory proteins, we have used the ligand binding domain of human ERα (aa 282-595), fused to glutathione-S-transferase (GST-LBD), to adsorb proteins from mammalian cell extracts whose association with ER is dependent upon the liganded state of the receptor. We too have isolated several other candidate proteins from cell extracts (T47D, CHO-K1, HeLa, MCF7k1) that recognize the transcriptionally active form of ERα by this technique. In the course of preliminary studies, *in vitro* kinase assays indicated that at least one of these proteins, which binds to GST-LBD only in the presence of estrogen agonists such as estradiol, diethylstilbestrol, and estriol, is a kinase that can phosphorylate the LBD in a ligand-dependent manner. OHT and ICI 182,780 were unable to promote phosphorylation by this kinase. Most studies of ERα phosphorylation have forcused on serine 118, shown to be

regulated by the MAP kinase pathway and to stimulate transcription through AF-1 (2). Serine 167 of hERα has previously been identified by amino acid sequencing as a ligand-induced phosphorylation site (21, 22). The Notides lab has suggested that phosphorylation of serine 167 is important for DNA binding and transcriptional activation (23) while more recent studies suggest that phosphorylation of serine 167 aids in regulating the transcriptional activity of AF-1, possibly coupling multiple signaling pathways (24). Because the kinase activity we have isolated represents an apparently novel phosphorylation site, is agonist-specific, and associated with the AF-2 region of ERα, we chose to pursue its identity and further characterize its binding to the ERα-LBD.

MATERIALS AND METHODS

Culture of Mammalian Cells

HeLa, CHO-k1, and CHO-ER cells were cultured in Dulbecco's Modified Eagle Medium/F-12 nutrient mixture (DMEM/F-12 1:1 mixture, without phenol red, Sigma) supplemented with 10% calf serum (Hyclone), 44 mM $NaHCO_3$, and 1X antibiotics-antimycotic liquid (penicillin, streptomycin, and amphotericin, GibcoBRL). 5 mg/L insulin was also added for CHO-k1 and CHO-ER cells. To maintain the expression and selection of the ER gene, 50 μM $ZnSO_4$ and 40 μM $CdSO_4$ were included in CHO-ER cultures and serum was charcoal stripped to remove steroids. MCF7-k1 cells were grown in Modified Eagle Medium (MEM with Hank's salts and phenol red, GibcoBRL) supplemented with 10% calf serum (Hyclone), 0.01 M HEPES, 1X penicillin/streptomycin (GibcoBRL), 5 mg/L Gentamicin Reagent Solution (GibcoBRL), and 44 mM $NaHCO_3$. For experiments requiring steroid-free media, MCF7-k1 cells were grown in phenol red-free MEM (Sigma) with 10% charcoal-stripped calf serum. All cells were grown at 37 C in a humidified, 5% CO_2 atmosphere.

For preparation of whole cell extracts, subconfluent cells were released from tissue culture vessels with a non-enzymatic cell dissociation solution (Sigma). The cell suspension was collected, pelleted gently at 1000 rpm for 10 minutes, and washed twice with phosphate buffered

saline (PBS). The cell pellet was resuspended in 4 volumes of detergent lysis buffer (50 mM Tris-HCl, pH 7.4, 400 mM NaCl, 2 mM EDTA, 1 mM DTT, 0.25% NP-40) containing protease inhibitors (leupeptin, chymostatin, pepstatin A, antipain, aprotinin and PEFABLOC). Cells were incubated for 20 minutes at 4 C to complete lysis followed by passage through a 25 gauge needle to sheer DNA. The cell debri was pelleted at 15,000 rpm for 20 minutes and supernatants were frozen in the presence of 5% glycerol and stored at -70 C until use.

Production of GST-ERα Fusion Proteins

The GST-LBD vector encoding amino acids 282-595 of human ERα fused to glutathione-S-transferase was transformed into the BL21 strain of *E.coli.* (Stratagene). Overnight cultures were diluted 1:10 and grown at room temperature in selective media (LB, 50 μg/ml ampicillin). Cells were induced with isopropyl-ß-D-thiogalactoside (0.1 mM) at an absorbance of 1.5 (at 600 nm). After three hours of induction, bacteria were collected by centrifugation, resuspended in four volumes of detergent lysis buffer (50 mM Tris-HCl, pH 7.4, 150 mM NaCl, 2 mM EDTA, 2 mM DTT, 0.5% NP-40) containing protease inhibitors. Extracts were cleared by sonication followed by centrifugation at 10,000 rpm for 20 minutes. Expression was monitored by western blotting with a rabbit polyclonal antibody against GST and an anti-ER monoclonal antibody (H222). Receptor levels were determined by controlled-pore glass bead (CPG) assay.

Site Directed Mutagenesis

Mutagenesis of GST-LBD was performed using the QuikChange™ Site-Directed Mutagenesis Kit (Stratagene) following manufacturer instructions. Briefly, plasmid DNA was denatured and appropriate oligonucleotide primers containing the desired mutation were annealed. *Pfu* DNA polymerase was used to extend and incorporate the mutagenic primers. Methylated, non mutated parental DNA was digested with *Dpn1* restriction enzyme and the resulting DNA was used to transform XL1-Blue supercompetent cells. Mutations were verified by automated DNA sequencing (University of Chicago Cancer Research Center DNA

Sequencing Facility). Mutants were retransformed into BL21 and proteins were expressed as described above. Resultant proteins were analyzed for ligand binding by CPG assay.

GST-Pulldown and *In vitro* Kinase Assays

Bacterial extracts of GST-LBD were preincubated with or without 1 μM of the appropriate ligand for 1 hour at 4 C. Affinity columns were prepared by immobilizing 30 pmole of GST-LBD on 10 μl glutathione-Sepharose-4B (Pharmacia). Columns were washed 5 times with washing buffer containing 20 mM HEPES, pH 7.4, 400 mM NaCl, 2.5 mM $MgCl_2$, 0.05% NP-40. Mammalian cell extracts were diluted so that the final composition of the buffer was 20 mM Tris-HCl, pH 7.4, 75 mM NaCl, 10 mM $MgCl_2$, 0.5 mM DTT, 20 mM ß-glycerophosphate, and 0.1 mM Na_3VO_4. Diluted extracts were mixed with prepared affinity columns and incubated for 3 hours at 4 C. Nonspecific proteins were removed by washing with buffer containing 20 mM HEPES, pH 7.4, 400 mM NaCl, 2.5 mM $MgCl_2$, 0.1 mM EDTA, and 0.05% NP-40.

For *in vitro* kinase assays, the pelleted sepharose beads were resuspended in kinase buffer (50 mM HEPES, pH 7.6, 150 mM NaCl, 12 mM $MgCl_2$, 2 mM $MnCl_2$, 10 μM Na_3VO_4, 0.5 mM DTT, 20 mM ß-glycerophosphate) containing 5 μM cold ATP and 1 μCi γ[32P]ATP/5 μl kinase buffer (3000 Ci/mmol, Amersham). After 20 minutes at 30 C, the reaction was terminated by repeated washes in column washing buffer as before. Proteins were eluted by incubation at 95 C in Laemmli sample buffer, resolved by SDS-PAGE, and visualized by Coomassie staining. GST-LBD phosphorylation was analyzed by autoradiography of dried gels.

For GRIP1 pulldown assays, the pSG5-GRIP1 construct (gift of M. Stallcup) was used for *in vitro* transcription and translation of ^{35}[S]-labeled GRIP1 protein using the TNT Coupled Reticulocyte Lysate System and manufacturer instructions (Promega). 2.5 μl of the reaction mixture, diluted to 300 μl in tris-buffered saline (TBS), was incubated with immobilized GST-LBD for an additional 2.5 hours, followed by five washes in TBS containing 0.05% NP-40.

Proteins were eluted by boiling beads for 10 minutes in 2X protein samples buffer. Bound ^{35}[S]-GRIP1 was analyzed by 10% SDS-PAGE followed by fluorography.

Purification of Kinase Activity

0-30% sucrose gradients were prepared (25 mM Tris-HCl, pH 7.4, 400 mM NaCl, 1 mM EDTA, 2 mM DTT, 1 mM NaN_3) by careful layering of 30, 25, 20, 15, 10% sucrose stock solutions followed by equilibration for 2 hour at 4 C.. Cell extracts were applied to the top of prepared centrifuge tubes and then fractionated for 15 hr at 50,000 rpm in a Beckman L8-70 ultracentrifuge. Gradient fractions were collected sequentially through the bottom of each tube. Fractions were analyzed for kinase activity by GST-LBD *in vitro* kinase assays.

Fractions containing kinase activity were further purified by ion exchange chromatography using the Pharmacia LCC FPLC system equipped with a HiTrapQ (Pharmacia) anion exchange column. Samples were applied in low salt buffer (50 mM HEPES, pH 7.4, 50 mM NaCl, 2.5 mM $MgCl_2$, 0.1 mM EDTA, 0.05% NP-40, 0.5 mM DTT) and washed for 10 minutes with a flow rate of 1 ml/min. A linear salt gradient from 50 mM to 1.0 M NaCl was applied for 20 minutes and then the column was washed for 10 minutes in 1.0 M NaCl. Samples containing the kinase activity, as assessed by *in vitro* kinase assays, were pooled.

Fractions were pre-cleared on GST-LBD columns in the absence of estradiol. Supernatants were reapplied to colunns containing GST-LBD in the presence of estradiol. After extensive washing in buffer containing 20 mM Tris-HCl, pH 7.4, 1.5 M NaCl, 2.5 mM $MgCl_2$, 0.05% NP-40, kinase activity was eluted by exchange of OHT for E2 for 30 minutes at room temperature in exchange buffer (50 mM Tris-HCl, 100 mM NaCl, 10 mM $MgCl_2$, 0.1 mM EDTA, 1 mM DTT, 0.05% NP-40). Purification was analyzed by SDS-PAGE followed by silver staining.

For the large scale preparation for microsequencing, HeLa cells were expanded over time and cells representing three hundred 150 cm^2 dishes were harvested. The final purified proteins were separated by 7.5% SDS-PAGE and were visible by coomassie blue staining. Selected proteins bands (E2, E3, E4) were excised from acryalmide gels, dehydrated by two washes in

50% acetonitrile, and stored in micrcentrifuge tubes at -20 C. Protein samples were sent to Dr. William Lane at the Harvard Microchemistry Facility. After in-gel tryptic digestion, HPLC separation of peptides, and screening by LC/MS, select peptides were sequenced by tandem mass spectrometry (MS/MS) on a Finnigan LCQ Quadrupole Ion Trap Mass Spectrometer. Resultant peptides were subjected to BLAST searches using the available databases from the NCBI. Sequences were aligned using the MacVector program.

Western Blotting

Partially purified cell extracts were separated by SDS-PAGE and transferred to nitrocellulose for western blotting. Membranes were incubated in blocking buffer (3% dry milk/TBS/0.2% Tween-20) for 1 hour at room temperature. Blots were then incubated with 1μg/ml of anti-CamKIIδ polyclonal antibody (Santa Cruz Biotechnology) diluted in a 1% dry milk/TBS/0.2% Tween-20 solution for 2 hour, followed by four 5 minute washes in TBS/0.2% Tween-20. Membranes were incubated in a 1:2,000 dilution of mouse-anti-goat IgG linked to horseradish peroxidase (Zymed) for 1 hour, followed by washing in TBS/0.2% Tween-20. Blots were visualized using the SuperSignal Chemiluminescent Substrate (Pierce) following manufacturer instructions.

Immunoprecipitation

CHO-ER cells, stably expressing the full-length ER, were stimulated for 5 minutes or 2 hour with 20 nM E2 or ethanol vehicle. Cells were lysed directly on tissue culture dishes by 3 cycles of freeze/thaw in liquid N_2 in the presence of lysis buffer (50 mM Tris, pH 7.4, 400 mM NaCl, 1 mM DTT, protease inhibitors). Lysates were recovered from dishes, DNA was sheared by passage through a 25 gauge needle, and cell debris was pelleted by centrifugation at 15,000 rpm at 4 C. Salt concentrations were diluted to 200 mM NaCl and lysates were incubated with 2 μg of an anti-ERα monoclonal antibody (H222) for 2 hours. 20 μl Protein-A-Sepharose (Pharmacia) was added to tubes and the incubation was continued for an additional hour. Immunoprecipitates were washed three times in TBS containing 0.05% NP-40 and bound proteins were released by boiling in 2X protein sample buffer. Proteins were separated on 7.5%

SDS-PAGE, transferred to nitrocellulose, and western blots were performed with the anti-CamKIIδ antibody as described above, with and without incubation with 5 μg/ml antigenic blocking peptide (Santa Cruz Biotechnology). Reactive proteins were visualized by chemiluminescence.

Transfection and Reporter Assays

MCF7-k1 cells, maintained in steroid-free media for at least 48 hours, were transfected with a reporter containing the chloramphenicol acetyl transferase (CAT) gene downstream of an estrogen responsive element (ERE) and collagenase promoter (ERE-collΔ60). The control vector (collΔ60) was used to determine background levels (reporters were gifts from P. Kushner). Transfections were performed in 6-well dishes using Superfect Transfection Reagent (Qiagen) and following manufacturer instructions. Following transfection, cells were stimulated with E2, KN-62 (Sigma), or vehicle for 24 hours. Cell lysates were prepared in 300 μl 1X Promoter Lysis Buffer (Promega) and a liquid scintillation method utilizing ^{3}[H]acetyl-CoA (NEN) and chloramphenicol was used to assay CAT activity (25, 26).

GRIP1 Peptide Binding and Competition

The human ERα-LBD$_{297-555}$ was overexpressed and purified as described previously (7). ERα-LBD, complexed to E2 or OHT, was incubated with or without a peptide corresponding to amino acids 686-699 of human GRIP1 at molar ratios of 1:2, 1:3, and 1:10. Incubations were performed on ice for 45 minutes in buffer containing 20 mM Tris, pH 8.1, 1 mM DTT, and 200 mM NaCl. Samples were then subjected to 6% native PAGE for 1 hour at 12 watts. Proteins were stained with GELCODE Blue stain reagent (Pierce).

For competition and release assays, GST-LBD columns were prepared as decribed above and incubated with purified kinase extracts in the presence of estradiol. Columns were then incubated for 30 minutes at room temperature in exchange buffer (50 mM Tris-HCl, 100 mM NaCl, 10 mM $MgCl_2$, 0.1 mM EDTA, 1 mM DTT, 0.05% NP-40) containing increasing

amounts of the GRIP1 peptide. Kinase activity remaining on GST-LBD columns was assessed by *in vitro* kinase assays. Released proteins were analyzed by SDS-PAGE and silver staining.

RESULTS AND DISCUSSION

We have continued to characterize a protein complex that binds *in vitro* to the ligand binding domain of the ERα in a hormone-dependent manner. Preliminary experiments had demonstrated that at least one protein contained in this complex is a kinase capable of phosphorylating the receptor. Phosphoamino acid analysis, tryptic peptide mapping, and mutagenesis identified the site of phosphorylation as serine 559 in the hERα. Progress was previously reported on the biochemical purification of the kinase activity, the major advance being the selective release of the kinase from GST-LBD columns upon treatment with a small excess of the estrogen antagonist 4-hydroxytamoxifen. The results discussed here represent our continued characterization of this interesting protein complex including identification of the kinase by microsequencing, demonstration of binding to the ERα *in vivo*, and mapping of the protein binding site on the ERα-LBD.

Large scale purification and microsequence analysis identifies the kinase.

We have used a combination of chromatographic steps to purify a protein complex containing kinase activity. Sucrose density gradient fractionation of cell extracts followed by *in vitro* kinase assays localized the activity to fractions representing a large molecular weight protein or complex of proteins. Subsequent ion exchange chromatography further purified the activity. The protein complex was purified to homogeneity after affinity chromatography on GST-LBD columns in the presence of estradiol and release by treatment of colums with the estrogen antagonist 4-hydroxytamoxifen as described in materials and methods. Analysis of proteins purified from HeLa cell extracts representing thirty 150 cm^2 tissue culture dishes followed by SDS-PAGE and silver staining indicates 4 prominant protein bands of molecular weight 31.8 (E1), 35.4 (E2), 51.6 (E3), and 62.1 kDa (E4) that bind in a hormone-dependent

manner to GST-LBD columns (**figure 1**). To obtain sufficient quantities for microsequence analysis, HeLa cells were expanded over time and lysates representing three hundred 150 cm^2 dishes were purified as described. After separation, the bands were visible by coomassie staining. Protein bands representing E2, E3, and E4 were sent to the Harvard Microchemistry Facility for microsequencing. Two peptide sequences were obtained for each protein (**figure 2**). BLAST searches of the available databases indicate that both E2 peptides match to several EST (expressed sequence tag) partial cDNA entries with homology to the 5' region of human pyrroline-5-carboxylate reductase. Sequence alignment of the two peptides shows 75% identity (**figure 3**). Pyrroline-5-carboxylate reductase (EC 1.5.1.2) is a cytosolic enzyme that catalyzes the NADPH-dependent conversion of pyrroline-5-carboxylate to proline (27). Due to the nature of the enzymatic activity catalyzed by this enzyme, its reported cytosolic localization, and the fact that this protein band was unique to protein complexes purified from HeLa cell extracts (data not shown), it is difficult to propose a roll for its association with the ER. It may be informative to purify the protein complex from HeLa nuclei to determine if this 35 kDa band is absent from the nuclear kinase complex, and therefore not required for kinase recruitment as we suspect.

Both peptides from sample E3 had strong homology to the delta subunit of rat Ca^{2+}/calmodulin-dependent protein kinase II (CamKIIδ) (**figure 4**). To date, no human form of the delta subunit has been cloned, although both peptides match predicted CamKIIδ sequences in the human EST database. Peptides from sample E4 show identity with CamKII gamma isoforms (**figure 5**). Therefore, we proposed that the kinase activity we have been following is most likely composed of at least 2 different CamKII isoforms.

CamKII is a well-known effector of the actions of Ca^{2+} and calmodulin, originally discovered in rat as a major protein in differentiated neuronal tissue where it was implicated in long-term potentiation and neurotransmitter release (28). CamKII has since been discovered in a variety of organisms including yeast, mold, fruit flies, and humans. The kinase functions as a multimer consisting of 8-12 subunits derived from one or more isoforms (α, β, γ, δ). Isozymes are encoded as single polypeptides, each containing a catalytic, regulatory, variable, and an

association domain. α, β, and β' isoforms predominate in brain and neuronal tissues. γ and δ are the most recently discovered isozymes and Northern blot analyses have shown widespread tissue distribution (29). The kinase is activated in response to increases in intracellular calcium and phosphorylates multiple substrates localized in the nucleus, cytoskeleton, membrane, and cytosol (30).

Western blotting verifies CamKII identification.

We obtained an antibody raised against an epitope within the C-terminus of the delta subunit of rat origin that has been reported to crossreact with proteins from human origin. GST-pulldown assays of sucrose density fractionated HeLa cell extracts were performed in the presence and absence of estradiol (E2). Bound proteins were released from GST-LBD columns and blotted for the presence of CamKIIδ. Positive bands of the expected molecular weight were observed most prominently in fractions #2-5 of the gradients (**figure 6**). Protein association was hormone-dependent. To verify that the observed immunoreactive band corresponds to the protein sent for microsequence analysis, a comparative silver stain and western blot were performed on kinase complexes purified from CHO-k1 and cell extracts in the absence and presence of E2. CHO-k1 samples did indeed show the expected 52 kDa band was immunoreactive (**figure 7**).

We have most recently obtained a CamKII antibody reported to crossreact with α, β, γ, and δ isoforms (Upstate Biotechnology). It will be informative to analyze the immunoreactivity of the purified protein complex as we expect the antibody to recognize at least two of the protein components according to our microsequence data to date.

CamKII associates with the ER in vivo.

To address whether CamKIIδ can associate with the ER in an intact cell, co-immunoprecipitations were attempted. CHO-ER cells, stably expressing the full-length ERα, were stimulated for 5 minutes or 2 hr with 20 nM E2 or ethanol vehicle. Cell lysates were incubated with anti-ER antibodies (H222) and protein-A-sepharose. After separation by SDS-PAGE and transfer to nitrocellulose, immunoprecipitated proteins were probed with the anti-

CamKIIδ antibody. **Figure 8** shows an immunoreactive band of the expected molecular weight in lanes from cells treated with E2 for 5 minutes and 2 hours. Importantly, this band is competable when immunizing peptide is included during blotting. While there are no previous reports of a direct interaction between nuclear receptors and CamKII, Le Bihan et al. recently reported that CamKII inhibitors inhibit progestin and glucocorticoid receptor-mediated transcription in the human breast cancer cell line T47D (31).

A CamKII inhibitor blocks ER-regulated transcription.

In order to start addressing what role CamKII may play in ER action, we performed transfection/reporter assays in the presence and absence of E2 and the CamKII inhibitor, KN-62. KN-62's efficacy is reported to result from the compound's ability to bind to the calmodulin binding site on CamKII, thereby blocking Ca2+/calmodulin binding and kinase activation competitively (32). MCF7k1 cells, expressing endogenous ERα, were transfected with a reporter containing the chloramphenicol acetyl transferase (CAT) gene downstream of an estrogen responsive element (ERE) and collagenase promoter (ERE-collΔ60). Cells were stimulated +/- E2 and +/- KN-62 for 24 hours. Results are presented in **figure 9.** A 5-fold induction of CAT activity is seen when cells are treated with 10 nM estradiol. KN-62 treatment decreases this induction significantly.

Kinase activity is recruited through a consensus co-activator interacting sequence.

Regions of the nuclear receptor co-activator protein GRIP1 which interact with ER have been mapped (13) (**figure 10**). To test if small peptides corresponding to these regions are able to bind to the ER, we analyzed complexes by native gel electrophoresis. Increasing amounts of a peptide corresponding to aa 686-699 of GRIP1 were incubated with purified ER-LBD bound to either estradiol (E2) or OHT. Native gel analysis shows a characteristic shift in LBD-E2 mobility with increasing amounts of peptide indicating the peptide is binding directly to the receptor (**figure 11**). Conversely, no shift is seen in the presence of the antagonist OHT.

This peptide contains the recently defined motif which appears to mediate transcriptional co-activator binding to members of the nuclear receptor family (LxxLL) (20). We were

interested in determining if this peptide might compete for kinase association and we therefore tested its ability to inhibit kinase activity in *in vitro* kinase assays. Indeed, increasing amounts of the GRIP1 peptide were able to block kinase activity in direct competition assays (data not shown). We next checked for the ability of the peptide to elute kinase activity from complexes preassembled on GST-LBD in the presence of E2. Again, a small excess of the GRIP1 peptide was able to diminish kinase activity (**figure 12**). Kinase activity could be reconstituted from unbound fractions after removal of the peptide by size exclusion chromatography. Analysis of released proteins show similar patterns to those obtained for OHT elutions (data not shown). Interestingly, both δ and γ isoforms of CamKII contain the consensus nuclear receptor coactivator interacting sequence LxxLL. In lieu of of the fact that the GRIP1 peptide will compete for kinase binding, it is tempting to speculate that these LxxLL sequences are responsible for recruitment of CamKII to the activated ER.

To investigate binding specificity further, we have made a series of mutations in putative surface residues of the GST-LBD proposed to be involved in recruitment of coactivator proteins (33, 34). Mutants were tested for their ability to recruit both GRIP1 and the kinase complex. **Figure 13** indicates that the ability to recruit GRIP1 exactly parallels the ability of the GST-LBD to recruit the kinase activity.

Taken together, our data support a model in which CamKII is capable of modulating transcriptional activity through ERα by direct association with the ligand binding domain of the receptor in the presence of agonists. What role phosphorylation may play is a topic of current interest in the lab. Many studies have focused on the effect that multiple signaliing pathways have on nuclear receptor action (35, 36). CamKII, a known effector of Ca^{2+} signals within the cell, may indeed help integrate these pathways at the point of nuclear receptor activity.

REFERENCES

1. M. Beato, P. Herrlich, G. Shultz, Steroid hormone receptors: many actors in search of a plot. *Cell* **83**, 851-857 (1995).

2. S. Kato, et al., Activation of the Estrogen Receptor Through Phosphorylation by Mitogen-Activated Protein Kinase. *Science* **270**, 1491-1494 (1995).

3. P. S. Danielian, R. White, J. A. Lees, M. G. Parker, Identification of a conserved region required for hormone-dependent transcriptional activation by steroid hormone receptors. *EMBO J.* **11**, 1025-1033 (1992).

4. J.-P. Renaud, et al., Crystal structure of the ligand-binding domain of the human nuclear receptor RXR-alpha. *Nature* **375**, 377-382 (1995).

5. J.-P. Renaud, et al., Crystal structure of the RAR-gamma ligand-binding domain bound to all-trans retinoic acid. *Nature* **378**, 681-689 (1995).

6. R. L. Wagner, et al., A structural role for hormone in the thyroid hormone receptor. *Nature* **378**, 690-697 (1995).

7. A. M. Brzozowski, et al., Molecular basis of agonism and antagonism in the oestrogen receptor. *Nature* **389**, 753-758 (1997).

8. D. M. Tanenbaum, Y. Wang, S. P. Williams, P. B. Sigler, Crystallographic comparison of the estrogen and progesterone receptor's ligand binding domain. *Proc. Natl. Acad. Sci. USA* **95**, 5998-6003 (1998).

9. K. B. Horwitz, et al., Nuclear Receptor Coactivators and Corepressors. *Molecular Endocrinology* **10**, 1167-1177 (1996).

10. S. Halachmi, et al., Estrogen Receptor-Associated Proteins: Possible Mediators of Hormone-Induced Transcription. *Science* **264**, 1455-1458 (1994).

11. V. Cavailles, S. Dauvois, P. S. Danielian, M. G. Parker, Interaction of proteins with transcriptionally active estrogen receptors. *Proc. Natl. Acad. Sci. USA* **91**, 10009-10013 (1994).

12. S. A. Onate, S. Y. Tsai, M.-J. Tsai, B. W. O'Malley, Sequence and characterization of a coactivator for the steroid hormone receptor family. *Science* **270**, 1354-1357 (1995).

13. H. Hong, K. Kohli, A. Trivedi, D. L. Johnson, M. R. Stallcup, GRIP1, a novel mouse protein that serves as a transcriptional coactivator in yeast for the hormone binding domains of steroid receptors. *Proc. Natl. Acad. Sci. USA* **93**, 4948-4952 (1996).

14. J. J. Voegel, M. J. S. Heine, C. Zechel, P. Chambon, H. Gronemeyer, TIF2, a 160 kDa transcriptional mediator for the ligand-dependent activation function AF-2 of nuclear receptors. *EMBO J.* **15**, 3667-3675 (1996).

15. S. L. Anzick, et al., AIB1, a Steroid Receptor Coactivator Amplified in Breast and Ovarian Cancer. *Science* **277**, 965-968 (1997).

16. B. Hanstein, et al., p300 is a component of an estrogen receptor coactivator complex. *Proc. Natl. Acad. Sci. USA* **93**, 11540-11545 (1996).

17. D. Chakravarti, et al., Role of CBP/p300 in nuclear receptor signalling. *Nature* **383**, 99-103 (1996).

18. J. Torchia, et al., The transcriptional co-activator p/CIP binds CBP and mediates nuclear-receptor function. *Nature* **387**, 677-684 (1997).

19. J. Xu, et al., Partial Hormone Resistance in Mice with Disruption of the Steroid Recpetor Coactivator (SRC-1) Gene. *Science* **279**, 1922-1925 (1998).

20. D. M. Heery, E. Kalkhoven, S. Hoare, M. G. Parker, A signature motif in transcriptional co-activators mediates binding to nuclear receptors. *Nature* **387**, 733-736 (1997).

21. S. F. Arnold, J. D. Obourn, H. Jaffe, A. C. Notides, Serine 167 Is the Major Estradiol-Induced Phosphorylation Site on the Human Estrogen Receptor. *Mol. Endo.* **8**, 1208-1214 (1994).

22. S. F. Arnold, J. D. Obourn, H. Jaffe, A. C. Notides, Phosphorylation of the Human Estrogen Receptor by Mitogen-activated Protein Kinase and Casein Kinase II: Consequence on DNA Binding. *J. Steroid Biochem. Molec. Biol.* **55**, 163-172 (1995).

23. E. Castano, D. P. Vorojeikina, A. C. Notides, Phosphorylation of serine-167 on the human oestrogen receptor is important for response element binding and transcriptional activation. *Biochem. J.* **326**, 149-157 (1997).

24. P. B. Joel, et al., pp90rsk1 regulates estrogen receptor-mediated transcription through phosphorylation of Ser-167. *Mol Cell Biol* **18**, 1978-1984 (1998).

25. J. R. Neumann, C. A. Morency, K. O. Russion, A Novel Rapid Assay for Chloramphenicol Acetyltransferase Gene Expression. *BioTechniques* **5**, 444-447 (1987).

26. A. Eastman, An Improvement to the Novel Rapid Assay for Chloramphenicol Acetyltransferease Gene Expression. *BioTechniques* **5**, 730-732 (1987).

27. K. M. Dougherty, M. C. Brandriss, D. Valle, Cloning human pyrroline-5-carboxylate reductase cDNA by complementation in Saccaromyces cerevisiae. *J. Biol. Chem.* **267**, 871-875 (1992).

28. H. Schulman, The multifunctional Ca2+/calmodulin-dependent protein kinases. *Curr Opin Cell Biol* **5**, 247-53 (1993).

29. P. Nghiem, S. M. Saati, C. L. Martens, P. Gardner, H. Schulman, Cloning and analysis of two new isoforms of multifunctional Ca2+/calmodulin-dependent protein kinase. Expression in multiple human tissues. *J Biol Chem* **268**, 5471-9 (1993).

30. R. R. White, Y. G. Kwon, M. Taing, D. S. Lawrence, A. M. Edelman, Definition of optimal substrate recognition motifs of Ca2+-calmodulin- dependent protein kinases IV and II reveals shared and distinctive features. *J Biol Chem* **273**, 3166-72 (1998).

31. S. Le Bihan, et al., Calcium/calmodulin kinase inhibitors and immunosuppressant macrolides rapamycin and FK506 inhibit progestin- and glucocorticosteroid receptor- mediated transcription in human breast cancer T47D cells. *Mol Endocrinol* **12**, 986-1001 (1998).

32. H. Hidaka, H. Yokokura, Molecular and cellular pharmacology of a calcium/calmodulin-dependent protein kinase II (CaM kinase II) inhibitor, KN-62, and proposal of CaM kinase phosphorylation cascades. *Adv Pharmacol 1996;36:193-219* ,

33. W. Feng, et al., Hormone-dependent coactivator binding to a hydrophobic cleft on nuclear receptors. *Science* **280**, 1747-9 (1998).

34. P. M. A. Henttu, E. Kalkhoven, M. G. Parker, AF-2 Activity and Recruitment of Steroid Receptor Coactivator 1 to the Estrogen Receptor Depend on a Lysine Residue Conserved in Nuclear Receptors. *EMBO* **17**, 1832-1839 (1997).

35. C. L. Smith, Cross-talk between peptide growth factor and estrogen receptor signaling pathways. *Biol Reprod* **58**, 627-32 (1998).

36. A. Migliaccio, et al., Activation of the Src/p21ras/Erk pathway by progesterone receptor via cross-talk with estrogen receptor. *Embo J* **17**, 2008-18 (1998).

FIGURE LEGENDS

Figure 1. Analysis of purified proteins shows a stoichiometric complex of 4 hormone-dpeendent proteins. (A) Kinase activity was purified in the absence (--) and presence of E2 (+E2) from HeLa and CHO-k1 cell extracts as described in materials and methods. Proteins were separated by 7.5% SDS-PAGE and silver stained. Interestingly, the two cell lines show somewhat different protein profiles. (B) Coomassie stained gel of large scale purification from HeLa cell extracts. Arrows indicate proteins sent for microsequencing(E2, E3, and E4).

Figure 2. Peptide sequences from E2, E3, and E4. Mass spectrometric data from the Harvard Microchemistry Facility for proteins E2, E3, and E4 show close correlation between predicted and observed molecular weights. Asterisks indicate isobaric amino acid residues (I/L=113, Q/K=128, F/Msx=147) that cannot be unambiguously differentiated in mass spectrometric sequencing.

Figure 3. Sequence alignment of peptides derived from sample E2 with human pyrroline-5-carboxylate-reducatase.

Figure 4. Sequence alignment of peptides derived from sample E3 with the rat CamKIIδ isozyme.

Figure 5. Sequence alignment of peptides derived from sample E4 with two isoforms of human CamKIIγ.

Figure 6. Western blotting verifies protein identification. HeLa cell extracts were fractionated by sucrose density gradients and fractions #1-6 were subjected to GST-LBD pulldown assays in the absence and presence of E2. Resultant proteins were analyzed for the

presence of CamKIIδ by western blotting show a roughly 52 kDa immunoreactive band assumed to correspond to CamKIIδ.

Figure 7. Comparison of silver stained and immunoreactive bands shows CamKIIδ immunoreactivity corresponds to the expected silver stained band. Kinase activity was purified from CHO-k1 cell extracts and described in materials and methods. Proteins were separated by 7.5% SDS-PAGE. Parallel lanes were silver stained or transferred to nitrocllulose and blotted for CamKIIδ. Arrows indicate the position of protein E3.

Figure 8. hERα and CamKIIδ associate *in vivo*. hERα immunoprecipitates from cells treated with E2 for 5 minutes or 2 hr were separated by 7.5% SDS-PAGE and blotted for the presence of CamKIIδ Addition of CamKIIδ immunizing peptide during western blotting shows the immunoreactive band at 52 kDa (arrows) to be specific.

Figure 9. The CamKII inhibitor KN-62 blocks estrogen induced gene expression. MCF7-k1 cells were transfected with ERE-CollΔ60-CAT or control CollΔ60-CAT reporter vectors and CAT activity was monitored after cells were treated with or without E2 (20 nM) or KN-62 (10 uM) for 24 hr. Transfections were performed in triplicate.

Figure 10. GRIP1 nuclear receptor interaction sites. Regions of GRIP1 which interact with ER have been mapped. All sites contain the concensus nuclear receptor interaction motif (LxxLL). The peptide used in these studies is marked with an arrow.

Figure 11. GRIP1 peptide binds to ER-LBD in the presence of E2 but not OHT. A) Increasing amounts of GRIP1 peptide were incubated with purified ER-LBD in the presence of E2. Samples were analyzed by 6% native gel electrophoresis followed by coomassie staining.

Peptide binding causes the ER-LBD band to shift. B) ER-LBD in the presence of OHT does not shifted after incubation with the GRIP1 peptide.

Figure 12. GRIP1 peptide is able to release kinase activity from GST-LBD columns. A) GST-LBD/kinase complexes were preassembled in the presence of E2. Increasing amounts of the GRIP1 peptide were applied to columns followed by analysis by *in vitro* kinase assays. Autoradiography demonstrates that 10-fold excess peptide vs. receptor is able to abolish kinase activity. B) Eluted samples were applied to G25 size exclusion columns to remove peptide and samples were reapplied to GST-LBD columns in the presence of E2. Kinase activity can be reconstituted from these samples demonstrating that the peptide can cause release of the kinase from GST-LBD.

Figure 12. Ability to recruit kinase activity parallels the ability to recruit the coactivator GRIP1 for GST-LBD mutants. (A) GST-LBD mutants were analyzed for the ability to recruit 35[S]-GRIP1 by GST pulldown assay with (+E2) and without (--) ligand. Bound proteins were analyzed by SDS-PAGE and fluorography. (B) Likewise, GST-LBD mutants were analyzed by *in vitro* kinase assays. GST-LBD phosphorylation was analyzed by SDS-PAGE and autoradiography.

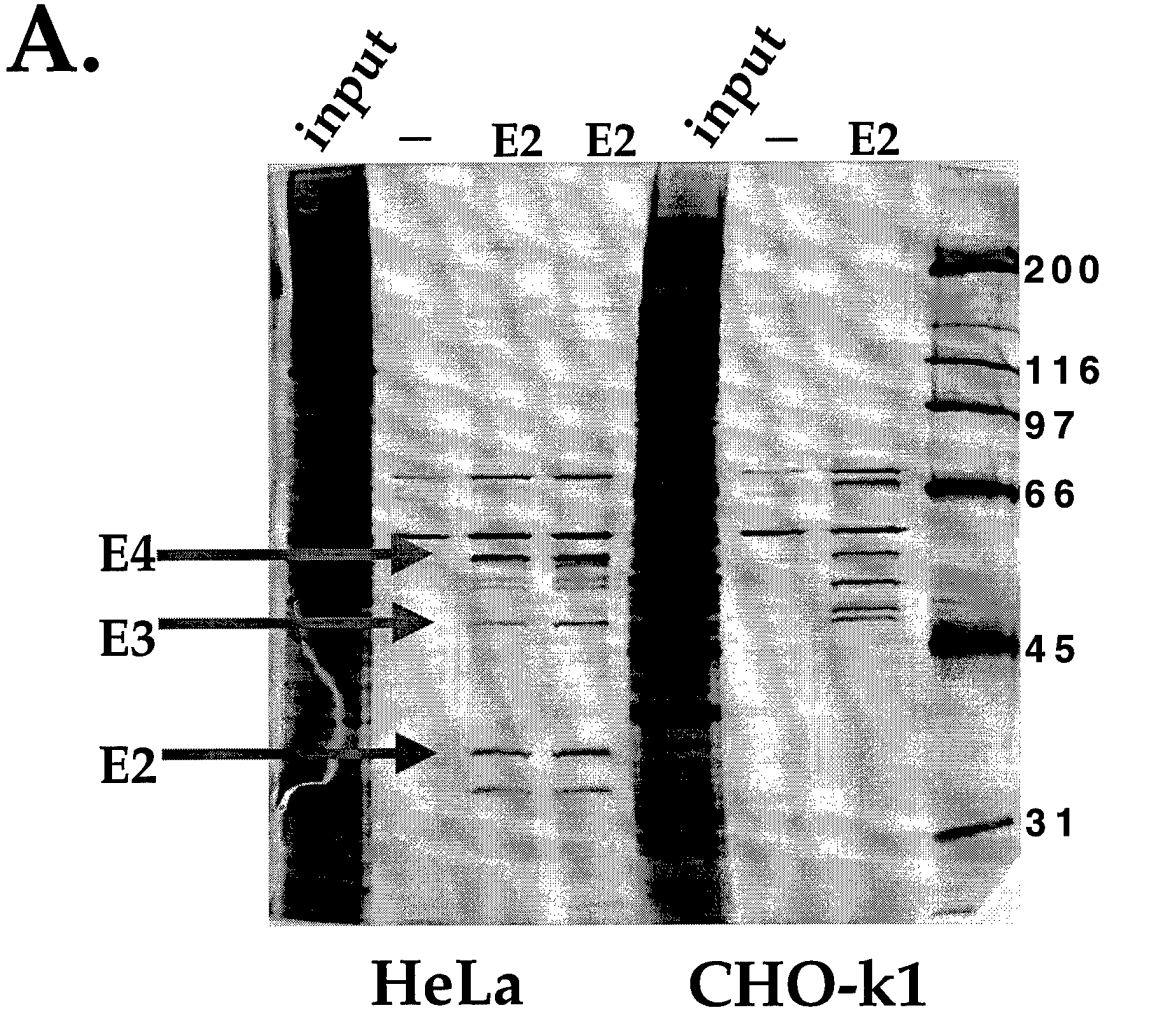
A.
input
—
E2
E2
input
—
E2
200
116
97
66
45
31
E4
E3
E2
HeLa
CHO-k1

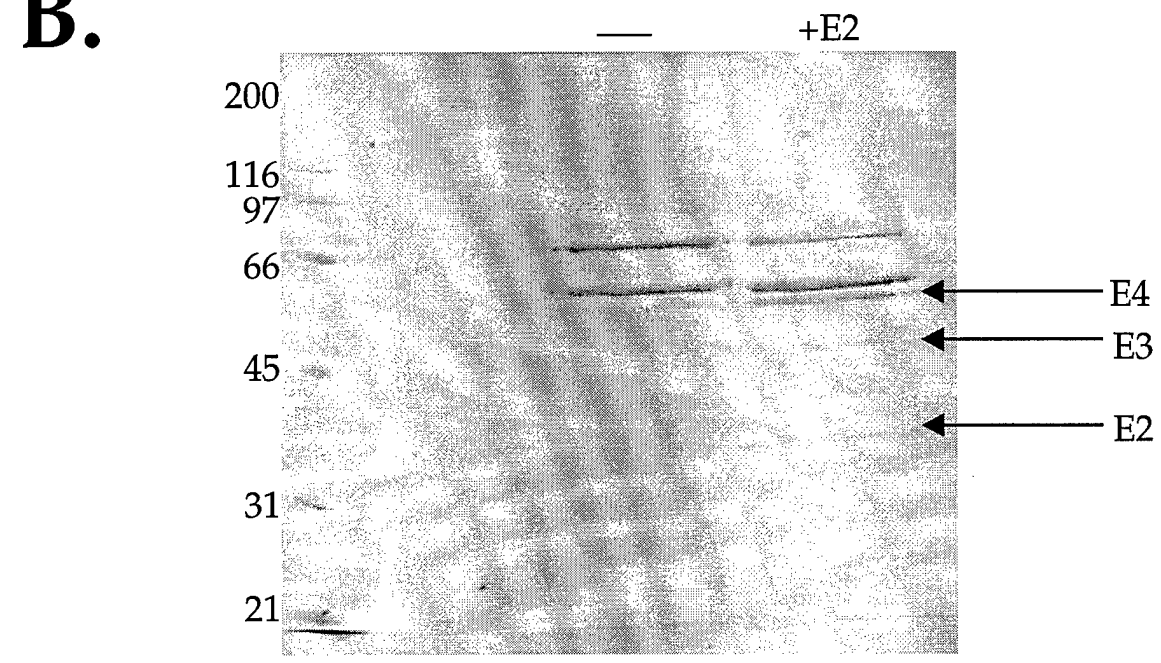
B.
—
+E2
200
116
97
66
45
31
21
E4
E3
E2

Figure 1.

E2 Peptides:

I*L*D E I*G A D V Q* A R

Peptide mass: 1298.69
Experimental: 1298.61

I*L*A S S P E M N L*P T V S A L* R

Peptide mass: 1813.97
Experimental: 1813.92

E3 Peptides:

F*T D E Y Q*L*F*E E L* G K*

Peptide mass: 1617.76
Experimental: 1617.60

W Q* N V H F*H R

Peptide mass: 1122.56
Experimental: 1122.58

E4 Peptides:

G A I*L*T T M L*V S R

Peptide mass: 1160.67
Experimental: 1160.44

F*T D D Y Q*L*F*E E L*G K*

Peptide mass: 1603.75
Experimental: 1603.70

Figure 2.

ClustalW Formatted Alignments

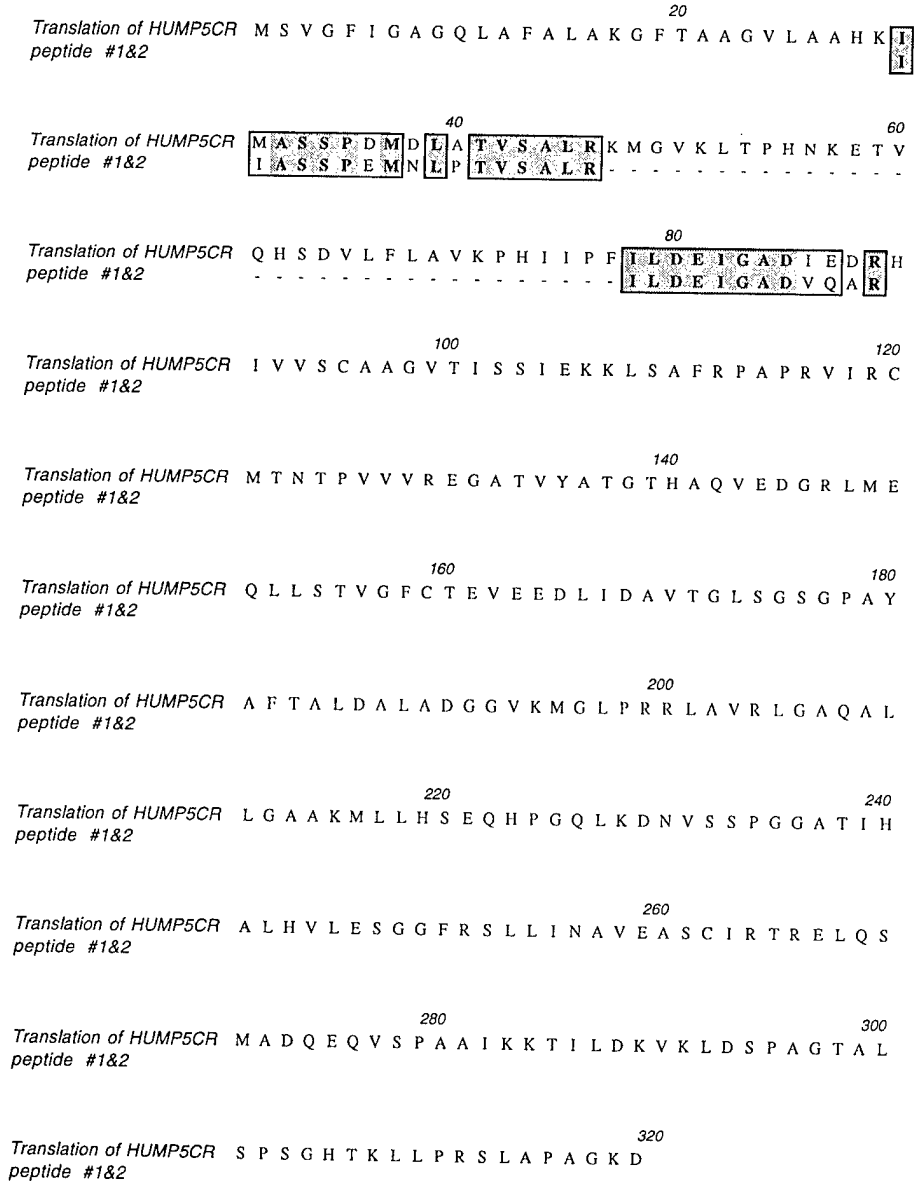

Figure 3.

ClustalW Formatted Alignments

```
                                        20
E3, peptide1                            FTDEYQLFEELGK
KCCD_RAT    MASTTTCTR                   FTDEYQLFEELGKGAFSVVRR
E3, peptide2

                    40                                  60
E3, peptide1
KCCD_RAT    CMKIPTGQEYAAKIINTKKLSARDHQKLER
E3, peptide2

                                        80
E3, peptide1
KCCD_RAT    EARICRLLKHPNIVRLHDSISEEGFHYLVF
E3, peptide2

                   100                                 120
E3, peptide1
KCCD_RAT    DLVTGGELFEDIVAREYYSEADASHCIQQI
E3, peptide2

                                       140
E3, peptide1
KCCD_RAT    LESVNHCHLNGIVHRDLKPENLLLASKSKG
E3, peptide2

                   160                                 180
E3, peptide1
KCCD_RAT    AAVKLADFGLAIEVQGDQQAWFGFAGTPGY
E3, peptide2

                                       200
E3, peptide1
KCCD_RAT    LSPEVLRKDPYGKPVDMWACGVILYILLVG
E3, peptide2

                   220                                 240
E3, peptide1
KCCD_RAT    YPPFWDEDQHRLYQQIKAGAYDFPSPEWDT
E3, peptide2
```

Figure 4.


```
                                       260
E3, peptide1
KCCD_RAT    VTPEAKDLINKMLTINPAKRITASEALKHP
E3, peptide2

                   280                                 300
E3, peptide1
KCCD_RAT    WICQRSTVASMMHRQETVDCLKKFNARRKL
E3, peptide2

                                       320
E3, peptide1
KCCD_RAT    KGAILTTMLATRNFSAAKSLLKKPDGVKIN
E3, peptide2

                   340                                 360
E3, peptide1
KCCD_RAT    NKANVVTSPKENIPTPALEPQTTVIHNPDG
E3, peptide2

                                       380
E3,. peptide1
KCCD_RAT    NKESTESSNTTIEDEDVKARKQEIIKVTEQ
E3, peptide2

                   400                                 420
E3, peptide1
KCCD_RAT    LIEAINNGDFEAYTKICDPGLTAFEPEALG
E3, peptide2

                                       440
E3, peptide1
KCCD_RAT    NLVEGMDFHRFYFENALPKINKPIHTIILN
E3, peptide2

                   460                                 480
E3, peptide1
KCCD_RAT    PHVHLVGDDAACIAYIRLTQYMDGNGMPKT
E3, peptide2

                                       500
E3, peptide1
KCCD_RAT    MQSEETRVWHRRDGK             SGSPTVP
E3, peptide2                WQNIHF HR
                            WQNVHR HR

                   520                                 540
E3, peptide1
KCCD_RAT    IKPPCIPNGKENFSGGTSLWQNI
E3, peptide2
```

ClustalW Formatted Alignments

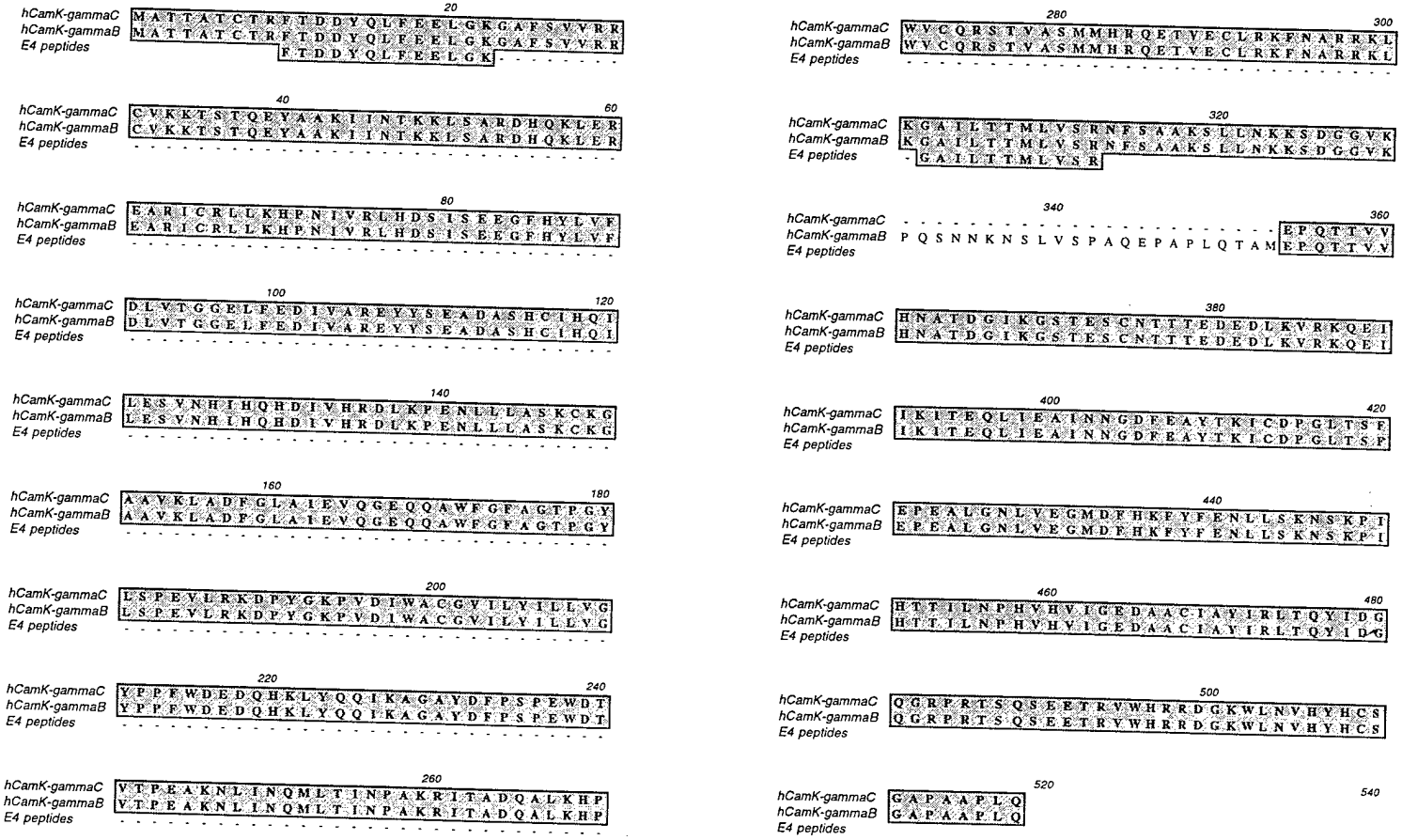

Figure 5.

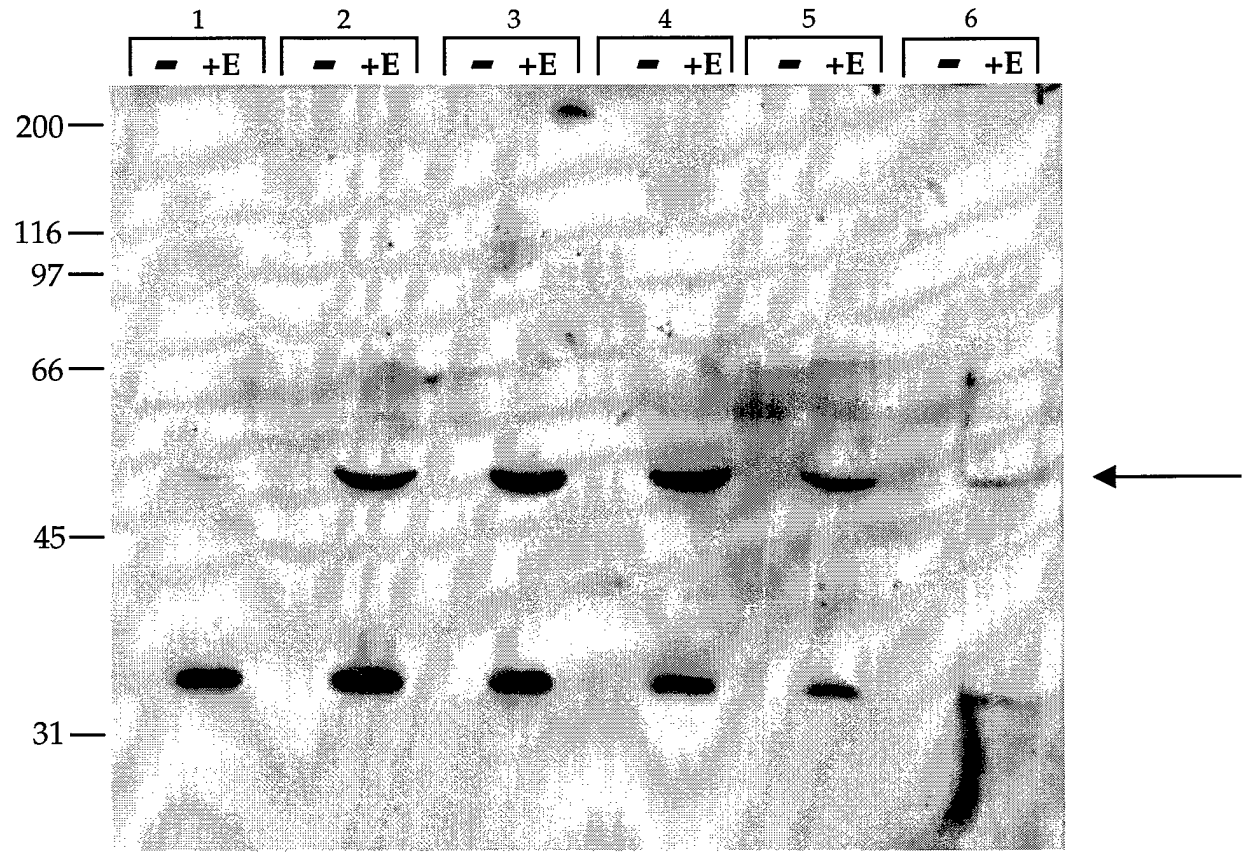

Figure 6.

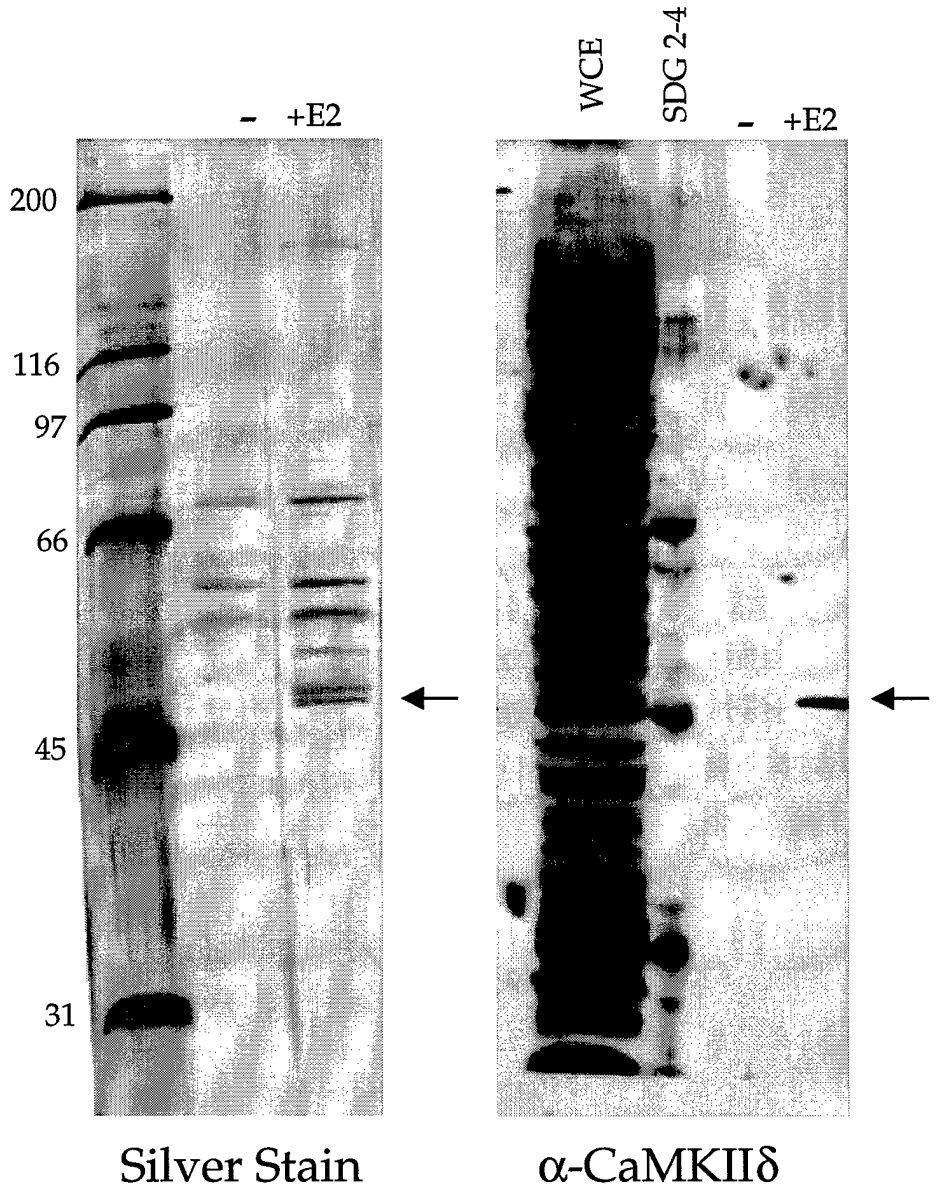

Figure 7.

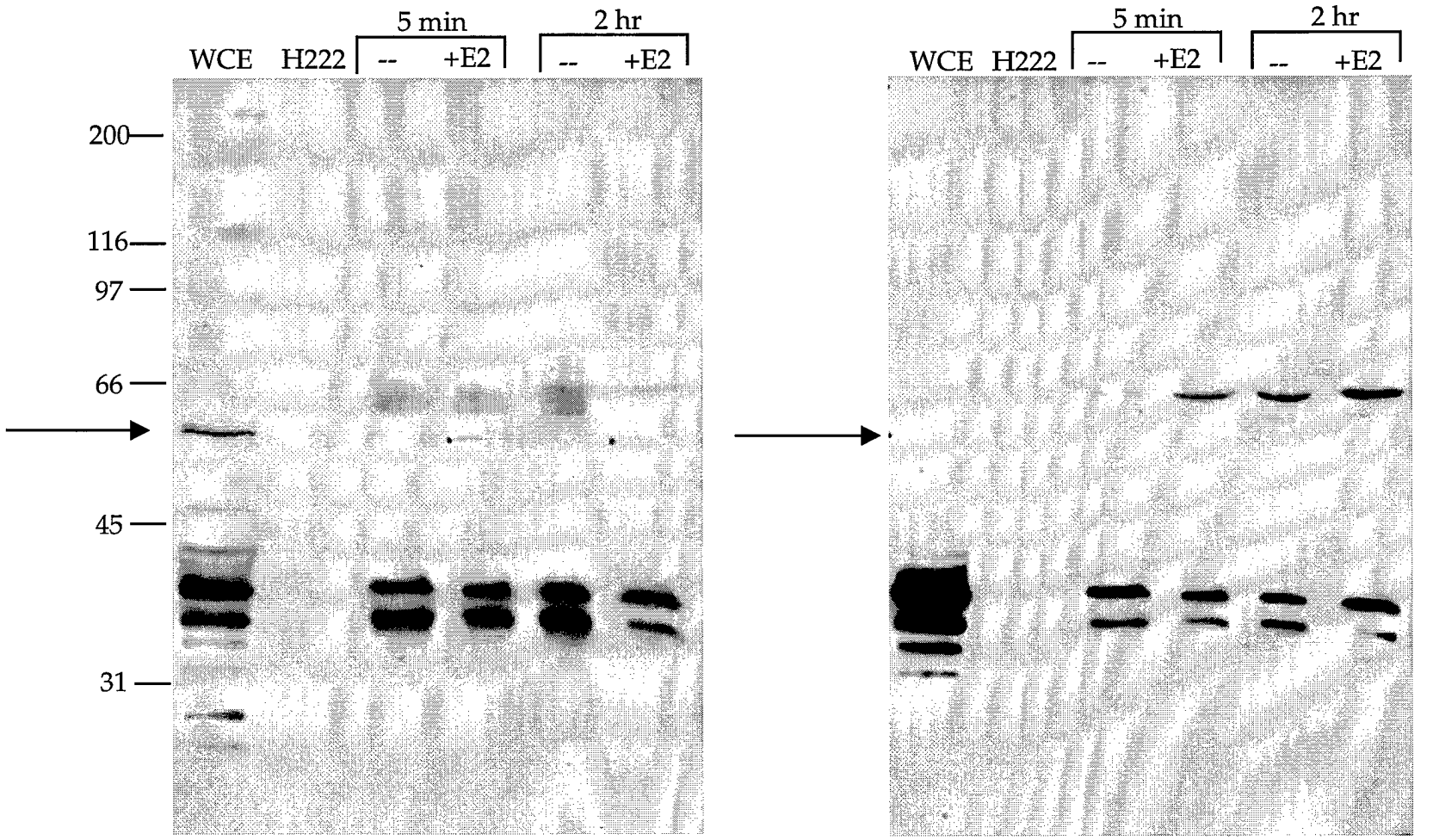
WCE
H222
5 min
2 hr
--
+E2
--
+E2
200
116
97
66
45
31
Western w/α-CaMKIIδ
WCE
H222
5 min
2 hr
--
+E2
--
+E2
Compete with antibody peptide

Figure 8.

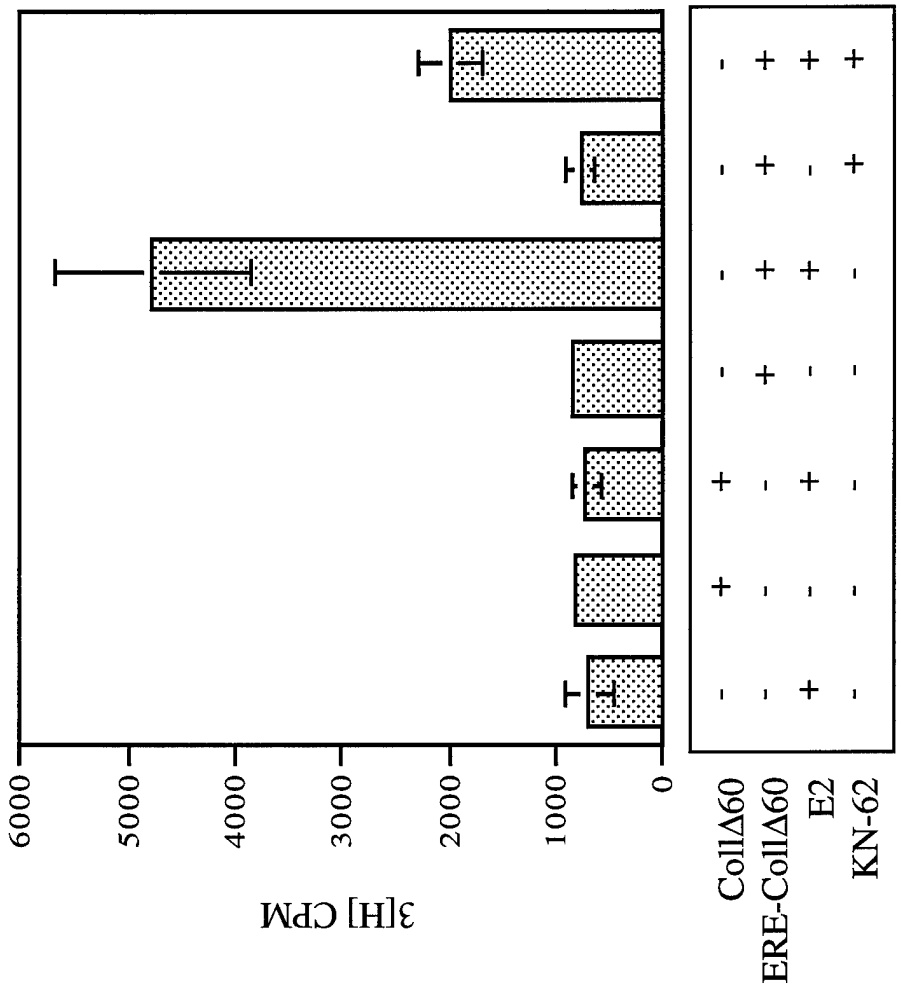
3[H] CPM
6000
5000
4000
3000
2000
1000
0
Coll Δ60
ERE-Coll Δ60
E2
KN-62

Figure 9.

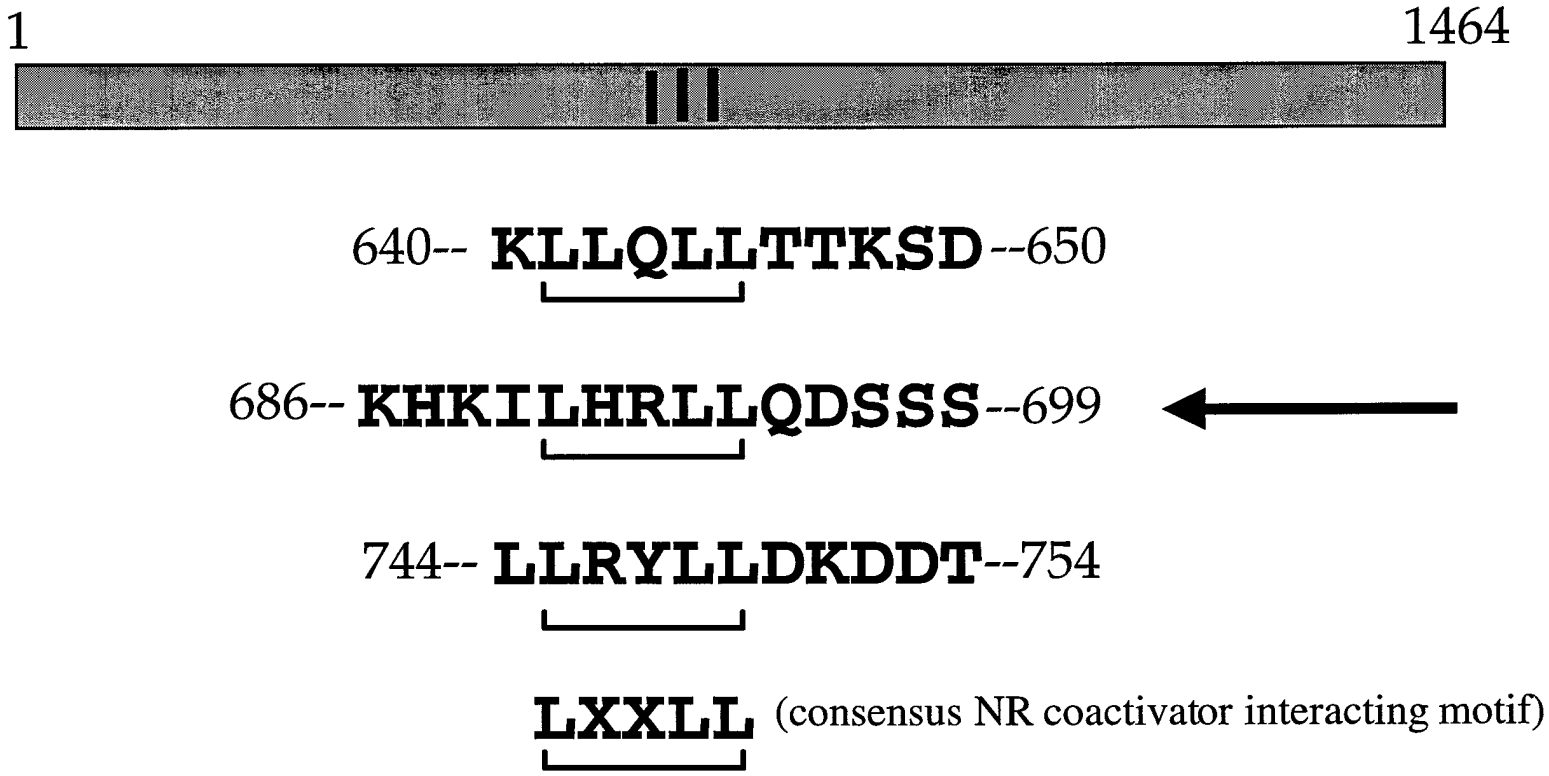
1
1464
640-- KLLQLLTTKSD --650
686-- KHKILHRLLQDSSS --699
744-- LLRYLLDKDDT --754
LXXLL (consensus NR coactivator interacting motif)

Figure 10.

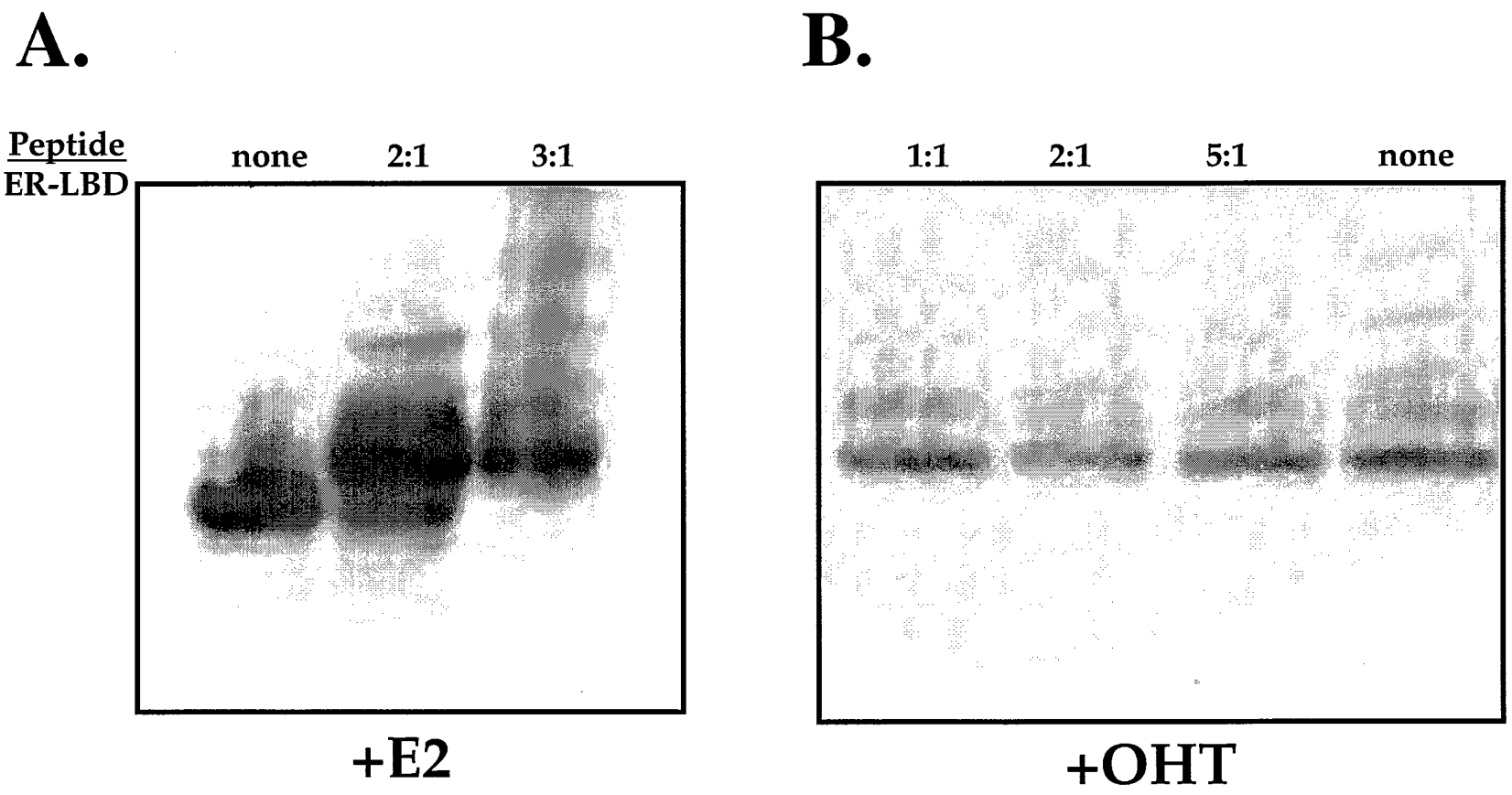

Figure 11.

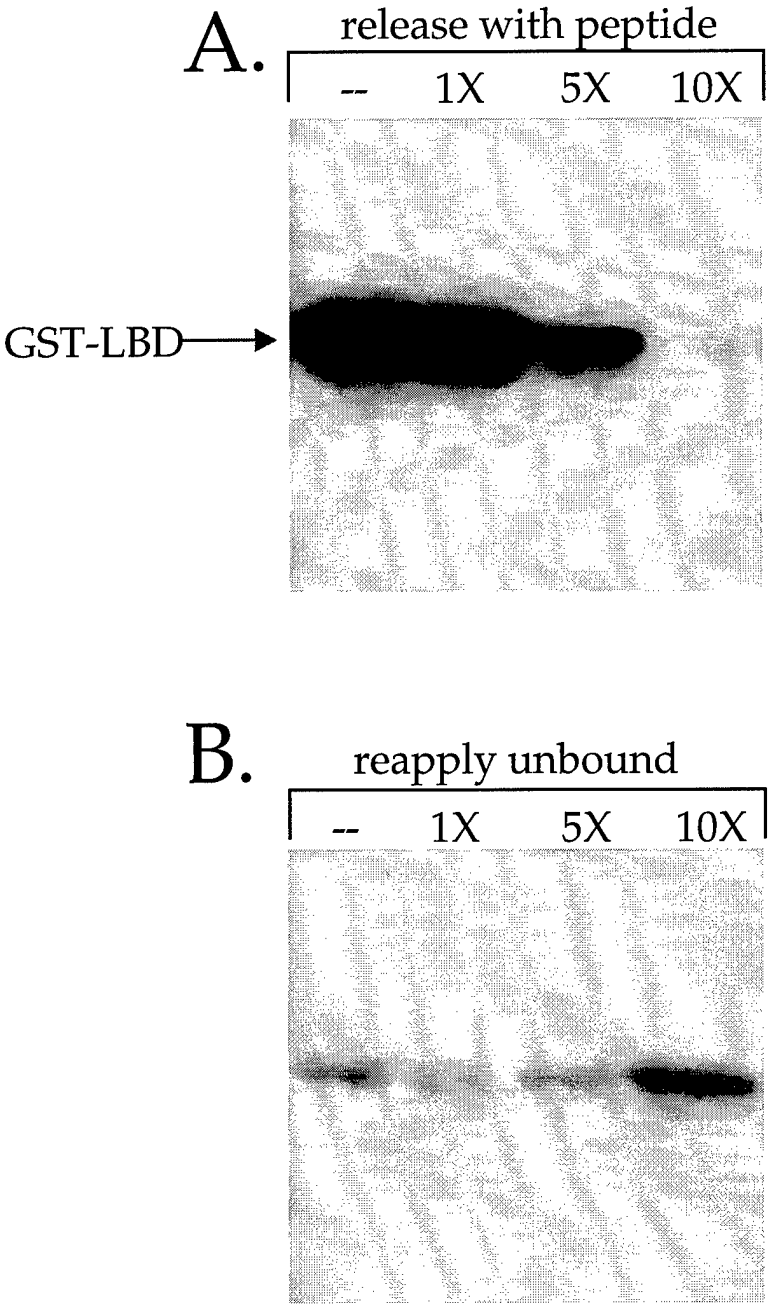
A.
release with peptide
--
1X
5X
10X
GST-LBD
B.
reapply unbound
--
1X
5X
10X

Figure 12.

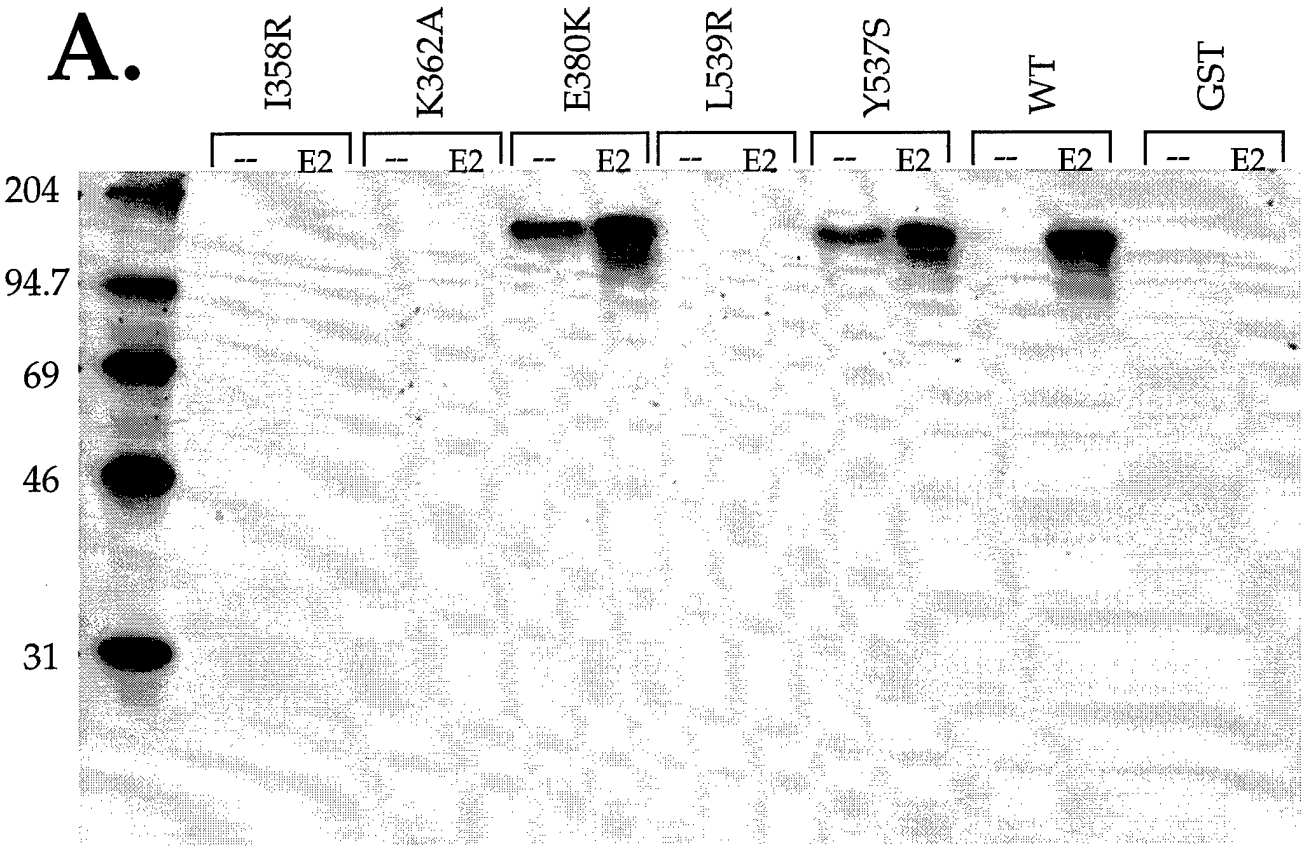
A.
I358R
K362A
E380K
L539R
Y537S
WT
GST
-- E2
204
94.7
69
46
31

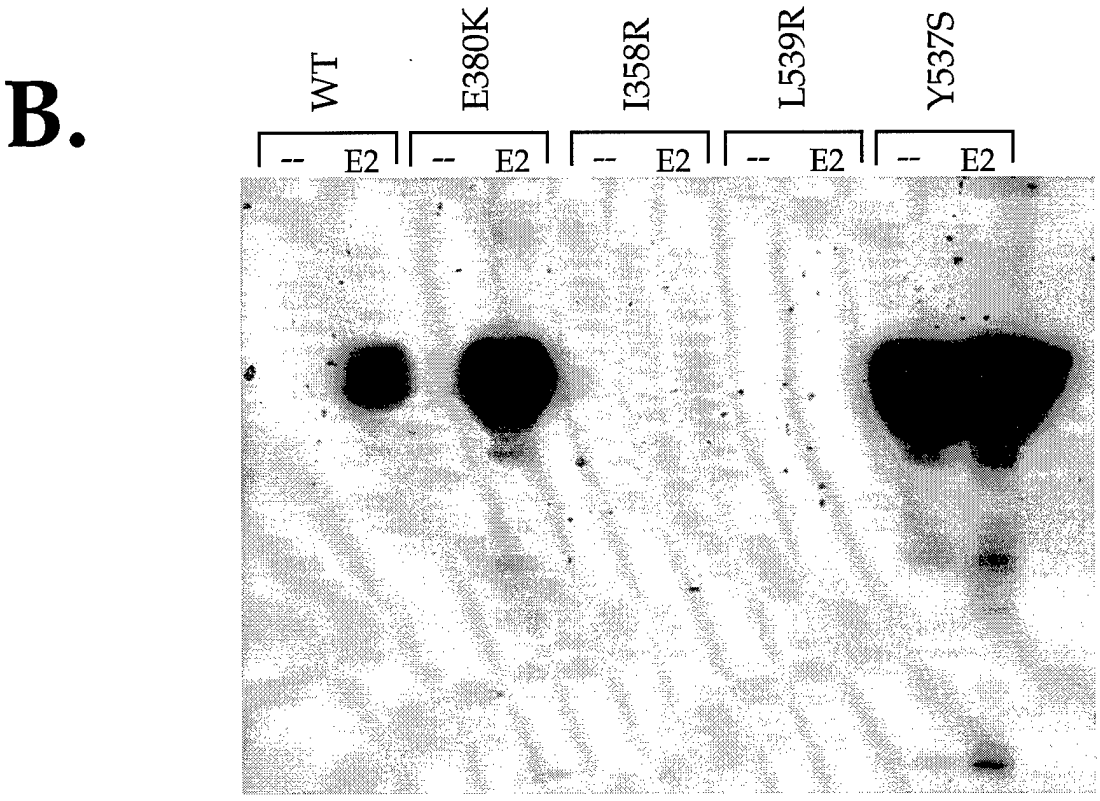
B.
WT
E380K
I358R
L539R
Y537S
-- E2

Figure 13.

ANNUAL REPORT FOR GRANT NO. DAMD17-94-J-4228

Appendix

Bibliography of pertinent publications

List of personnel supported

Three copies each of three publications

Publications (1994-1998)

1. C.C. Landel, P.J. Kushner and G.L. Greene. The interaction of human estrogen receptor with DNA is modulated by receptor-associated proteins. Mol. Endocrinol. 8(10):1407-1419 (1994).
2. D.A. Seielstad, K.E. Carlson, J.A. Katzenellenbogen, P.J. Kushner and G.L. Greene. Molecular characterization by mass spectrometry of the human estrogen receptor ligand-binding domain expressed in *Escherichia coli*.. Mol. Endocrinol. 9, 647-658 (1995).
3. D.A. Seielstad, K.E. Carlson, J.A. Katzenellenbogen, P.J. Kushner and G.L. Greene. Analysis of the structural core of the human estrogen receptor ligand binding domain by selective proteolysis / mass spectrometric analysis. Biochemistry, 34(39), 12605-12615 (1995).
4. C.C. Landel, P.J. Kushner and G.L. Greene. Estrogen receptor accessory proteins: Effects on receptor-DNA interactions. Environmental Health Perspectives, 103 (7)23-28 (1995).
5. A Nardulli, L Romine, C Carpo, G Greene and B Rainish, Estrogen Receptor Affinity and Location of Consensus and Imperfect Estrogen Response Elements Influence Transcription Activation of Simplified Promoters. Mol. Endocrinol., 10, 694-704 (1996).
6. E. DeSombre, A. Hughes, C. Church-Landel, G. Greene, J. Schwartz, R. Hanson. Cellular and subecullar studies of the radiation effects of Auger electron-emitting estrogens. Acta Oncologica Vol. 35, No. 7, 833-840 (1996).
7. S. Kim-Schulze, K.A. McGowan, S.C. Hubchak, M.C. Cid, M.B. Martin, H.K. Kleinman, G.L. Greene, W. Schnaper. Expression of an Estrogen Receptor by Human Coronary Artery and Umbilical Vein Endothelial Cells. Circulation, 94, 1402-1407 (1996).
8. G. L. Greene, V. S. Sharma and L. Cheng. Estrogen Receptor Structure and Function in Breast Cancer Cells. In: Accomplishments in Cancer Research 1996, J. G. Fortner & P.A. Sharp, Eds. Lippencott-Raven, Philadelphia. pp 147-156 (1997).
9. C.C. Landel, S.J. Potthoff, A.M. Nardulli, P.J. Kushner, and G.L. Greene. Estrogen Receptor Accessory Proteins Augment Receptor-DNA Interaction and DNA Bending. J. Steroid Biochem. Molec. Biol. 63, No. 1-3, pp. 59-73 (1997)
10. A.M. Brzozowski, A.C.W. Pike, Z Dauter, R.E. Hubbard, T. Bonn, O. Engstrom, L. Ohman, G.L. Greene, J.A. Gustafsson, and M. Carlquist. Molecular basis of agonism and antagonism in the oestrogen receptor. Nature 389, 753-758 (1997).
11. J.R. Wood, G.L. Greene and A.M. Nardulli, Estrogen response elements function as allosteric modulators of estrogen receptor conformation. Mol Cell Biol, 18, 1927-1934 (1998).

Personnel (7/25/94-7/24/98)

Greene, Geoffrey L.
Barstad, Danielle
Black-Loria, Paula
Chen, Donny
Cheng, Lin
Church-Landel, Carolyn
Dizon, Resty
Hospelhorn, Chris
Poinsette, Margarette
Sharma, Vandana
Smith, Janice
Yang, Schuseng

Pergamon

PII: S0960-0760(97)00073-3

J. Steroid Biochem. Molec. Biol. Vol. 63, No. 1–3, pp. 59–73, 1997

Printed in Great Britain
0960-0760/97 $19.00 + 0.00

Estrogen Receptor Accessory Proteins Augment Receptor–DNA Interaction and DNA Bending

Carolyn Church Landel,[3] Sara J. Potthoff,[1] Ann M. Nardulli,[1] Peter J. Kushner[2] and Geoffrey L. Greene[3]*

[1]Department of Molecular and Integrative Physiology, University of Illinois at Urbana-Champaign, Urbana, IL 61801, U.S.A.; [2]Metabolic Research Unit, University of California, San Francisco, CA 94143, U.S.A. and [3]The Ben May Institute for Cancer Research and Department of Biochemistry and Molecular Biology, University of Chicago, 5841 South Maryland Avenue, MC 6027, Chicago, IL 60637, U.S.A.

Increasing evidence suggests that accessory proteins play an important role in the ability of the estrogen receptor (ER) and other nuclear hormone receptors to modulate transcription when bound to *cis*-acting hormone response elements in target genes. We have previously shown that four proteins, hsp70, protein disulfide isomerase (PDI) and two unknown proteins (p48 and p45), copurify with ER that has been isolated by site-specific DNA chromatography (BERE) and influence the interaction of ER with DNA *in vitro*. To better define the nature of these effects, we used filter binding and electrophoretic mobility shift assays to study the ability of these proteins to alter the kinetics of ER–DNA interaction and to influence the ability of ER to bend DNA when bound to an estrogen response element (ERE). The results of both assays indicate that ERE-purified ER, with its four associated proteins (hsp70, PDI, p48, p45), has a greater ability to bind to the vitellogenin A2 ERE than ER purified by estradiol–Sepharose chromatography in the absence (ESeph) or presence (EATP) of ATP, in which p48, p45 (ESeph) and hsp70 (EATP) are removed. Surprisingly, the rates of association and dissociation of ER and ERE were essentially the same for all three mixtures, suggesting that one or more ER-associated proteins, especially p45 and p48, may be required for ER to attain maximum DNA binding activity. In addition, circular permutation and phasing analyses demonstrated that the same ER-associated proteins produced higher order ER–DNA complexes that significantly increased the magnitude of DNA distortion, but did not alter the direction of the ER-induced bend of ERE-containing DNA fragments, which was toward the major groove of the DNA helix. These results suggest that p45 and/or p48 and possibly hsp70, play an important role both in the specific DNA binding and bending activities of ER and thus contribute to the overall stimulation of transcription in target genes that contain *cis*-acting EREs.

J. Steroid Biochem. Molec. Biol., Vol. 63, No. 1–3, pp. 59–73, 1997

INTRODUCTION

The estrogen receptor (ER) is a member of the nuclear hormone receptor family of transcription factors. In addition to the steroid receptors, the superfamily includes receptors for thyroid hormone and vitamins such as retinoic acid and vitamin D. A number of other orphan nuclear receptors, whose ligands have yet to be identified, have been described as well [1]. For ER, as well as other steroid receptors, binding of ligand results in activation of the receptor, a process that includes conformational changes, post-translational modifications and changes in receptor–protein interactions. These changes enable the receptor to bind with high affinity to *cis*-acting hormone response elements (HREs), typically positioned upstream of hormone-responsive genes. Once bound

Current address: Program in Molecular Medicine, University of Massachusetts, Worcester, MA 01605, U.S.A.
*Correspondence to G. L. Greene. Tel: (773) 702 6964; Fax: (773) 702 6260; e-mail: ggreene@ben-may.bsd.uchicago.edu.
Received 8 Jan. 1997; accepted 9 Jun. 1997.

to these sites, the activated receptor modulates the rate of transcription of responsive genes.

Although much has been learned about the behavior of ER functional domains and the nature of target DNA sequences, the molecular details of ER-mediated transcriptional regulation remain unclear. It is possible that ER enhances the formation of an RNA polymerase II preinitiation complex by stabilizing or recruiting the assembly of a template-committed complex of transcription factors. For progesterone receptor (PR), such a stablized complex is postulated to be poised for rapid initiation of transcription by the polymerase and includes multiple factors other than receptor, such as TFIID, IIA, IIB and IIE/F [2]. The precise roles of each of these factors in the initiation process are only partially understood. What is clear, however, is that steroid receptors do not act in isolation, but rather in concert with various receptor-associated proteins.

The identities and functions of receptor-associated proteins are only beginning to emerge. Steroid receptors can interact with other transcription activators (*e.g.* AP-1) [3] as well as various co-regulators (*e.g.* CBP and SRC-1) [4–6] and members of the basal transcription apparatus. For example, the basal transcription factor TFIIB interacts with both the progesterone and estrogen receptors *in vitro* [7]. Furthermore, as measured by an *in vitro* assay, TFIIB was able to stimulate receptor-mediated transcriptional activation, suggesting that interaction of the receptors with TFIIB may be a critical component to receptor-mediated activation. Still other reports suggest that nuclear accessory factors or coactivators are needed for receptor-mediated transactivation. A 55-kDa nuclear accessory factor (NAF) appears to be essential for maximal binding of the vitamin-D receptor to the vitamin-D response element from the human osteocalcin promoter [8]. Similarly, a 65-kDa factor termed triiodothyronine receptor-auxiliary protein (TRAP), which exhibits limited independent DNA binding, enhances thyroid receptor binding to DNA [9]. The non-histone high mobility group chromatin protein, HMG-1, can substitute for an unidentified factor present in partially purified PR fractions and is responsible for promoting PR–DNA binding [10]. More recent studies have identified a protein, Trip-1 (thyroid hormone receptor interacting protein), that interacts with both thyroid hormone receptor (TR) and retinoic-X receptor (RXR) in a ligand-dependent fashion [11]. Trip1 has significant homology with the yeast transcriptional mediator Sug1. Significantly, Trip1 can functionally substitute for Sug1 in yeast, and both proteins interact *in vitro* with the thyroid hormone receptor.

Identification of proteins that associate with activated ER has been the focus of many recent investigations. TIF1 was identified as a protein which stimulated RXR transcriptional activity in yeast and was subsequently shown to potentiate ER activity as well [12]. Another study identified a 45-kDa single-strand DNA-binding protein (DNA-binding stimulatory factor; DBSF) that stimulated the interaction of purified ER with an estrogen response element (ERE) *in vitro* [13]. Biochemical analysis recently revealed a 160-kDa ER-associated protein (ERAP160) that exhibits estradiol-dependent binding to the receptor [14]. Significantly, mutational analysis of the receptor demonstrated that its ability to activate transcription paralleled its ability to bind ERAP160. Furthermore, antiestrogens were unable to promote ERAP160 binding and could block the estrogen-dependent association in a dose-dependent manner. In a similar study, another set of ER-associated proteins (receptor-interacting proteins; RIPs) were identified by two *in vitro* techniques, GST pull-down assay and far-Western blotting [15]. The far-Western technique identified three RIPs with molecular masses of 160, 140 and 80 kDa. The GST pull-down assay failed to detect RIP140 and RIP80, but did detect RIP160 as well as two additional RIPs with molecular weights of 100 and 50 kDa. Importantly, these interactions were only observed with the transcriptionally active, estrogen-occupied ER and were abolished by antiestrogens. It is thought that these proteins may contribute to hormone-dependent transcriptional activation by ER. A recent study suggests that CREB binding protein (CBP) may represent a common, limiting factor that integrates the transcriptional activities of nuclear receptors by interacting with both receptor and SRC-1, p160 and p140 co-activators [4]. In addition, we have previously described four proteins, including hsp70, protein disulfide isomerase (PDI), and two unknown proteins (p48 and p45), that copurify with ER using three chromatographic techniques [16]. Gel shift experiments demonstrated that these ER-associated proteins influenced the ER–ERE interaction [16]. Thus, while a number of receptor-associated proteins have been identified, the mechanisms by which these proteins alter ER activity *in vivo* is still unknown.

Because many prokaryotic and eukaryotic transcription factors alter DNA structure upon binding to their recognition sequences [17–22], it has been proposed that DNA distortion and bending may be involved in transcription activation. Several members of the nuclear receptor superfamily including estrogen, progesterone, thyroid, retinoid X and glucocorticoid receptors and the orphan receptor RORα induce conformational changes in DNA structure upon binding to their cognate recognition sequences [23–29]. The TATA binding protein, which is instrumental in forming the basal transcription initiation complex, also induces a sharp bend in DNA [30].

Evidence to support a role for DNA bending in transcription activation includes the observation that intrinsically bent DNA can replace a protein binding site in the promoter and mediate either repression or

activation of transcription in a number of systems [31–34]. The ER DNA-binding domain, which is less effective in activating transcription than full length ER, binds specifically to the ERE and induces a 34° distortion angle in ERE-containing DNA fragments [26]. The full-length human ER, when expressed in yeast, MCF-7, or COS cells, induces a significantly larger 56–65° distortion angle [34,35]. Thus, there appears to be a relationship between the magnitude of DNA bending and transcription activation. Because these earlier experiments with the full-length ER utilized a complex array of cellular proteins in addition to the receptor, it was of interest to examine the ER–ERE interaction using more highly purified ER preparations to determine if ER-associated proteins influence ER-induced DNA distortion and/or bending.

In this study, extracts from CHO–ER cells [36], which express high levels of human ER, were used as a source of affinity purified ER to examine the effects of several associated proteins (hsp70, PDI, p45, p48) on ER–ERE interactions in filter binding and electrophoretic mobility shift assays. Surprisingly, we find that one or more of these proteins influences the absolute ability of purified ER to interact with ERE, but not the rate of association or dissociation of ER and ERE. In addition, the same ER-associated proteins significantly influence the magnitude, but not the direction, of ER-induced bending of ERE-containing DNA fragments. Higher order ER–ERE–protein complexes displayed distortion angles as high as 97°, compared to 62–66° for the smaller and more abundant ER–ERE complexes normally observed. Our results suggest that one or more ER-associated proteins may play an important role in both the DNA binding and bending activities of ER and thus contribute to the overall transcriptional stimulation of target genes.

MATERIALS AND METHODS

Culture of mammalian cells

CHO-ER cells [36] were cultured in Dulbecco's Modified Eagle Medium/Ham F-12 Nutrient Mixture (1:1; Sigma, St. Louis, MO) without phenol red (Sigma) with 10% iron-supplemented newborn calf serum (Sigma) that did not require charcoal treatment, as previously described [16], 44 mM $NaHCO_3$, 1X antibiotic–antimycotic liquid (penicillin, streptomycin and amphotericin; Gibco BRL, Grand Island, NY) and 5 mg/l insulin. To maintain expression and selection of the ER gene, 50 μM $ZnSO_4$ and 40 μM $CdSO_4$ were also included in the medium.

Cell fractionation

For the preparation of whole cell and nuclear extracts, subconfluent cells were released from tissue culture vessels with a non-enzymatic cell dissociation solution (Sigma, St. Louis, MO). The releasing action was inactivated by the addition of serum-containing media. Cells were pelleted gently at $800 \times g$ for 5 min and washed three times with PBS. To prepare whole cell extracts, the cell pellet was resuspended in 4 volumes of ice cold extraction buffer (50 mM Tris, pH 7.9, 2 mM DTT, 400 mM NaCl (high salt buffer), 5 μg/ml aprotinin, 10 μg/ml leupeptin and 0.2 mM PEFABLOC). Cells were lysed in an ice bath with a dounce (type B pestle) homogenizer, pelleted at 4°C by centrifugation at $10\,000 \times g$ and the supernatant was frozen in aliquots and stored at −80°C. ER content was determined by the controlled-pore glass bead (CPG) assay as previously described [16,37,38] following treatment of the extract with excess [6,7-^{3}H]estradiol (Amersham Life Sciences, Arlington Heights, IL).

To obtain nuclear ER, pelleted CHO-ER cells were resuspended in 10 volumes of PBS containing 10% glycerol and 60 nM [6,7-^{3}H]estradiol and incubated for 30 min at room temperature with rocking. Cells were pelleted and the procedure was repeated. The final cell pellet was resuspended in 4 volumes of 50 mM Tris, pH 7.9, 2 mM DTT (salt-free buffer) that contained a protease inhibitor cocktail. The cells were then lysed in an ice bath by dounce homogenization and the mixture was centrifuged for 30 min at $10\,000 \times g$ at 4°C. The crude nuclear pellet was resuspended in salt-free buffer and centrifuged again to remove residual cytosolic proteins. To extract the retained [6,7-^{3}H]estradiol–ER complex, the crude nuclear pellet was resuspended in four times the original packed cell volume of 50 mM Tris, pH 7.9, 2 mM DTT, 400 mM NaCl (high salt buffer) containing protease inhibitor cocktail and incubated for 60 min on ice with occasional dounce homogenization. The homogenate was centrifuged as before and the supernatant was collected as the nuclear fraction, which was further clarified by centrifugation for 30 min at $50\,000 \times g$ and stored at −80°C. The [6,7-^{3}H]estradiol–ER content in the nuclear fraction was determined by direct liquid scintillation counting and by specific adsorption to controlled pore glass beads (CPG) as described above.

Purification of hER from CHO-ER extracts

Estradiol–sepharose chromatography (ESeph and EATP). To obtain ESeph-purified proteins, 2.5 ml of CHO-ER whole cell extract, adjusted to contain 0.7 M NaCl and 1 M urea, was applied to a 200 μl estradiol–Sepharose column and incubated batchwise for 1 h at 4°C, as described previously [16]. The column was washed with 20 bed volumes each of loading buffer (20 mM Tris, pH 7.4, 1 mM EDTA, 1 mM DTT, 700 mM NaCl, 1 M urea) and the same buffer with 400 mM NaCl and 3 M urea. Bound ER was eluted with 2×10^{-5} M [6,7-^{3}H]estradiol in a buffer that contained 20 mM Tris, pH 7.4, 1 mM EDTA,

1 mM DTT, 200 mM NaCl and 5 M urea. The yield of ER was determined by specific adsorption to controlled-pore glass beads. To obtain EATP-purified proteins, CHO-ER whole cell extract was treated with ATP prior to purification of hER by E-Seph chromatography, which significantly reduced the amount of associated hsp70, consistent with the reported behavior of hsp70 proteins [39].

DNA-affinity chromatography (BERE). To obtain BERE-purified proteins, 2.5 ml of CHO-ER whole cell extract was labeled with excess [6,7-^{3}H]estradiol for 1 h at 4°C and then dialyzed against a buffer containing 20 mM Tris, pH 7.4, 1 mM EDTA, 1 mM DTT, 100 mM NaCl and 1 M urea. The ER content in the extract was determined by CPG assay [16]. Excess biotinylated ERE was added to the extract at a ratio of 5 pmol of ERE to 1 pmol of ER along with 50 mg poly(dIdC) and 10 mg of the progesterone response element (PRE) (TGACTTGGTTTGGTACAAAATGTTCTGATCTG) from the MMTV long terminal repeat as carrier DNA. This mixture was incubated for 20 min at 22°C, followed by an additional incubation for 40 min at 4°C and applied to a 200 ml UltraAvidin-agarose column and incubated batchwise for 1 h at 4°C. The column was washed with 20 bed volumes of loading buffer (20 mM Tris, pH 7.4, 1 mM EDTA, 1 mM DTT, 100 mM NaCl, 1 M urea). Bound ER was eluted in a buffer containing 20 mM Tris, 1 mM EDTA, 1 mM DTT, 1 M NaCl, 1 M urea and quantitated by CPG assay as well as by direct counting in scintillation cocktail. When CHO-ER nuclear extracts were used, the procedure was the same as described except that incubation with [6,7-^{3}H]estradiol was not necessary since the cells were pre-labeled with [6,7-^{3}H]estradiol in culture.

Labeling of oligonucleotides for filter binding assays

Oligonucleotides (10 pmol) were end-labeled with [γ-^{32}P]-ATP as previously described [16]. Crude radiolabeled oligonucleotides were purified by electrophoresis on 9% polyacrylamide-bis (29:1) gels containing 0.045 M Tris-borate, 0.001 M EDTA, pH 8.0 (0.5× TBE). The desired double-stranded oligonucleotides were located by autoradiography, extracted from excised gel slices, precipitated from ethanol in the presence of 10 μg of tRNA (Sigma, St. Louis, MO) carrier and pelleted by centrifugation. The resulting pellets were washed with 70% ethanol, dried and resuspended in 10 mM Tris, pH 8.0 and 1.0 mM EDTA [16]. The specific activity of each labeled oligonucleotide was determined prior to purification by thin layer chromatography on polyethyleneimine-impregnated cellulose developed in 0.5 M KH_2PO_4, pH 3.4. The oligonucleotide remains at the origin, whereas ATP and inorganic phosphate migrate in the direction of the solvent front.

Nitrocellulose filter binding assay

In a 96-well microtiter plate, 30-μl reaction mixtures containing 1 μg poly(dIdC), 30 μg BSA, 20 mM Tris, pH 7.9, 1 mM DTT and 0.1 M NaCl were prepared. 30 fmol of ER were delivered from either a crude extract or a partially purified ER fraction and the plate was incubated on ice for 5 min. Specific competitor, when used, was added at this stage at the desired molar excess. The plate was then centrifuged briefly in a refrigerated table top centrifuge at 800 rpm to bring all liquid to the bottom of the well. While on ice, 120 fmol of ^{32}P-labeled ERE (37-mer; (AGCTTGTCCAAAGTCA**GGTCACAGTGACC**-**T**GATCAAA) derived from the vitellogenin A2 gene was added to the side of each well. The plate was again spun briefly to mix the probe with the reaction mixture. The reaction mixture was then incubated for 30 min at room temperature. A 96-well nitrocellulose multiscreen plate was prepared in a vacuum manifold (both from Millipore, Bedford, MA) by prewetting each well with 20 mM Tris, pH 7.9, 1 mM DTT, 0.1 M NaCl (washing buffer). 100 μl of washing buffer was left in each well for sample dispersion. Following the 30 min incubation, samples were transferred from the microtiter plate using a multichannel pipetman into the appropriate wells of the multiscreen plate. Once all samples were transferred, vacuum was applied to the manifold. All wells were then washed three times with 200 μl of washing buffer containing 0.01% NP-40. Once washing was complete, the vacuum was increased to dry the membranes. When dry, the multiscreen plate was removed from the manifold and 40 μl of scintillation fluor was added to each well. The plates were counted in a Packard Top Count microtiter plate scintillation counter.

Preparation of DNA fragments for electrophoretic assays

The circular permutation vector, ERE BendI [40], was digested with *Eco*RI, *Hin*dIII, *Eco*RV, *Nhe*I, or *Bam*HI to produce 427 bp fragments containing a consensus ERE at the 3′ end, an intermediate 3′ position, the middle, intermediate 5′ position, or at the 5′ end of the DNA fragment, respectively. ^{32}P-labeled DNA fragments were prepared as previously described [40]. All 427 basepair DNA fragments contained the same nucleotide sequence. The only difference in the fragments was the placement of the ERE.

For phasing analysis, the phasing vectors, ERE26, ERE28, ERE30, ERE32, ERE34 and ERE36 [34], each of which contained a consensus ERE separated from an intrinsic DNA bend by 26, 28, 30, 32, 34 or 36 basepairs, respectively, were digested with *Eco*RI and *Hin*dIII. The resulting 281–291 basepair DNA fragments were labeled with [γ^{32}P]-ATP as described [34]. DNA bending standards [22] were digested and labeled as previously described [34].

Circular permutation and phasing analysis electrophoretic assays

Gel mobility shift assays were carried out with BERE-, ESeph- and EATP-purified proteins. 250 fmol of BERE-purified proteins or 100 fmol of ESeph- or EATP-purified proteins were incubated with 1 μg poly (dI-dC), 10% glycerol, 8 mM KCl, 15 mM Tris, pH 7.9, 0.2 mM EDTA, pH 8.0 and 4 mM DTT at 4°C for 15 min. The reactions were then incubated at room temperature for 15 min with 10 000 cpm of the ^{32}P-labeled DNA fragment. Protein–DNA mixtures were fractionated on low ionic strength acrylamide gels [41] at 4°C with buffer recirculation. For supershift experiments, 240 ng of the ER-specific monoclonal antibody H222 was included in the binding reaction and the room temperature incubation was extended to 20 min. For competition assays, equimolar amounts of specific or nonspecific competitor were added to the initial binding reaction. 15.3 ng of a 30 bp annealed oligo containing a consensus ERE was used as the specific competitor. A 54 bp annealed oligo comprised of sequence from the *Xenopus laevis* vitellogenin B1 noncoding sequence was used as the nonspecific competitor.

Calculation of distortion and bending angles

A Molecular Dynamics phosphorimager and Image Quant software (Molecular Dynamics, Sunnyvale, CA) were utilized to determine the migration distance of each ER–DNA complex and free probe. The magnitude of the distortion angle (α_D) was determined by comparing the relative mobility of each ER–DNA complex with the relative mobilities of DNA bending standards [22] as previously described [26, 40]. The magnitude of a directed DNA bending angle (α_B) was determined using the empirical formula of Kerppola and Curran [40, 42]:

$$\tan(k\alpha_B/2) = \frac{A_{PH}/2}{\tan(k\alpha_C/2)}$$

where α_B is the ER-induced distortion angle, α_C is the intrinsic DNA bend angle, A_{PH} is the phasing amplitude and k is a coefficient used to adjust for electrophoretic conditions. By comparing the relative mobility of 5 sets of DNA bending standards with the known bend angles, a value of $k = 0.991$ was determined using the formula $\mu_M/\mu_E = \cos(k\alpha_D/2)$, where μ_M is the relative mobility of the ER–DNA complex when the ERE is in the middle of the DNA fragment and μ_E is the relative mobility of the ER–DNA complex when the ERE is at the end of the DNA fragment [22]. To determine if there were statistical differences in distortion and directed bending angles, determination of variance was followed by two-sample *t*-tests using Microsoft Excel.

RESULTS

Measurement of the rate of ER–ERE association

We first characterized the ER–ERE interaction using a nitrocellulose filter binding assay. The filter binding assay is a simple method of quantitating DNA bound to protein and is based on the ability of nitrocellulose to bind proteins but not double-stranded DNA. Free DNA will pass through the nitrocellulose filter while protein and any interacting DNA is retained. The use of radioactively labeled DNA allows one to quantitate the association and dissociation rates of the differentially purified ER preparations and to examine the specificity of the ER–ERE interaction. ER and various associated proteins were purified from high salt extracts of CHO-ER cells by specific adsorption of ER to Sepharose-bound estradiol (ESeph, EATP) or biotinylated vitellogenin A2 ERE (BERE), as described previously [16, 43] and summarized in Table 1. The association rate of the vitellogenin A2 ERE with each ER mixture was measured by analyzing the DNA binding reaction at time points from 0–30 min following the addition of [^{32}P]ERE (Fig. 1). As observed previously, the amount of ER–DNA complex formed in the presence of excess unlabeled ERE was significantly greater for the BERE-purified proteins (hsp70/hER/PDI/p48/p45) than for either the ESeph- (hsp70/hER/PDI) or EATP- (hER/PDI) purified proteins. In addition, it appeared that under these experimental conditions, maximal ER–ERE binding occurred by 10 min for all mixtures. Although the initial rates of association, reflected by the slopes of the curves prior to saturation, appeared to differ for each ER mixture, the large differences in the height of each curve (total binding) made a visual comparison difficult. Reduction of the incubation temperature to 4°C did not alter the profiles significantly (data not shown). Therefore Scatchard analyses as well as analyses of the rates of dissociation of each ER–ERE complex were performed to clarify this issue.

Table 1. *Summary and properties of ER-associated proteins isolated by different chromatographic techniques*

Source of ER[a]	Proteins present (kDa)[b]	Relative DNA binding
NE	total nuclear proteins	+ + + +
BERE	70, 66, 55, 48, 45	+ + + +
ESeph	70, 66, 55	++
EATP	66, 55	+

[a]Methods used to isolate ER from CHO-ER cells: nuclear extract (NE), site-specific DNA-affinity chromatography (BERE), estradiol–Sepharose affinity chromatography (ESeph) and estradiol–Sepharose affinity chromatography in the presence of ATP (EATP).

[b]The identity of the proteins indicated in the table are: 70 = hsp70; 66 = ER; 55 = PDI; 48 and 45 are unidentified. Adapted from Landel, Kushner and Greene [43].

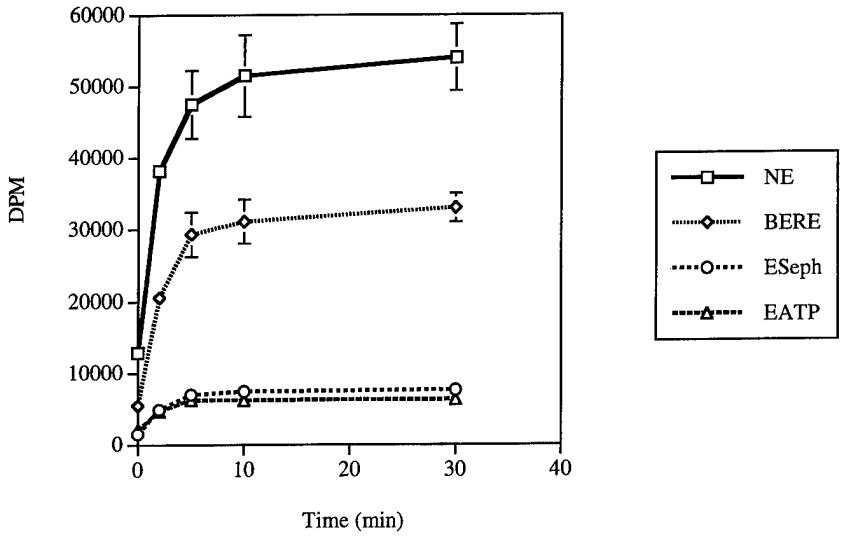

Fig. 1. Graph of the ER–ERE rate of association. ^{32}P-labeled vitellogenin A2 ERE (37-mer; 120 fmol; -AGGTCAcagTGACCT-) was added to partially purified ER complexes (30 fmol) and incubated at 25°C for 0–30 min. At the indicated time points, aliquots of the reaction mixture were removed. The samples were immediately applied to nitrocellulose filters and washed thoroughly to stop the reaction. The time course was performed with CHO-ER nuclear extract and BERE-, ESeph- and EATP-purified proteins.

Measurement of the rate of ER–ERE dissociation

A variation of the filter binding assay was used to measure the rate of ER–ERE dissociation. These experiments were performed by incubating CHO-ER nuclear extract or the BERE-, ESeph- or EATP-purified proteins with [^{32}P]ERE. After the reactions had reached equilibrium (30 min), they were diluted tenfold to quench the forward reaction. Subsequent to dilution, an aliquot of each reaction was removed and spotted onto nitrocellulose as the initial time point. Either TE control, ERE, mtERE (2 bp inversion in the second half of the palindrome: -AGGTCAcagTG**CA**CT-), or nonspecific PRE was then added to the reaction mixtures and time points were collected for 60 min. As shown in Fig. 2, no dissociation of ER from [^{32}P]ERE was observed in the absence (TE) or presence of PRE, whereas both mtERE and ERE were able to displace [^{32}P]ERE when present at a 200-fold molar excess. Notably, the dissociation rate profiles among the four ER mixtures were not significantly different within each competitor series (Fig. 2). Therefore, the ER-associated proteins do not appear to exert their influence on the rate of ER–ERE dissociation.

Partially purified ER protein complexes exhibit different binding capacities for the vitellogenin A2 ERE

To independently assess any differences in the capacities of ER/ERE interactions, equilibrium saturation binding studies were carried out with the BERE-, ESeph- and EATP-purified proteins. The experiments were performed by incubating fixed amounts (30 fmol) of the BERE-, ESeph- and EATP–purified ER complexes with increasing amounts of [^{32}P]ERE. The equilibrium binding constants were then determined by Scatchard analysis for each partially purified ER-containing fraction. As expected from the association and dissociation rate data, no significant differences in equilibrium dissociation constants (K_d=3–5 $\times$ 10^{-9} M) were observed among these complexes. Only the absolute ER-ERE binding capacities (B_{max}) were different, as shown in Fig. 3.

Effect of associated proteins on the ER–ERE interaction in the presence of competitor DNA

The filter binding assay was also used to examine the specificity of the interaction between the ER complexes and the ERE. These experiments were performed by incubating ER complexes with [^{32}P]ERE in the presence of three doses of either ERE, mtERE, or PRE competitor. For each competitor, the binding profiles for the BERE-, ESeph- and EATP-purified ER complexes, as well as ER in nuclear extracts, appeared to be virtually identical (Fig. 4), although a difference between the effectiveness of mtERE and ERE was readily apparent. From these data, we conclude that the specificity of the ER–ERE interaction was not altered by the associated proteins. This result contrasts with previously published gel shift data that appeared to show a greater sensitivity of the ESeph- and EATP-purified proteins to competition by the mtERE than the BERE-purified proteins [16]. However, these earlier experiments were performed under somewhat different binding conditions with only one dose (200-fold molar excess) of competitor. It is also possible that the gel shift assay is more strin-

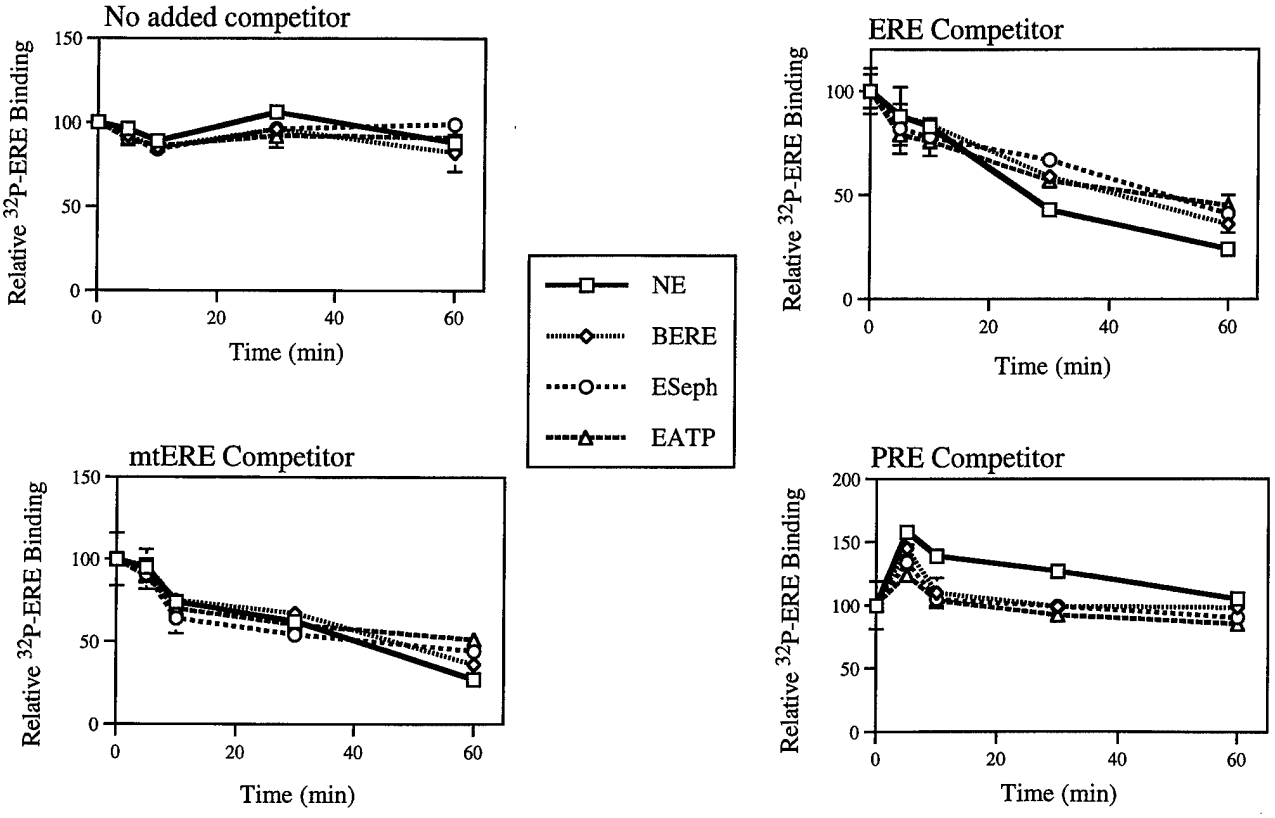

Fig. 2. Graph of the ER–ERE rate of dissociation. Partially purified ER complexes (30 fmol) were incubated for 30 min at 25°C with [^{32}P]ERE (120 fmol) to allow the ER–ERE complexes to reach equilibrium. The reaction mixtures were then diluted 10-fold to quench the forward reaction. At indicated time points following the addition of either TE (control) or a 200-fold molar excess of ERE, mtERE (-AGGTCAcagTGCACT-) or PRE, samples were applied to nitrocellulose filters and washed thoroughly. The time course was performed with CHO-ER nuclear extract and BERE-, ESeph- and EATP-purified proteins.

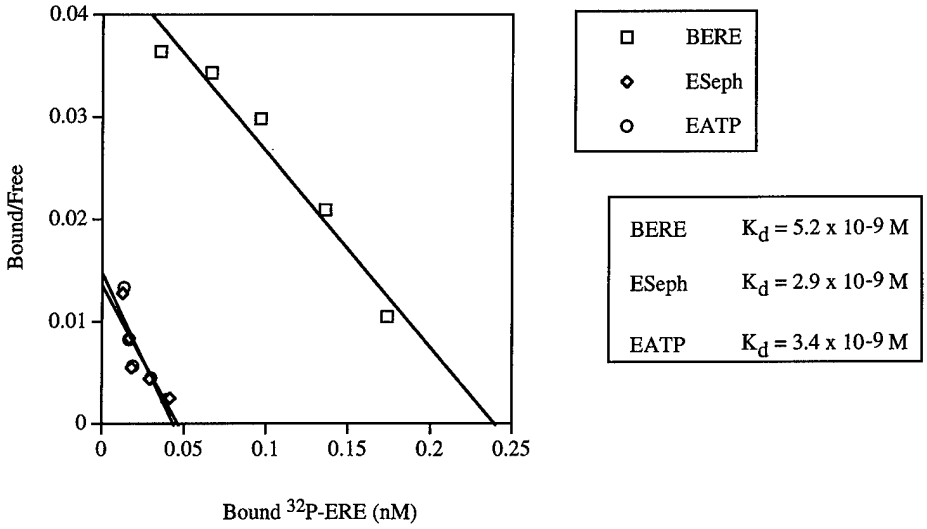

Fig. 3. Scatchard analysis of the [^{32}P]ERE binding affinity and capacity of three different ER complexes. ER complexes (30 fmol) were incubated for 30 min at 25°C with five different concentrations of [^{32}P]ERE (30–500 fmol). Each reaction was then applied directly to nitrocellulose filters and washed to stop the reaction and remove unbound [^{32}P]ERE. The negative reciprocal of the slope of each line was used to calculate the equilibrium dissociation constant (K_d). The analysis was performed with BERE-, ESeph- and EATP-purified proteins.

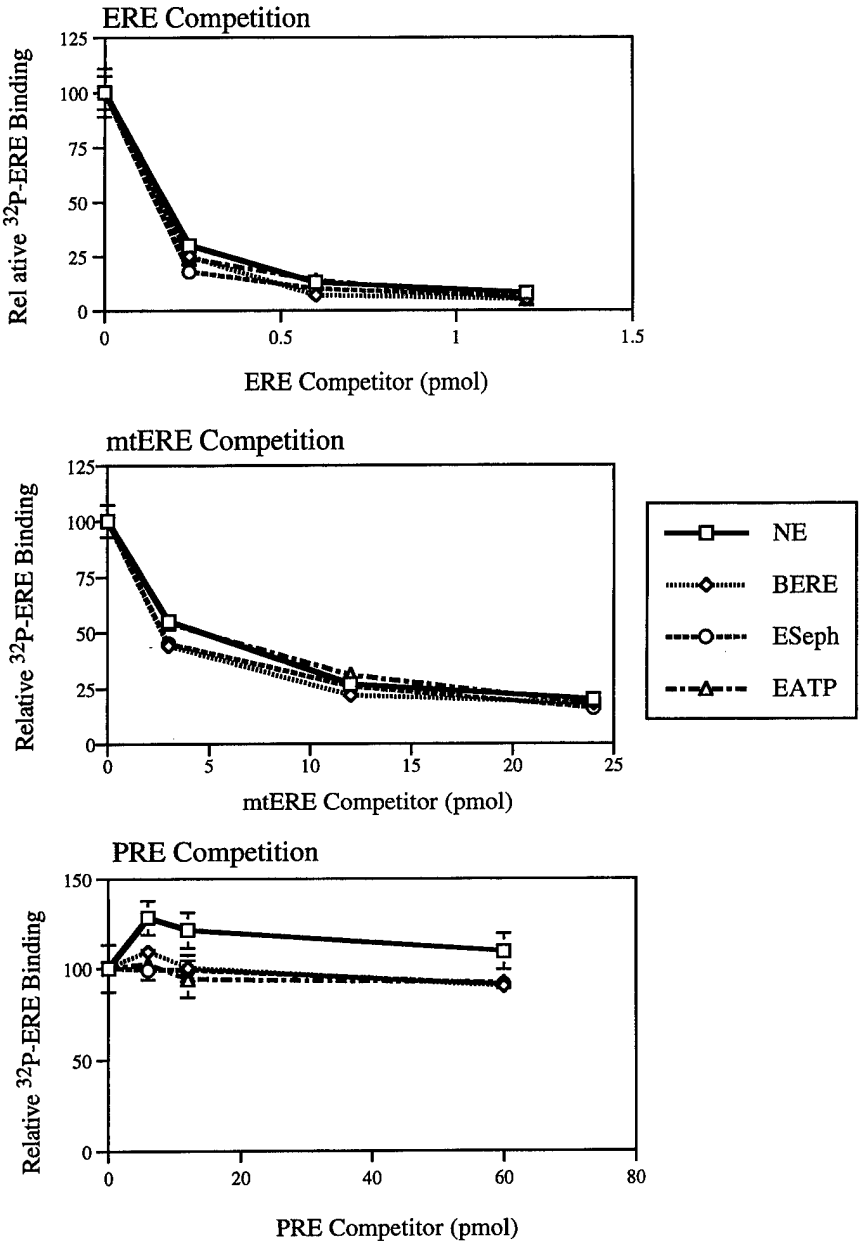

Fig. 4. Graph to assess the specificity of the ER–ERE interaction. Partially purified ER complexes (30 fmol) were incubated for 30 min at 25°C with [^{32}P]ERE (120 fmol) in the presence of three different doses of either ERE, mtERE or PRE. The samples were then applied to nitrocellulose filters and washed thoroughly. The analysis was performed with CHO-ER nuclear extract and BERE-, ESeph- and EATP-purified proteins.

gent than the filter binding assay and therefore facilitates the disruption of weaker ER–ERE complexes.

ER binds specifically to ERE-containing DNA fragments in gel mobility shift assays

Although the filter binding assays provided detailed information about the kinetics of ER association and dissociation with the ERE, they did not provide information about the composition of the ER–ERE complex. To determine if the different ER–ERE complexes varied in composition, BERE-, ESeph-, or EATP-purified proteins were incubated with 427 bp ^{32}P-labeled DNA fragments containing a consensus ERE. When the protein-DNA mixtures were fractionated on a low ionic strength, nondenaturing acrylamide gel, five ER–DNA complexes (1, 2, 3a, 3b and 4) were observed in the BERE-purified proteins and two ER–DNA complexes were observed (1 and 2) with the ESeph- and EATP-purified proteins (Fig. 5). Although complexes 3a and 3b were sometimes present in both the ESeph and EATP purified extracts, these complexes were consistently far less prominent than complexes 1 and 2. Antibody supershift experiments were performed to determine if the protein–

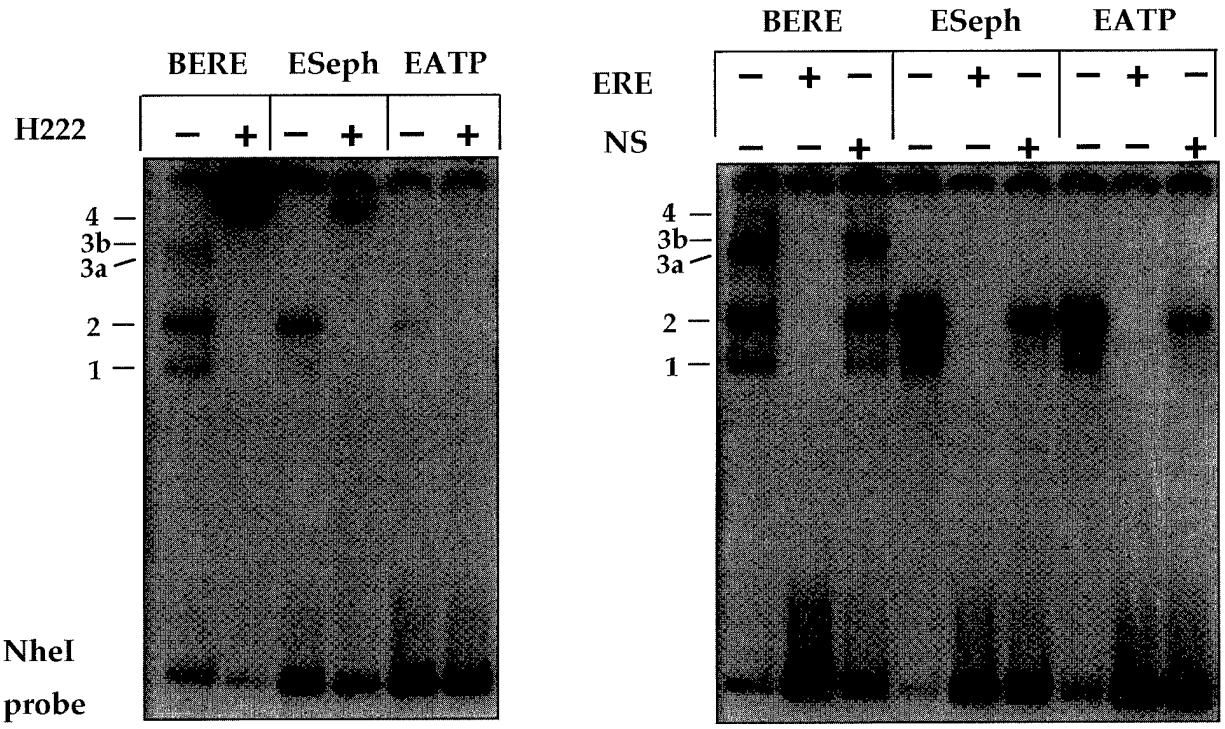

Fig. 5. BERE-, ESeph- or EATP-purified proteins interact specifically with ERE-containing DNA fragments. Nhe I cut ^{32}P-labeled DNA fragments were incubated with BERE-, ESeph- or EATP-purified proteins and then fractionated on a nondenaturing 8% acrylamide gel. The ER-specific monoclonal antibody H222 was included in the binding reaction as indicated (+H222). Binding reactions contained either no competitor DNA (–), a 100-fold excess of unlabeled ERE (ERE), or a 100-fold excess of unlabeled nonspecific DNA fragment (NS). ER–DNA complexes are identified by numbers at the left of each figure.

DNA complexes observed contained ER. When the ER-specific monoclonal antibody H222 was included in the binding reactions, the protein–DNA complexes were supershifted, indicating that ER-specific binding was occurring (Fig. 5).

Competition experiments were also carried out to determine if binding of the ER to the ERE-containing DNA fragments was specific. An oligo containing either the consensus ERE or a nonspecific DNA sequence was included in binding reactions. Although the ERE-containing oligo competed with the ^{32}P-labeled probe for ER binding (Fig. 5, panel B), the oligo containing a nonspecific DNA sequence failed to compete (Fig. 5, panel B, NS lanes). These data indicated that the 13 bp ERE present in the large ^{32}P-labeled DNA fragment was responsible for the ER–DNA complexes observed.

ER-induced distortion of ERE-containing fragments is influenced by additional proteins

We have previously demonstrated that human ER from transfected COS cell nuclear extracts, MCF-7 whole cell extracts, and partially purified yeast extracts induces 56–65° distortion angles in ERE-containing DNA fragments [34, 40, 44]. By using the more highly purified ER present in BERE-, ESeph- and EATP-purified mixtures, we were able to determine if the associated proteins (hsp70, PDI, p45 and p48) altered ER-induced distortion of DNA. Each DNA fragment used in these circular permutation assays contained a single consensus ERE located at various positions within the 427 bp fragment. Earlier studies demonstrated that a DNA fragment with a bend in the middle migrates more slowly on an acrylamide gel than a DNA fragment with a bend at the end [22]. Thus, by observing the migration of ER–DNA complexes formed with DNA fragments containing an ERE at the end or in the middle of the DNA fragment, it is possible to detect and quantitate the magnitude of the distortion induced by ER binding to ERE-containing DNA fragments. BERE-, ESeph- and EATP-purified proteins were incubated with ^{32}P-labeled DNA fragments containing an ERE at the end, at an intermediate position, or in the middle of the fragment. When the ERE was at the 3′ or 5′ end of the DNA fragment, the migration of the ER–DNA complex was more rapid (Fig. 6, RI and B, respectively) than when the ERE was at an intermediate 3′ or 5′ position (H and N, respectively). The ER–DNA complex with the slowest migration was formed with the DNA fragments containing an ERE in the middle (RV). This differential migration of the ER–DNA complexes indicates that ER binding caused distortion in the DNA fragments. The magnitude of the distortion was calculated by comparing the relative mobility of the ER–DNA complex with

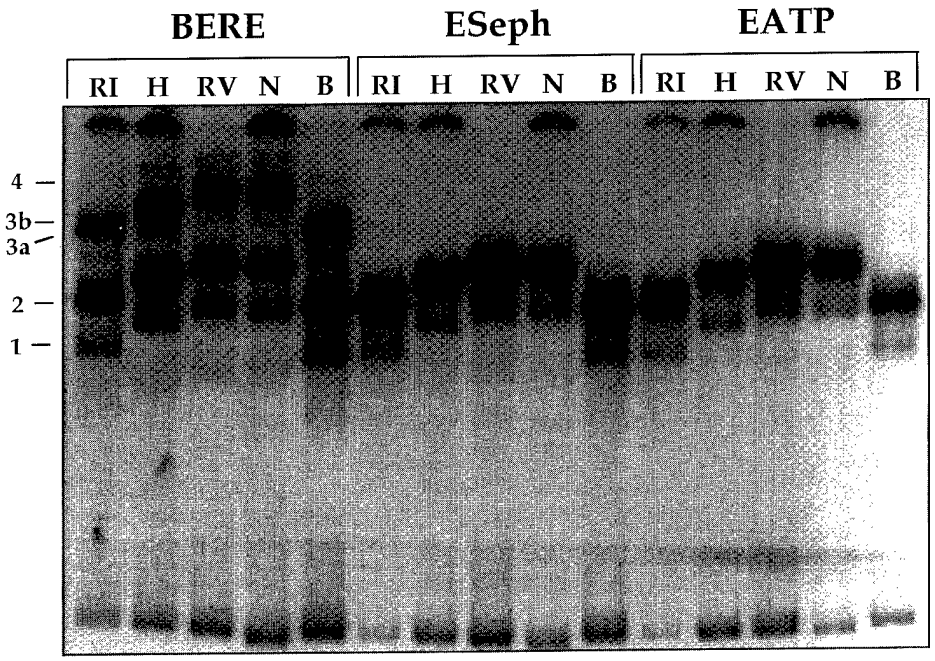

Fig. 6. Circular permutation analysis demonstrates that ER-associated proteins influence ER–DNA complex formation and distortion of ERE-containing DNA fragments. BERE-, ESeph- and EATP-purified proteins were incubated with 427 basepair ^{32}P-labeled DNA fragments that had been isolated from the circular permutation vector ERE Bend I[26] after digestion with *Eco*RI, *Hin*dIII, *Eco*RV, *Nhe*I or *Bam*HI (RI, H, RV, N and B) and end labeling with [γ^{32}P]ATP. The protein–DNA mixtures were fractionated on an 8% nondenaturing polyacrylamide gel. The gel was dried and radioactive bands were visualized by autoradiography. ER–DNA complexes are identified by numbers at the left of the figure.

the migration of DNA bending standards [22]. The results of several combined experiments are shown in Table 2. ER-purified proteins induced distortion angles of 62° and 66° in complexes 1 and 2, respectively. These two smaller ER–DNA complexes were observed with all three of the ER mixtures tested. Three higher order complexes were observed in the BERE-purified mixtures, which contain p48 and p45 in addition to the hsp70, ER and PDI (p55). Complexes 3a and 3b, which were always observed with the BERE-purified proteins, occasionally with the ESeph-purified proteins, but rarely with the EATP-purified proteins, displayed distortion angles of 75° and 93°, respectively. The largest distortion angle of 97° was observed only with the BERE-purified proteins (complex 4). No differences in the center of the bend were detected with any of the ER preparations.

Table 2. ER-induced distortion and bending angles

Purified ER	Complex	Distortion angle	Bend angle
BERE	1	62 ± 0.9 (5)	6.7 ± 0.1 (3)
	2	66 ± 0.6 (5)	7.0 ± 0.3 (3)
	3a	75 ± 1.9 (5)	6.5 ± 0.2 (3)
	3b	93 ± 1.6 (5)	12.2 ± 2.2 (3)
	4	97 ± 2.5 (5)	15.7 ± 2.3 (3)
ESeph	1	62 ± 0.9 (4)	5.7 ± 0.3 (4)
	2	65 ± 0.4 (4)	6.9 ± 0.3 (5)
EATP	1	62 ± 1.0 (5)	5.4 ± 0.6 (5)
	2	64 ± 0.5 (4)	6.0 ± 0.2 (5)

Distortion angles and directed bending angles induced by ER binding to ERE-containing DNA fragments were determined by circular permutation and phasing analysis, respectively. Values are reported as the mean + S.E. The number of individual determinations is indicated in parenthesis. The protein composition of each purified ER mixture is listed in Table 1.

ER-associated proteins influence the magnitude but not the direction of an ER-induced DNA bend

Phasing analysis was carried out to determine the direction of the DNA bends induced by ER in the BERE-, ESeph- and EATP-purified mixtures. This method uses DNA fragments that have an intrinsic DNA bend separated from a single consensus ERE by 26, 28, 30, 32, 34 or 36 nucleotides. The spacing between the intrinsic and ER-induced DNA bends is incrementally varied over one turn of the DNA helix so that there will be a point at which the two bends are out of phase and will have the effect of straightening the DNA fragment and a point at which the two bends will be in phase and form a larger overall bend. When the intrinsic and ER-induced DNA bends are in phase, the ER–DNA complex will be inhibited in its migration and when the DNA bends are out of phase, the ER–DNA complex will migrate more rapidly through an acrylamide matrix. By observing the migration of the DNA fragments containing an ERE separated from an intrinsic DNA bend by various increments, we can determine the direction of an ER-induced DNA bend.

^{32}P-labeled DNA fragments containing an ERE and an intrinsic DNA bend separated by 26–36 basepairs were incubated with BERE-, ESeph- and EATP-purified proteins and then separated on a nondenaturing acrylamide gel. With all three of the ER mixtures, the DNA fragments that contained 32 basepairs between the ERE and the intrinsic DNA bend migrated most rapidly through the acrylamide gel (Fig. 7). This 32 basepair separation places the ERE and the intrinsic DNA bend on the same side of the DNA helix and indicates that the bends are out of phase. Because the intrinsic DNA bend is toward the minor groove of the DNA helix, the ER-induced DNA bend must be directed toward the major groove of the DNA helix. These findings are consistent with previous phasing analysis experiments carried out with MCF-7 and COS expressed ER [34, 35].

Phasing analysis can also be used to determine the degree of directed DNA bending associated with ER binding to ERE-containing DNA fragments. Data from several phasing analysis experiments were combined and utilized to determine the degree of directed ER-induced DNA bending, as previously described [35]. All ER preparations contained complexes 1 and 2, which induced directed DNA bending angles of 5° to 7°. The BERE-purified proteins induced formation of complexes 3a, 3b and 4, which represented directed DNA bends of 7°, 12° and 16°.

DISCUSSION

We have used two complementary methods to examine the interaction of BERE-, ESeph- and EATP-purified ER complexes with the vitellogenin A2 ERE [45, 46]. Both filter binding (Figs 1–3) and electrophoretic mobility shift assays (Figs 5–7) indicate that BERE-purified ER, with its four associated proteins (hsp70, PDI, p48, p45), has a greater capacity for interaction with the vitellogenin A2 ERE than either ESeph- or EATP-purified ER, in which p48, p45 (ESeph) and hsp70 (EATP) are missing (Table 1). These findings are consistent with previously published gel shift experiments [16]. Filter binding analyses were performed to determine whether this differential binding was related to the association (Fig. 1) or dissociation (Fig. 2) rate of the ER–DNA complex or whether the absolute capacity of the ER and its associated proteins to bind to the ERE differed (Fig. 3). Analysis of the rates of association and dissociation for all three ER mixtures revealed no significant difference in these parameters, suggesting that the enhanced formation of the ER–DNA complex with BERE-purified proteins reflected the overall ability of ER and its associated proteins to bind to the ERE. Scatchard analysis demonstrated that the equilibrium ER–ERE dissociation constants (K_d=3–5 × 10^{-9} M) for BERE-ESeph- or EATP-purified proteins were not significantly different (Fig. 3).

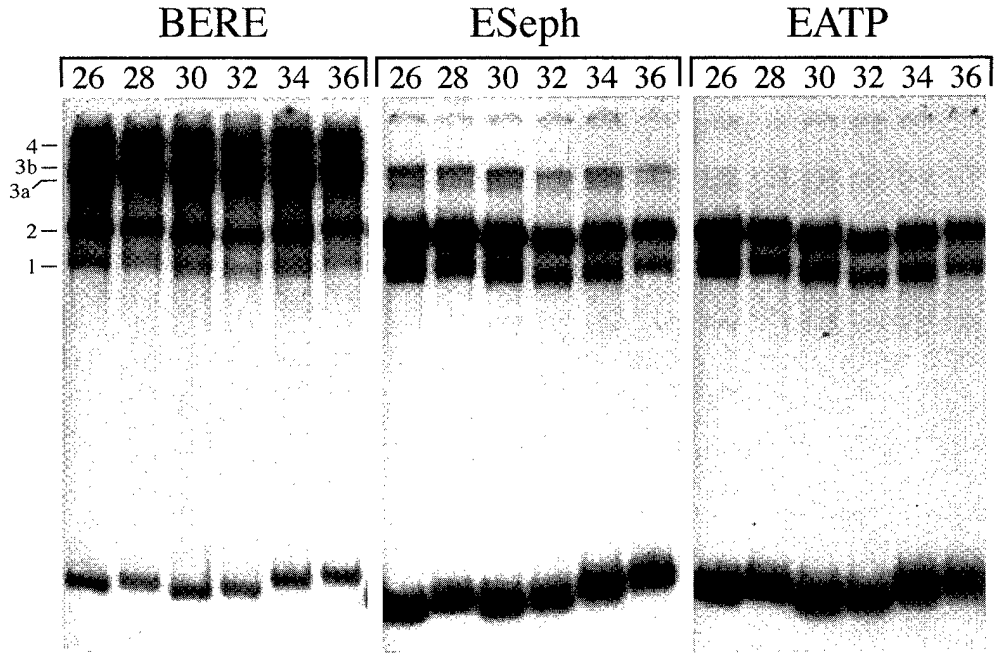

Fig. 7. Phasing analysis demonstrates that BERE-, ESeph- and EATP-purified proteins induce directed bends in ER-containing DNA fragments. BERE-, ESeph- and EATP-purified proteins were incubated with 281–291 basepair ^{32}P-labeled DNA fragments containing an intrinsic DNA bend separated from a consensus ERE by 26, 28, 30, 32, 34 or 36 basepairs. ER–DNA mixtures were fractionated on a nondenaturing acrylamide gel. The gel was dried and subjected to autoradiography. ER-DNA complexes are identified by numbers at the left of the figure.

Furthermore, the Scatchard analysis clearly identified an enhanced capacity of the BERE-purified ER mixture to interact with an ERE when compared to the ESeph- and EATP-purified proteins. These data suggest that one or more receptor-associated proteins may facilitate the conversion of ER from an inactive state (unable to bind ERE) to an active state (able to bind to the ERE), or perhaps stabilize the active state, independent from ligand binding activity.

The decreased binding of more highly purified receptors to their cognate recognition sequences has been reported by others [10, 13]. We have observed an inverse relationship between the number of ER-associated proteins present in the ER preparation and the ability of the receptor to interact with ERE. The most highly purified ER preparation, which contains only ER and PDI (EATP; Table 1), was the least able to form stable ER–DNA complexes. The presence of hsp70 (ESeph-purified proteins) increased ER–DNA complex formation. BERE-purified ER, which contains four detectable associated proteins (Table 1), afforded the most ER–DNA complex in the presence of excess ERE. Thus, similar to the DNA-binding stimulatory factor described by Mukherjee [13], ER-associated proteins, and especially p45 and p48, may promote absolute ER DNA-binding activity. Although we cannot rule out the possibility that denaturation contributes to the decreased ER activity of highly purified ER, our data strongly suggest that one or more of the proteins we have isolated contributes directly to the formation of ER complexes with enhanced affinity for ERE and increased bending. Our own previously published reconstitution experiments have confirmed that addition of p48/p45 and hsp70 to the EATP-purified ER can enhance the ER–ERE interaction [16]. Significantly, this process could not be mimicked by the addition of other proteins (e.g. albumin, insulin). As shown here and discussed below, these proteins appear to participate in the formation of higher order ER complexes with improved ERE binding and bending abilities, suggesting that these proteins do not simply renature defective ER molecules.

Although the DNA fragments used in circular permutation and phasing analysis experiments were different, the ER–DNA complexes observed were quite similar for both assays. While all three of the ER preparations (Table 1) formed complexes 1 and 2, only the BERE-purified proteins consistently formed complexes 3a and 3b and only BERE-purified proteins formed complex 4 (Figs 5–7). Thus, p45 and p48, which are present in the BERE preparations, but not in the ESeph or EATP preparations, may be instrumental in the consistent formation of complexes 3a and 3b and are absolutely required for the formation of complex 4. Complexes 3a and 3b are sometimes present in small amounts with ESeph-purified proteins, but are rarely observed with EATP-purified proteins. These findings suggest that hsp70, which is present in the ESeph preparation, but not in the EATP preparation, may be involved in the formation of complexes 3a and 3b, but that p45 and p48 are required to maintain these two higher order complexes. We have also observed higher order ER–ERE complexes with MCF-7 whole cell, nuclear and cytosolic extracts [34], indicating that similar complexes can form *in vivo*. Thus, both circular permutation and phasing analysis experiments indicate that the observed multiplicity of ER–DNA complexes reflects the population of associated proteins present in the different ER preparations. ER and PDI are involved in formation of complexes 1 and 2. Although hsp70 may be involved in forming Complex 3a and 3b, maintenance of complexes 3a, 3b and 4 requires the presence of p45 and p48. Interestingly, complexes 1 and 2 have the same mobility as two ER–DNA complexes formed with yeast-expressed ER, which was purified on an estradiol–sepharose column [44], suggesting that the ER may associate with similar proteins even though the cellular context is distinctly different. The number of ER–DNA complexes described here differs from an earlier study that used the same ER preparations, but a much smaller DNA probe, different gels and buffers, and different receptor:probe ratios [16]. However, the ability of the BERE-purified proteins to more readily form higher order complexes was observed in both studies.

Electrophoretic assays have been used to examine various characteristics of DNA structure. Circular permutation is typically used to detect regions of undirected, increased flexibility in DNA structure and phasing analysis is used to detect bends with a fixed spatial orientation [21]. We have used circular permutation analysis to determine whether ER-associated proteins might alter the magnitude of distortion induced by the binding of ER to ERE-containing DNA fragments. Complexes 1 and 2 induced distortion angles of 62° and 66°, respectively, in ERE-containing DNA fragments with all of the ER preparations utilized. These finding are in agreement with our previous determinations of the distortion angle induced by human ER isolated from yeast, MCF-7 and COS cells [34, 40, 44]. Complexes 3a, 3b and 4, which were most prominent when BERE-purified proteins were used, induced significantly larger distortion angles of 75°, 93° and 97°, respectively (Table 2). Thus, receptor-associated proteins were responsible for producing new, higher order ER–DNA complexes, which caused greater distortion in DNA structure. The ER-associated proteins did not, however, appear to alter the distortion angles of complexes 1 and 2.

Phasing analysis was utilized to examine the ability of ER-associated proteins to affect the magnitude and the direction of the ER-induced DNA bending. As

seen with the circular permutation experiments, the formation of higher order ER–DNA complexes caused an increase in the magnitude of the directed DNA bend (Table 2). However, the direction of the ER-induced DNA bend, which was toward the major groove of the DNA helix, was unaltered by the presence of the ER-associated proteins. Thus, both circular permutation and phasing analysis experiments support the idea that ER and its associated proteins promote the formation of higher order complexes (3a, 3b and 4) that induce greater distortion and directed bending angles in ERE-containing DNA fragments. The ER-induced DNA bend was directed toward the major groove of the DNA helix. This is the same orientation as ROR-, RXR- and PR-induced bends [23, 24, 47]. The observation that all nuclear receptor superfamily members examined to date induce DNA bends toward the major groove of the DNA helix may result from the homologous structure of these proteins.

The relationship between alterations in DNA structure and transcription activation is unclear. Because such a large number of transcription factors, including nuclear receptors, induce DNA to bend, it has been hypothesized that distortion or bending of DNA might facilitate the interaction of regulatory proteins with members of the basal transcription complex and thus be required for transcription activation [7, 23, 48]. ER-mediated transactivation probably requires a large repertoire of proteins to maintain function. Association of ER with one set of proteins may maintain the receptor in a quiescent state. The change in ER conformation induced by hormone binding may dissociate some of these proteins and recruit others. Likewise, interaction of ER with DNA, which induces conformational changes in the dimerization interface of the DNA binding domain [49], could initiate more global changes in ER structure and modulate receptor–protein associations. Therefore, we propose a model (Fig. 8) in which the unliganded ER is associated with PDI and hsp70, as well as hsp90, hsp56 and perhaps other as yet unidentified factors. Following ligand binding, hsp90 and hsp56 dissociate, while hsp70 and PDI remain associated with the 'activated' ER, although the hsp70 interaction is perhaps weakened [39]. The 'activated' ER complex then recruits or stabilizes the binding of at least two additional proteins, p45 and p48, when ER binds to an ERE, resulting in an increased ability of ER to bind ERE. The resulting change in DNA structure generated by the binding of this complex is likely to contribute to effective transcriptional stimulation. In this model, the ER that does not interact with the ERE dissociates from hsp70, thereby rendering it inactive. Additional proteins identified by other laboratories (e.g. TFIIB, p140, CBP/p300, SRC-1) may participate in one or more of these steps as well [4, 5, 7, 15]. Clearly, a better understanding of the role of p45 and/or p48 in ER action will require the separation and identification of these two proteins. In addition, the contribution of DNA bending to the formation and/or stabilization of an active transcription complex will ultimately be determined by a more detailed structural analysis of a functional transcription unit.

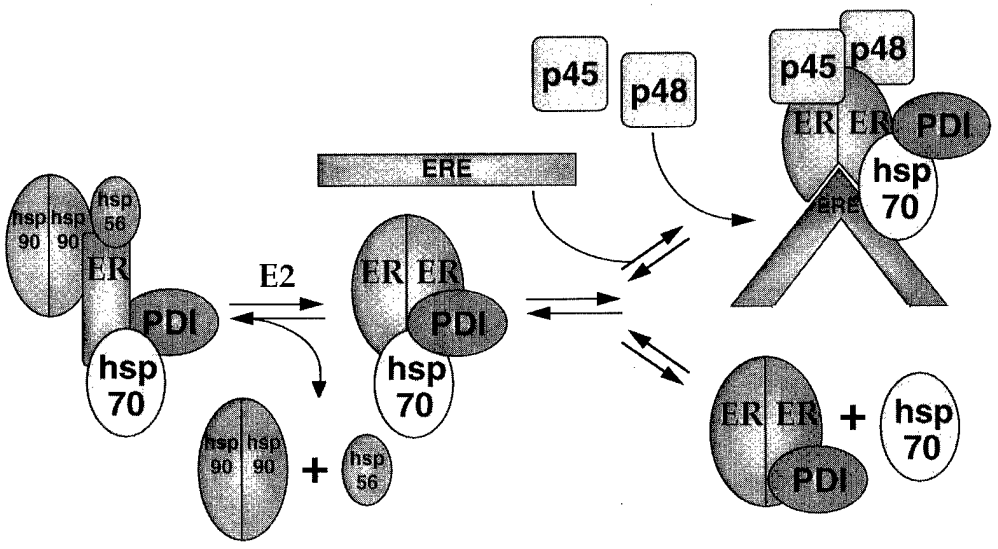

Fig. 8. Model of ER-associated proteins. This model is based on our current results as well as some additional data reported by others for ER. The model depicts the hormone dependent dissociation of hsp90, as well as significant conformational changes associated with hormone binding, dimerization and DNA binding. Further dissociation of ER-associated proteins can occur in the presence of estradiol, namely loss of hsp70. However, in the presence of an ERE, both PDI and hsp70 are retained. Significantly, the presence of p45 and p48 appear to be necessary for high capacity ER–ERE interaction. The contact sites between ER and p45, p48, PDI and hsp70 are unknown, as are the true stoichiometric relationships among the proteins present in the complexes depicted.

Acknowledgements—We gratefully acknowledge Adito Rao, Chris Hospelhorn and Lin Cheng for excellent technical assistance and Marsha Rosner for providing helpful comments during the preparation of this manuscript. We also thank Pat Fields for assistance in the use of the Packard Top Count microtiter plate scintillation counter. This work was supported in part by U.S. Army Medical and Research Materiel Command grant DAMD 17-94-J-4228 (G. L. G. and C. C. L.), Cancer Center Support Grant P30 CA-14599 from the NCI (G. L. G. and C. C. L.) and NIH HD21399 (A. M. N.).

REFERENCES

1. Parker M. G., Mechanisms of action of steroid receptors in the regulation of gene transcription. *J. Reprod. Fert.* **88** (1990) 717–720.
2. Klein-Hitpass L., Tsai S., Weigel N., Allan G., Riley D., Rodriguez R., Schraeder W., Tsai M. and O'Malley B., The progesterone receptor stimulates cell-free transcription by enhancing the formation of a stable preinitiation complex. *Cell* **60** (1990) 247–257.
3. Pfahl M., Nuclear receptor/AP-1 interaction. *Endocr. Rev.* **14** (1993) 651–658.
4. Kamei Y., Xu L., Heinzel T., Torchia J., Kurokawa R., Gloss B., Lin S.-C., Heyman R. A., Rose D. W., Glass C. K. and Rosenfeld M. G., A CBP integrator complex mediates transcriptional activation and AP-1 inhibition by nuclear receptors. *Cell* **85** (1996) 403–414.
5. Onate S. A., Tsai S. Y., Tsai M. J. and O'Malley B. W., Sequence and characterization of a coactivator for the steroid hormone receptor superfamily. *Science* **270** (1995) 1354–1357.
6. Horwitz K., Jackson T., Bain D., Richer J., Takimoto G. and Tung L., Nuclear receptor coactivators and corepressors. *Mol. Endocrinol.* **10** (1996) 1167–1177.
7. Ing N., Beekman J., Tsai S., Tsai M.-J. and O'Malley B., Members of the steroid hormone receptor superfamily interact with TFIIB (S300-II). *J. Biol. Chem.* **267** (1992) 17617–17623.
8. Sone T., Ozono K. and Pike W. J., A 55-kDa accessory factor facilitates vitamin D receptor DNA binding. *Mol. Endocrinol.* **5** (1991) 1578–1586.
9. Darling D., Beebe J., Burnside J., Winslow E. and Chin W., 3,5,3′-triiodothyronine (T_3) receptor-auxiliary protein (TRAP) binds DNA and forms heterodimers with the T_3 receptor. *Mol. Endocrinol.* **5** (1991) 73–93.
10. Prendergast P., Onate S., Christensen K. and Edwards D., Nuclear accessory factors enhance the binding of progesterone receptor to specific target DNA. *J. Steroid Biochem. Molec. Biol.* **48** (1994) 1–13.
11. Lee J. W., Ryan F., Swaffield J. C., Johnston S. A. and Moore D. D., Interaction of thyroid-hormone receptor with a conserved transcriptional mediator. *Nature* **374** (1995) 91–93.
12. Le Douarin B., Zechel C., Garnier J.-M., Lutz Y., Tora L., Pierrat B., Heery D., Gronemeyer H., Chambon P. and Losson R., The N-terminal part of TIF1, a putative mediator of the ligand-dependent activation function (AF-2) of nuclear receptors, is fused to B-raf in the oncogenic proteins T18. *EMBO J.* **14** (1995) 2020–2033.
13. Mukherjee R. and Chambon P., A single-stranded DNA-binding protein promotes the binding of the purified oestrogen receptor to its responsive element. *Nucl. Acids Res.* **18** (1990) 5713–5716.
14. Halachmi S., Marden E., Martin G., MacKay H., Abbondanza C. and Brown M., Estrogen receptor-associated proteins: Possible mediators of hormone-induced transcription. *Science* **264** (1994) 1455–1458.
15. Cavailles V., Dauvois S., Danielian P. S. and Parker M. G., Interaction of proteins with transcriptionally active estrogen receptors. *Proc. Natl. Acad. Sci. USA* **91** (1994) 10009–10013.
16. Landel C., Kushner P. and Greene G., The interaction of the human estrogen receptor with DNA is modulated by receptor-associated proteins. *Mol. Endocrinol.* **8** (1994) 1407–1419.
17. Gartenberg M. R. and Crothers D. M., DNA sequence determinants of CAP-induced bending and protein binding affinity. *Nature* **333** (1988) 824–831.
18. Shuey D. J. and Parker C. S., Bending of promoter DNA on binding of heat shock transcription factor. *Nature* **323** (1986) 509–513.
19. Verrijzer C. P., van Oosterhout J. A. W. M., van Weperen W. W. and van der Vliet P. C., Pou proteins bend DNA via the Pou-specific domain. *EMBO J.* **10** (1991) 3007–3014.
20. Vignais M. L. and Sentenac A., Asymmetric DNA bending induced by the yeast multifunctional factor TUF. *J. Biol. Chem.* **264** (1989) 8463–8466.
21. Kerppola T. and Curran T., Fos-Jun heterodimers and Jun homodimers bend DNA inopposite orientations: Implications for transcription factor cooperativity. *Cell* **66** (1991) 317–326.
22. Thompson J. and Landy A., Empirical estimation of protein-induced DNA bending angles: Applications to λ site-specific recombination complexes. *Nucl. Acids Res.* **16** (1988) 9687–9705.
23. McBroom L., Flock G. and Giguere V., The nonconserved hinge region and distinct amino-terminal domains of the RORα orphan nuclear receptor isoforms are required for proper DNA bending and RORα-DNA interactions. *Mol. Cell. Biol.* **15** (1995) 796–808.
24. Lu S., Eberhardt N. and Pfahl M., DNA bending by retinoid X receptor-containing retinoid and thyroid hormone receptor complexes. *Mol. Cell. Biol.* **13** (1993) 6509–6519.
25. Sabbah M., Estrogen receptor-induced bending of the Xenopus vitellogenin A2 gene hormone response element. *Biochem. Biophys. Res. Commun.* **185** (1992) 944–952.
26. Nardulli A. M. and Shapiro D. J., Binding of the estrogen receptor DNA binding domain to the estrogen response element induces DNA bending. *Mol. Cell. Biol.* **12** (1992) 2037–2042.
27. Petz, L., Nardulli, A., Kim, J., Horwitz, K., Freedman, L., Shapiro, D. DNA bending is induced by binding of the glucocorticoid receptor DNA binding domain and progesterone receptor to their response element. *J. Steroid Biochem. Molec. Biol.* **60** (1997) 31–41.
28. Leidig F., Apriletti J., Baxter J. and Eberhardt N., Thyroid hormone receptors induce DNA bending: Potential importance for receptor action (Abstr.). *Clin. Res.* **38** (1990) 474A.
29. King I., Thyroid hormone receptor-induced bending of specific DNA sequences is modified by an accessory factor. *J. Biol. Chem.* **268** (1993) 495–501.
30. Kim Y., Geiger J., Hahn S. and Sigler P., Crystal structure of a yeast TBP/TATA-box complex. *Nature* **365** (1993) 512–520.
31. Perez-Martin J. and Espinosa M., Protein-induced bending as a transcriptional switch. *Science* **260** (1993) 805–807.
32. Rojo F. and Salas M., A DNA curvature can substitute phage ϕ29 regulatory protein p4 when acting as a transcriptional repressor. *EMBO J.* **10** (1991) 3429–3438.
33. Bracco L.*et al.*, Synthetic curved DNA sequences can act as transcriptional activators in *Escherichia coli*. *EMBO J.* **8** (1989) 4289–4296.
34. Nardulli A. M., Grobner C. and Cotter D., Estrogen receptor-induced DNA bending: Orientation of the bend and replacement of an estrogen response element with an intrinsic DNA bending sequence. *Mol. Endocrinol.* **9** (1995) 1064–1076.
35. Potthoff S., Romine L. and Nardulli A., Effects of wild type and mutant estrogen receptors on DNA flexibility, DNA bending and transcription activation. *Mol. Endocrinol.* **10** (1996) 1095–1106.
36. Kushner P., Hort E., Shine J., Baxter J. and Greene G., Construction of cell lines that express high levels of the human estrogen receptor and are killed by estrogens. *Mol. Endocrinol.* **4** (1990) 1465–1473.
37. Gormley G., Hospelhorn V., Khan M. and Jensen E., A controlled pore glass bead assay for the measurement of cytoplasmic and nuclear glucocorticoid receptors. *J. Steroid Biochem. Molec. Biol.* **22** (1985) 693–698.
38. Greene G., Harris K., Bova R., Kinders R., Moore B. and Nolan C., Purification of T47D human progesterone receptor and immunochemical characterization with monoclonal antibodies. *Mol. Endocrinol.* **2** (1988) 714–726.
39. Kost S., Smith D., Sullivan W., Welch W. J. and Toft D., Binding of heat shock proteins to the avian progesterone receptor. *Mol. Cell. Biol.* **9** (1989) 3829–3838.

40. Nardulli A., Greene G. and Shapiro D., Human estrogen receptor bound to an estrogen response element bends DNA. *Mol. Endocrinol.* 7 (1993) 331–340.
41. Chodosh, L., Mobility shift DNA-binding assay using gel electrophoresis. In *Current Protocols in Molecular Biology*, ed F. Ausubel. Greene Publishing Associates and Wiley Interscience, New York, 1989, pp. 12.2.1–12.2.10.
42. Kerppola T. and Curran T., DNA bending by Fos and Jun: The flexible hinge model. *Science* **254** (1991) 1210–1214.
43. Landel C., Kushner P. and Greene G., Estrogen receptor accessory proteins: Effects on receptor–DNA interactions. *Environ. Health Perspect.* **103** (1995) 23–28.
44. Nardulli A., Romine L., Carpo C., Greene G. and Rainish B., Estrogen receptor affinity and location of consensus and imperfect estrogen response elements influence transcription activation of simplified promoters. *Mol. Endocrinol.* **10** (1996) 694–704.
45. Klein-Hitpass L., Tsai S., Greene G., Clark J., Tsai M. and OMalley B., Specific binding of estrogen receptor to the estrogen response element. *Mol. Cell. Biol.* **9** (1989) 43–49.
46. Klein-Hitpass L., Ryffel G. U., Heitlinger E. and Cato A. C. B., A 13 bp palindrome is a functional estrogen responsive element and interacts specifically with estrogen receptor. *Nucl. Acids Res.* **16** (1988) 647–663.
47. Prendergast P., Pan Z. and Edwards D., Progesterone receptor-induced bending of its target DNA: Distinct effects of the A and B receptor forms. *Mol. Endocrinol.* **10** (1996) 393–407.
48. Jacq X., Brou C., Lutz Y., Davidson I., Chambon P. and Tora L., Human TAFII30 is present in a distinct TFIID complex and is required for transcriptional activation by the estrogen receptor. *Cell* **79** (1994) 107–117.
49. Schwabe J., Neuhaus D. and Rhodes D., Solution structure of the DNA-binding domain of the oestrogen receptor. *Nature* **348** (1990) 458–461.

MOLECULAR AND CELLULAR BIOLOGY, Apr. 1998, p. 1927–1934
0270-7306/98/$04.00+0

Vol. 18, No. 4

Estrogen Response Elements Function as Allosteric Modulators of Estrogen Receptor Conformation

JENNIFER R. WOOD,[1] GEOFFREY L. GREENE,[2] AND ANN M. NARDULLI[1]*

Department of Molecular and Integrative Physiology, University of Illinois, Urbana, Illinois 61801,[1] and Ben May Institute, University of Chicago, Chicago, Illinois 60637[2]

Received 23 June 1997/Returned for modification 8 August 1997/Accepted 29 December 1997

The estrogen receptor (ER) is a ligand-dependent transcription factor that regulates the expression of estrogen-responsive genes. ER-mediated transcriptional changes are brought about by interaction of the ER with the estrogen response element (ERE). In this study, we examined the interaction of the *Xenopus laevis* ER DNA binding domain (DBD) and the intact ER with the *X. laevis* vitellogenin A2 ERE and the human pS2 ERE. Using gel mobility shift, DNase I footprinting, and methylation interference assays, we demonstrated that the DBD bound only as a dimer to the A2 ERE. However, the DBD bound as a monomer to the consensus pS2 ERE half site at lower DBD concentrations and then as a homodimer to the consensus and imperfect pS2 ERE half site at higher DBD concentrations. Antibody supershift experiments carried out with partially purified, yeast-expressed full-length ER demonstrated that three ER-specific antibodies interacted differentially with A2 and pS2 ERE-bound ER, indicating that receptor epitopes were differentially exposed. Furthermore, partial digestion of the A2 and pS2 ERE-bound ER with chymotrypsin or trypsin produced distinct protease cleavage patterns. Taken together, these data provide evidence that differential interaction of the DBD with the A2 and pS2 EREs brings about global changes in ER conformation. The conformational changes in ER induced by individual ERE sequences could lead to association of the receptor with different transcription factors and assist in the differential modulation of estrogen-responsive genes in target cells.

Estrogen is a hormone of central importance in regulating the development, growth, and maintenance of reproductive tissues. Estrogen's actions are mediated by the intracellular estrogen receptor (ER), which interacts with estrogen response elements (EREs) present in target genes to bring about changes in transcription. Although the ER-ERE interaction plays a crucial role in regulating gene expression, the mechanisms by which this interaction leads to changes in transcription are unclear.

A number of thermodynamic and structural studies have demonstrated that specific contacts between protein and DNA are often accompanied by conformational changes in protein, DNA, or both (1, 9, 31, 39, 42, 48). These findings have led to the hypothesis that DNA can act as an allosteric modulator of protein conformation in a number of different systems (9, 39). For example, basic regions of leucine zipper proteins are poorly ordered in solution but are induced to form α-helical structures upon binding to DNA (31, 43). Nuclear factor NF-κB p50 subunits form chymotrypsin-resistant homodimers that serve as powerful transcriptional activators when bound to some recognition sequences (10). However, when bound to other recognition sequences, the same p50 subunits are degraded by chymotrypsin and are poor transcription activators. This differential sensitivity to protease digestion implies that homodimer conformations differ and that conformational variations can lead to differences in transcription activation.

The ER DNA binding domain (DBD) and the glucocorticoid receptor DBD undergo conformational changes on binding to their cognate hormone response elements. X-ray crystallographic studies demonstrate that local DBD regions, which are unfolded in solution, assume more ordered structures when bound to DNA (15, 21, 36, 37). In addition, crystallographic analysis of the ER DBD bound to the vitellogenin B1 ERE2 (AGTCAnnnTGACC [50]), which differs from the vitellogenin A2 ERE (GGTCAnnnTGACC [16]) by a single base pair (underlined), has demonstrated that the substitution of an adenine for a guanine in the 5′ half site causes the rearrangement of a lysine side chain, disruption of a salt bridge between lysine and glutamic acid residues, and destruction of a hydrogen bond with the guanine residue (38). When the DBD is bound to the vitellogenin B1 ERE2, the lysine residue accommodates the nucleotide substitution by forming hydrogen bonds with a nearby tyrosine residue and the substituted adenine residue. Thus, the change of one nucleotide requires the formation of a new and different interconnected hydrogen bond network and implies that each ERE sequence may induce unique conformational changes in DBD structure.

At this point, it is uncertain whether changes in DBD conformation can be transmitted to other receptor regions and thereby alter receptor function. Starr et al. (41) have provided evidence that mutation of a single amino acid in the glucocorticoid receptor DBD induces conformational changes in a transcription activation domain of the receptor. However, other studies have demonstrated that ER DNA and ligand binding domains function as independent entities, which can be fused to heterologous units and still effectively activate transcription (12, 20, 45, 51).

A number of laboratories have demonstrated that EREs with imperfect ERE half sites are weaker transcriptional activators than the A2 ERE (6, 22, 32). Interestingly, we recently demonstrated that the orientation of a consensus or an imperfect ERE relative to the TATA sequence can have profound effects on the expression of an estrogen-responsive reporter plasmid (28). The A2 ERE maximally activates transcription when it is separated from the TATA sequence by 2.6 or 3.6 helical turns, whereas the pS2 ERE maximally activates tran-

*Corresponding author. Mailing address: Department of Molecular and Integrative Physiology, University of Illinois at Urbana-Champaign, 524 Burrill Hall, 407 South Goodwin Ave., Urbana, IL 61801. Phone: (217) 244-5679. Fax: (217) 333-1133. E-mail: anardull@uiuc.edu.

scription when it is separated from the TATA sequence by 3 helical turns. From these studies, we hypothesized that the ERE may act as an allosteric modulator of ER conformation and that these DNA-induced changes in ER conformation could in turn influence ER-protein interactions and lead to changes in transcription activation.

To determine if an ERE sequence could induce specific changes in receptor conformation, we have characterized the interaction of the ER DBD and the intact ER with the vitellogenin A2 and the pS2 ERE sequences. The *Xenopus laevis* vitellogenin A2 ERE is a perfectly palindromic, consensus ERE sequence (GGTCAnnnTGACC [16]) and differs from the human pS2 ERE in the 3′ half site by one base pair (GG TCAnnnTGGCC [30]). We detect differences in the interaction of the purified ER DBD with the A2 and pS2 EREs in gel mobility shift, DNase I footprinting, and methylation interference assays. The differential interaction of ER-specific antibodies with A2 and pS2 ERE-bound ER implies that there are differences in ER conformation. Protease sensitivity assays provide further evidence that the conformations of the A2 and pS2 ERE-bound ER are distinct. We believe that these DNA-induced conformational changes in ER can form the basis for differential transcription of estrogen-responsive genes.

MATERIALS AND METHODS

Preparation of ^{32}P-labeled DNA fragments, ER DBD, and ER. For gel mobility shift assays, DNase I footprinting, and methylation interference experiments, 5 μg of circular permutation plasmids B3consERE and B3pS2ERE (28) were digested with *Eco*RV and *Hin*dIII to produce 278-bp ERE-containing DNA fragments containing the A2 and pS2 EREs, respectively, flanked by identical nucleotide sequence. To label the coding strand, the ERE-containing DNA fragments were combined with 50 mM Tris (pH 8.0), 10 mM $MgCl_2$, 50 mM NaCl, 25 pmol (150 μCi) of [α-^{32}P]dATP, 25 pmol (150 μCi) of [α-^{32}P]dGTP, 140 μM dTTP, 140 μM dCTP, and 1 U of Klenow DNA polymerase in a final volume of 40 μl. After 20 min at room temperature, 140 μM dATP and 140 μM dGTP were added to the samples, and the reaction mixture was incubated for another 5 min at room temperature. DNA fragments were fractionated on a 5% acrylamide gel, excised, isolated by electroelution, precipitated, and resuspended in TE (10 mM Tris [pH 8.0], 1 mM EDTA). ERE-containing DNA fragments were also labeled on the noncoding strand and used in DNase I footprinting and methylation interference experiments. To label the noncoding strand, plasmids B3consERE and B3pS2ERE were cut with *Eco*RV and *Nhe*I to produce 388-bp ERE-containing DNA fragments. The fragments were filled in on the noncoding strand as described above except that 25 pmol (150 μCi) of [α-^{32}P]dCTP, 25 pmol (150 μCi) of [α-^{32}P]dTTP, 140 μM dATP, and 140 μM dGTP were used. After 20 min, 140 μM dCTP and 140 μM dTTP were added to the reaction mixture. ^{32}P-labeled probes were fractionated on an acrylamide gel and electroeluted as described for the coding strand.

For the antibody supershift experiments, 5 μg of each of plasmids B3consERE and B3pS2ERE was cut with *Hin*dIII and ^{32}P labeled as described above for the coding strand. The 425-bp, end-labeled, ERE-containing DNA fragments were gel purified on a 5% acrylamide gel, excised, electroeluted, precipitated, and resuspended in TE.

For protease sensitivity experiments, 5-μg aliquots of plasmids B3consERE and B3pS2ERE were cut with *Eco*RI and *Bam*HI to produce 55-bp ERE-containing DNA fragments. The fragments were gel purified and labeled as described above except that 49.5 pmol (300 μCi) of [α-^{32}P]dATP and 16.5 pmol (100 μCi) of [α-^{32}P]dGTP were used. The probes were gel purified a second time on a 5% acrylamide gel, excised, electroeluted, precipitated, and resuspended in TE.

The expression and purification of the 111-amino-acid *X. laevis* ER DBD (amino acids 171 to 281) and the partially purified yeast-expressed human ER have been described elsewhere (27, 28). These studies were carried out exclusively with the ERα DBD and full-length receptor, not the recently discovered ERβ (18).

Gel mobility shift assays. Gel mobility shift assays were carried out as previously described (29). Briefly, *Eco*RV/*Hin*dIII ^{32}P-labeled DNA fragments (0.05 to 0.1 pmol) containing the A2 ERE were combined with 0 to 0.37 pmol of purified DBD in binding reaction buffer (15 mM Tris [pH 7.9], 0.2 mM EDTA, 10% glycerol, 4 mM dithiothreitol) with 80 mM KCl and 50 ng of poly(dI-dC) to a final volume of 20 μl. The DBD-DNA mixture was incubated for 15 min at room temperature and then fractionated on an 8% low-ionic-strength acrylamide gel. ^{32}P-labeled DNA fragments containing the pS2 ERE were identically processed except that 0 to 1.83 pmol of purified DBD were used in the binding reactions.

DNase I footprinting. *Eco*RV/*Hin*dIII-digested A2 ERE-containing DNA fragments (0.5 to 1.0 pmol), which had been labeled on the coding strand, were combined with 0 to 7.34 pmol of purified DBD in binding reaction buffer with 80 mM KCl, 50 ng of poly(dI-dC), 1.25 mM $MgCl_2$, and 0.5 mM $CaCl_2$ to a final volume of 20 μl. DNA fragments containing the pS2 ERE were identically processed except that 0 to 36.7 pmol of purified DBD was used. Ovalbumin was also included in each reaction so that the total protein concentration was 2.5 μg. The binding reaction mixtures were incubated for 15 min at room temperature. Then 0.4 U RQ1 RNase-free DNase I (Promega, Madison, Wis.) was added in the absence of the DBD, and 0.8 U of DNase I was added to reactions containing the DBD. The samples were cleaved for 1.5 or 2.5 min, respectively, after which digestion was terminated by addition of 20 μl of DNase I stop solution (200 mM NaCl, 1% sodium dodecyl sulfate, 30 mM EDTA). The DNA was extracted with phenol-chloroform, precipitated, washed twice with 70% ethanol, and dried. The A2 and pS2 ERE-containing DNA fragments were resuspended in loading buffer, incubated at 90°C for 1.5 min, and electrophoresed on an 8% sequencing gel. The gel was dried and visualized by autoradiography.

The protection of each A2 and pS2 ERE half site was quantitated by using a PhosphorImager and ImageQuant software (Molecular Dynamics, Sunnyvale, Calif.). Each lane was normalized to account for unequal loading, and then the level of radioactivity in each ERE half site was quantitated before and after addition of increasing amounts of DBD. The level of protection, which is expressed as the percentage of cleaved DNA, was calculated by determining the amount of cleaved DNA in each ERE half site in the presence of DBD relative to the amount of cleaved DNA in each ERE half site in the absence of DBD.

Methylation interference. *Eco*RV/*Hin*dIII-digested, end-labeled DNA fragments (8 to 10 pmol; 10^6 cpm) were methylated in 211 μl of DMS (dimethyl sulfate) buffer (50 mM sodium cacodylate [pH 8.0], 1 mM EDTA) with 0.5% DMS. After 3 min, the reaction was terminated with 50 μl of DMS stop solution (1.5 M sodium acetate [pH 7.0], 1 M β-mercaptoethanol, 100 μg of tRNA per ml) and 750 μl of cold ethanol. The modified DNA was precipitated twice and resuspended in TE. Then 1.5 to 3.0 pmol of methylated A2 or pS2 ERE-containing probe was combined with 3.7 or 7.4 pmol of purified DBD, respectively, in binding reaction buffer with 80 mM KCl and 50 ng of poly(dI-dC). The 20-μl reaction mixture was fractionated on an 8% nondenaturing polyacrylamide gel. The free probe and protein-DNA complexes were detected by autoradiography of the wet gel and excised. The modified DNA was isolated by electroelution, precipitated, and then cleaved for 30 min with 10% piperidine at 90°C. The piperidine solution was evaporated, and the modified DNA was resuspended in 30 μl of water, lyophilized, resuspended in 20 μl of water, and lyophilized. The A2 and pS2 ERE-containing DNA fragments were resuspended in loading buffer, incubated at 90°C for 1.5 min, and electrophoresed on an 8% sequencing gel. The gel was dried and visualized by autoradiography.

Antibody supershifts. Monoclonal antibody P1A3 was made against purified *X. laevis* ER DBD at the Immunological Resource Center, University of Illinois at Urbana-Champaign. The production of antibodies ER 21, H226, D547, H222, and D75 has been described previously (4, 13). Polyclonal antibodies ER6 and ER1 and monoclonal antibody h151 were provided by Robin Fuchs-Young (M. D. Anderson Cancer Center, University of Texas, Smithville) and Dean Edwards (University of Colorado, Denver), respectively.

Gel mobility supershift assays were carried out with partially purified, yeast-expressed human ER (28). For these assays, 0.05 to 0.1 pmol of the *Eco*RV/*Hin*dIII-digested, end-labeled DNA fragments containing the A2 or pS2 ERE were combined with 285 or 570 fmol of ER in binding reaction buffer with 10 μg of bovine serum albumin, 1 μg of poly(dI-dC), 20 mM KCl, 50 μM $ZnCl_2$, and 10^{-7} M 17β-estradiol (E2). The reaction mixtures were incubated for 10 min at room temperature before one of the indicated ER-specific antibodies was added to the A2 or pS2 ERE-containing samples. After 5 min at room temperature, the protein-DNA complexes were fractionated for 4 h at 300 V on a nondenaturing 8% acrylamide gel and processed as described above. The amount of free and bound DNA was determined with a PhosphorImager and ImageQuant software.

Partial ER proteolysis. The 55-bp, ^{32}P-labeled DNA fragments (0.05 to 0.1 pmol) containing either the A2 or pS2 ERE were combined with 285 or 570 fmol of ER, respectively, as described above. After a 10-min incubation, 0, 0.05, 0.5, 1.25, 2.5, 3.75, or 5 ng of chymotrypsin (Sigma, St. Louis, Mo.) was added to the A2 and pS2 ERE-containing reaction mixtures. The samples were incubated for an additional 10 min and loaded onto a running, 8% nondenaturing acrylamide gel. The gel was electrophoresed for 2 h at 300 V, dried, and visualized by autoradiography. A2 or pS2 ERE-ER complexes were also exposed to trypsin cleavage and processed similarly except that 0, 0.05, 0.5, 1.25, 2.5, 3.75, or 5 ng of trypsin (Worthington Biochemical Corporation, Freehold, N.J.) was added to each sample.

RESULTS

To be certain that the ER-ERE interaction was not influenced by other proteins, we began our investigations by using highly purified preparations of *X. laevis* ER DBD. There are several advantages to using the DBD. First, it is easily expressed in bacteria and can be highly purified in a two-step chromatographic procedure (27). Second, the DBD retains many of the characteristics of the intact receptor including specific interaction with the ERE, differential binding to EREs

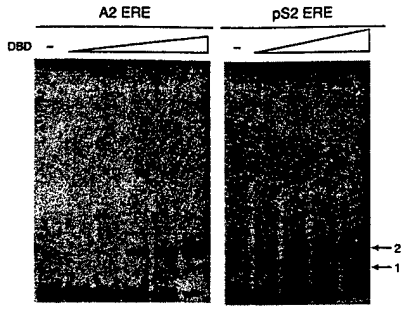

FIG. 1. The DBD forms one complex with the A2 ERE but forms two complexes with the pS2 ERE. Increasing concentrations of purified DBD (0, 0.007, 0.03, 0.07, 0.18, or 0.36 pmol for the A2 ERE; 0, 0.07, 0.36, 0.73, or 1.83 pmol for the pS2 ERE) were incubated with ^{32}P-labeled A2 or pS2 ERE-containing DNA fragments as described in Materials and Methods. The binding reactions were fractionated on a nondenaturing acrylamide gel, and the gel was dried and subjected to autoradiography. Complexes 1 and 2, formed between the DBD and A2 or pS2 EREs, are indicated to the right.

that deviate from the consensus sequence, and activation of an estrogen-responsive reporter construct (6, 27). Third, the DBD structure has been defined in detail by nuclear magnetic resonance and X-ray crystallographic techniques (36–38). Fourth, because the amino acid sequence of steroid hormone receptor DBDs is highly conserved, delineating how one DBD interacts with its cognate response element may also help to delineate how other members of the nuclear receptor superfamily activate transcription.

Differential interaction of the DBD with A2 and pS2 EREs is detected in gel mobility shift assays. To begin characterizing the DBD-ERE interaction, gel mobility shift assays were carried out. ^{32}P-labeled DNA fragments containing the A2 ERE or the pS2 ERE were combined with increasing amounts of purified DBD and fractionated on nondenaturing polyacrylamide gels. The DBD formed a single complex with the A2 ERE regardless of DBD concentration, suggesting that the DBD occupied both of the consensus ERE half sites (Fig. 1). These results are consistent with previous X-ray crystallographic and gel mobility shift assays which demonstrate that even at extremely low DBD concentrations, the DBD bound as a dimer to a consensus ERE sequence (27, 36, 38). In contrast to our findings with the A2 ERE, DNA fragments containing the pS2 ERE formed two complexes with the DBD. Complex 2 had the same mobility as the single complex formed with the A2 ERE, indicating that the DBD was probably binding as a dimer to the pS2 ERE (Fig. 1, arrow 2). Complex 1 migrated more rapidly than complex 2 and probably represents one DBD monomer interacting with the pS2 ERE-containing DNA fragments (Fig. 1, arrow 1). The disappearance of complex 1 and the appearance of complex 2 with increasing DBD concentration supports the idea that a monomer-to-dimer transition was occurring with the pS2 ERE. Although the DBD bound to both the A2 and pS2 EREs, significantly lower levels of DBD were required for occupation of the consensus A2 ERE than for occupation of the imperfect pS2 ERE. This was not surprising since we have previously demonstrated that the affinity of the intact receptor is twofold lower for the pS2 ERE than for the A2 ERE (28).

DNase I footprinting demonstrates that the DBD dimer interacts with the A2 ERE but that both the DBD monomer and dimer interact with the pS2 ERE. To determine if the complexes formed in the gel shift assays corresponded to DBD monomer and dimer binding and to further characterize the interaction of the DBD with the A2 and pS2 EREs, DNase I footprinting was carried out. This technique utilizes the nonspecific cleavage properties of DNase I to identify DNA regions that are protected by proteins. DNA fragments containing the A2 ERE or the pS2 ERE were ^{32}P-labeled on the coding strand and then combined with increasing amounts of purified DBD. The reactions were subjected to DNase I digestion, and the resulting cleavage products were separated on a sequencing gel. As seen in Fig. 2, the DBD interacted only with the region of the DNA fragments that included either the A2 ERE or the pS2 ERE. Although the areas of protection were similar for the A2 and pS2 EREs, there were distinguishable differences in the pattern of cleavage. Quantitative analysis of the A2 and pS2 ERE half sites demonstrated that both A2 ERE half sites were equally protected regardless of protein concentration (Fig. 3). These findings indicated that the DBD bound to each ERE half site with equal affinity and confirmed that only the DBD dimer bound to the A2 ERE. The pS2 ERE half sites, however, were differentially protected with the consensus pS2 ERE half site (GGTCA), requiring lower DBD concentrations for protection than the imperfect pS2 ERE half site (TGGCC). Thus, the DBD bound to the pS2 ERE as a monomer at lower DBD concentrations and as a dimer at higher DBD concentrations. It should be noted, however, that higher DBD concentrations were required for protection of the pS2 ERE than for protection of the A2 ERE (Fig. 2 and 3). Interestingly, hypersensitive sites were observed at the 3′ ends of both the A2 and pS2 ERE footprints (Fig. 2, *).

DNA fragments containing the A2 or the pS2 ERE were also ^{32}P-labeled on the noncoding strand and subjected to DNase I cleavage. Like the coding strand, the region protected on the noncoding strand included only the A2 or the pS2 ERE (Fig. 4), the A2 ERE half sites were equally protected, and lower DBD concentrations were required for protection of the

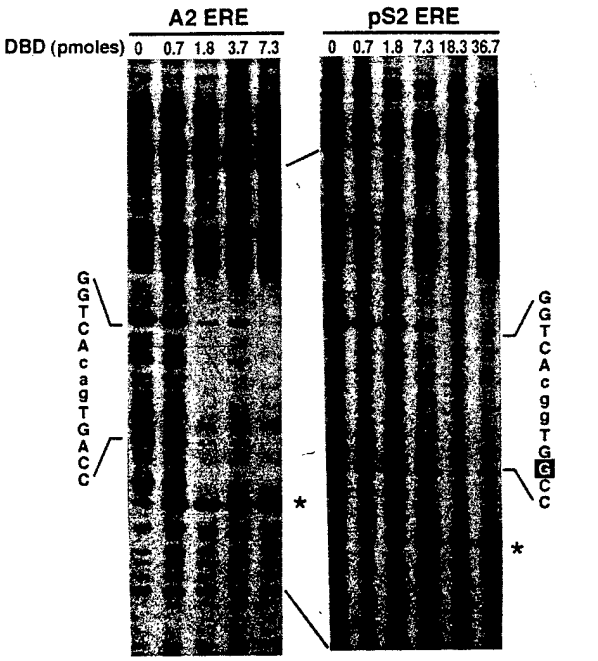

FIG. 2. DNase I footprinting defines regions of the coding strand that are involved in DBD binding. Increasing concentrations of purified DBD were incubated with A2 or pS2 ERE-containing DNA fragments which had been labeled on the coding strand. The binding reactions were subjected to limited DNase I digestion, and the cleaved DNA was fractionated on a denaturing acrylamide gel. The gel was dried and subjected to autoradiography. The positions and sequences of the A2 ERE and the pS2 ERE and DNase I-hypersensitive sites (*) are indicated.

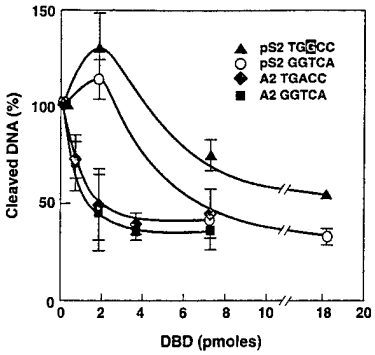

FIG. 3. Lower DBD concentrations are required to protect the A2 ERE than the pS2 ERE. The level of A2 and pS2 ERE half site protection on the coding strand is expressed as the percentage of cleaved DNA and was calculated by determining the amount of cleaved DNA in each ERE half site in the absence of DBD relative to the amount of cleaved DNA in each ERE half site in the presence of DBD. Each point represents the mean ± standard error of the mean from three to four independent experiments.

pS2 ERE consensus half site than for protection of the imperfect pS2 ERE half site. Lower DBD concentrations were again required to protect the A2 ERE than the pS2 ERE. These data from the noncoding strand demonstrate that the DBD bound only as a dimer to the A2 ERE, while both the DBD monomer and dimer bound to the pS2 ERE.

Guanine residues in the A2 and pS2 EREs are required for DBD dimer binding, but only guanine residues in the pS2 ERE consensus half site are necessary for DBD monomer binding. Because DNase I is a large globular protein, steric hindrance of this molecule with other proteins may result in an overestimation of the DNA region protected by bound proteins.

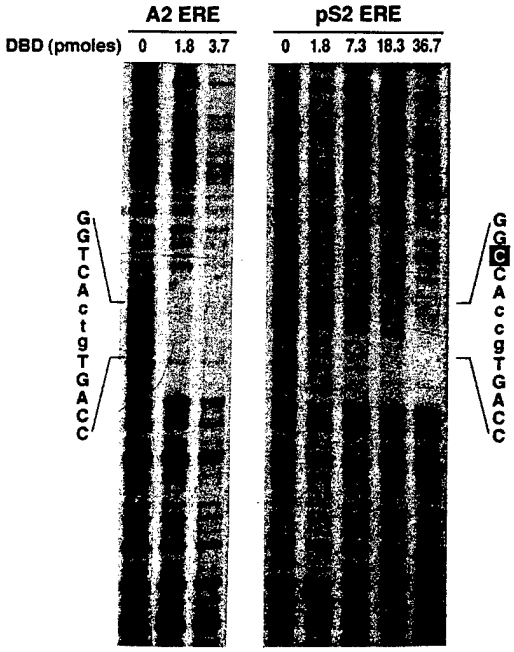

FIG. 4. DNase I footprinting defines regions of the noncoding strand that are involved in DBD binding. Increasing concentrations of purified DBD were incubated with A2 or pS2 ERE-containing DNA fragments which had been labeled on the noncoding strand. The binding reaction was subjected to limited DNase I digestion, and the cleaved DNA was fractionated on a denaturing acrylamide gel. The gel was dried and subjected to autoradiography. The positions and sequences of the A2 and pS2 EREs are indicated.

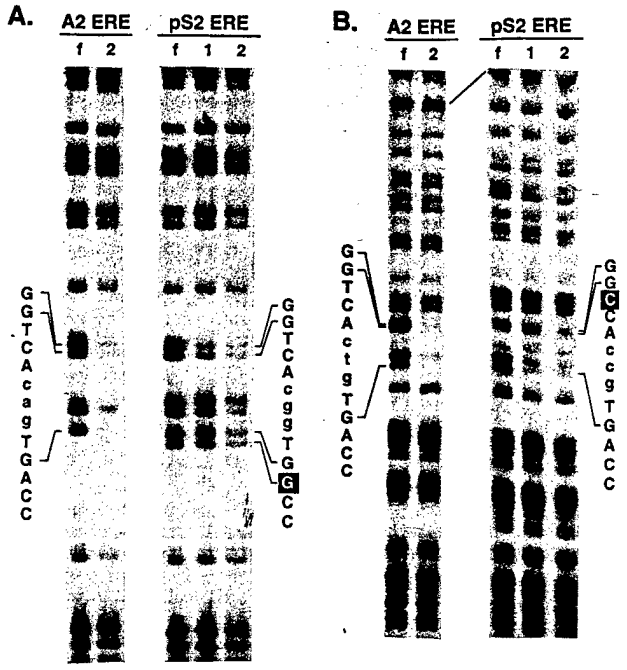

FIG. 5. Methylation interference experiments delineate guanine residues required for efficient binding of the DBD to the A2 and pS2 EREs. A2 or pS2 ERE-containing DNA fragments which had been labeled on the coding (A) or noncoding (B) strand were modified with DMS. The modified DNA fragments were incubated with purified DBD and fractionated on a nondenaturing acrylamide gel. The free probe (lanes f), DBD-ERE complex 1 (lanes 1), and DBD-ERE complex 2 (lanes 2) were detected by autoradiography. The DNA from each band was isolated, cleaved, fractionated on a denaturing gel, and visualized by autoradiography. The positions and sequences of the A2 and pS2 EREs are indicated.

Therefore, to more specifically define and compare the contacts between the DBD and the A2 and pS2 ERE sequences, methylation interference assays were carried out. This method of footprinting uses DMS, a small molecule, to modify guanine residues. The modified DNA is then incubated with a DNA binding protein that specifically interacts with a recognition sequence present in the DNA strand. Because methylation of guanine residues in a recognition sequence inhibits protein binding, guanine residues that are required for efficient protein-DNA interaction can be identified.

A2 ERE- or pS2 ERE-containing DNA fragments were modified by DMS treatment and combined with 5.5 or 29.3 pmol of purified DBD, respectively, so that approximately 50% of the DNA fragments were bound to the DBD. Free DNA and DBD-DNA complexes were fractionated on a nondenaturing acrylamide gel, isolated, cleaved, and resolved on a denaturing gel. Methylation of guanine residues in the A2 and pS2 ERE half sites strongly inhibited DBD binding, as indicated by the diminished intensity of the bands corresponding to these nucleotides (Fig. 5). Specific DBD binding required the participation of guanine residues (bold faced) in both half sites of the A2 ERE (**GG**TCAcag**T**GACC). Interaction of the DBD dimer with the pS2 ERE also required unmodified guanine residues in both the consensus and imperfect half sites (**GG**TCAcgg**TGGC**C). These findings are consistent with X-ray crystallographic studies carried out with the ER DBD and methylation interference assays carried out with the full-length ER (17, 36). Of particular interest was the interaction of the DBD monomer with the pS2 ERE, which required only the participation of guanine residues in the consensus half site

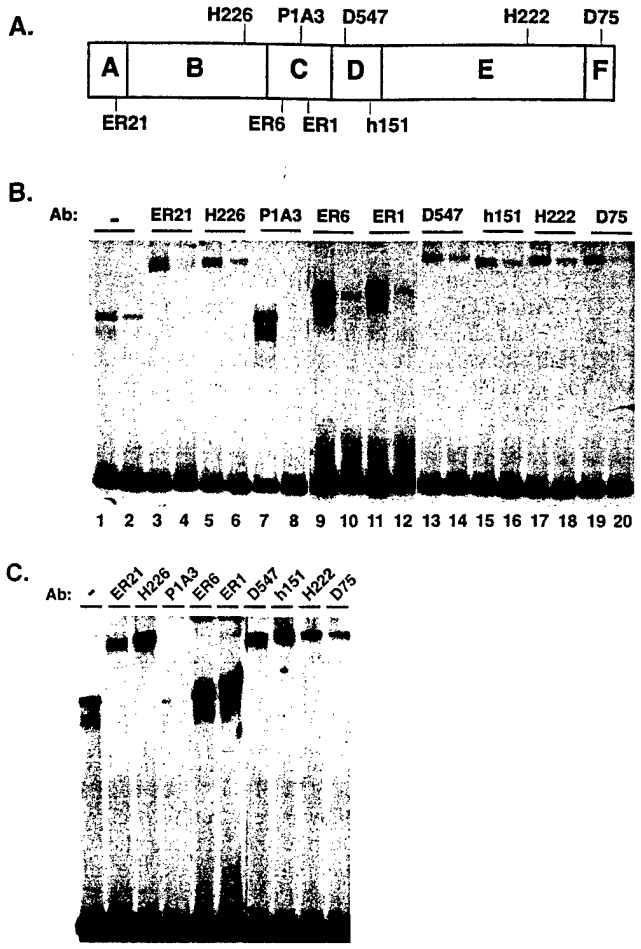

FIG. 6. Antibodies to various ER epitopes can detect differences in conformation of the A2 and pS2 ERE-bound receptor. (A) Schematic representation of the epitopes for ER-specific antibodies used. (B) Partially purified, yeast-expressed ER (285 fmol) was incubated with A2 ERE-containing DNA fragments (odd-numbered lanes) or pS2 ERE-containing DNA fragments (even-numbered lanes). After a short incubation, antibodies (Ab) were added to the binding reactions as indicated and the complexes were fractionated on a nondenaturing acrylamide gel. The complexed DNA and free probe were visualized by autoradiography. (C) Partially purified, yeast-expressed ER (570 fmol) was incubated with pS2 ERE-containing DNA fragments. Samples were processed as for panel B.

(Fig. 5). These data are in good agreement with our DNase I footprinting results (Fig. 2 to 4) and provide additional evidence that first the DBD binds as a monomer to the consensus pS2 ERE half site and then a second monomer binds to the imperfect pS2 ERE half site as DBD concentrations are increased.

Differences in ER epitope availability are detected in antibody supershift experiments when the receptor is bound to the A2 or the pS2 ERE. The gel shift and footprinting experiments established that the DBD interacted differently with the A2 and pS2 EREs but did not provide direct evidence that DBD conformation was different when bound to these two EREs. We reasoned that subtle changes in DBD structure might be translated to other ER regions, resulting in more global conformational changes in the intact receptor. Therefore, monoclonal and polyclonal antibodies directed against several ER regions (Fig. 6A) were used in antibody supershift experiments to determine if differences in epitope availability could be detected when the ER was bound to the A2 or pS2 ERE. Partially purified, yeast-expressed ER was combined with ^{32}P-labeled A2 or pS2 ERE-containing DNA fragments. Antibodies directed against different ER epitopes were then added to the binding reaction mixtures, and the resulting complexes were fractionated on nondenaturing polyacrylamide gels. The level of each receptor-DNA complex was quantitated so that the effect of each antibody on the A2 and the pS2 ERE-ER complex formation could be assessed. The most striking difference in epitope availability was observed with monoclonal antibody P1A3, which was made against purified *X. laevis* DBD. P1A3 enhanced the ER-A2 ERE complex formation approximately sixfold (Fig. 6B; compare lanes 1 and 7) and strongly inhibited ER-pS2 ERE complex formation (compare lanes 2 and 8) but failed to supershift either the A2 or pS2 ERE-ER complex. Two other antibodies also discriminated between the pS2 and A2 ERE-bound ER. ER21 and D75, which are directed against the amino and carboxy termini of the receptor, respectively, did not alter the supershifted ER-A2 ERE complex formation but decreased formation of the ER-pS2 ERE complex (Fig. 6B; compare lane 2 with lanes 4 and 20). The decreased pS2 ERE-ER complex formation was more apparent when increased amounts of receptor were included in the binding reaction (Fig. 6C). The other antibodies tested (H226, ER6, ER1, D547, h151, and H222) supershifted both the A2 and pS2 ERE-containing complexes in a similar manner. The differential interaction of three ER-specific antibodies with A2 and pS2 ERE-bound ER implied that there were differences in ER epitope availability not only in the DBD but also in the amino and carboxy termini of the receptor.

Sequence-mediated changes in ER conformation are detected after limited protease digestion of the A2 and pS2 ERE-bound ER. The antibody supershift experiments provided evidence that ER epitopes were differentially exposed when the receptor was bound to the A2 and pS2 EREs and therefore that differences in receptor conformation may exist. To more directly assess possible differences in receptor conformation, protease sensitivity assays were carried out with A2 and pS2 ERE-bound ER. This assay utilizes limited proteolysis of a DNA-bound protein to produce a pattern of digestion based on amino acid accessibility and provides information about native protein conformation (35, 44). ^{32}P-labeled DNA fragments containing the A2 or pS2 EREs were combined with 285 or 570 fmol of partially purified yeast-expressed ER, respectively. This twofold difference in ER concentration was used to account for the lower binding affinity of the intact ER for the pS2 ERE (28). The protein was then subjected to limited proteolysis by exposure to increasing concentrations of chymotrypsin, and the resulting complexes were fractionated on nondenaturing polyacrylamide gels. The differences in the digestion patterns observed with the A2 ERE-bound ER and the pS2 ERE-bound ER were striking (Fig. 7A). Limited digestion of the A2 ERE-bound ER produced a larger stable ER-DNA complex (C3) than was observed with the pS2 ERE-bound ER after chymotrypsin treatment (C5). The numbers of intermediate ER-DNA complexes observed with A2 and pS2 ERE-bound ER were also quite distinct. While chymotrypsin digestion of the A2 ERE-bound receptor produced several ER-DNA complexes of intermediate size (C1 to C5), digestion of the pS2 ERE-bound ER produced few intermediate-size ER-DNA complexes.

The difference in digestion patterns observed with these two EREs was not due to differences in ER or DNA concentrations, since different amounts of ER and DNA produced the same digestion pattern, nor was it due to a difference in chymotrypsin concentrations, since the same digestion patterns were produced at higher and lower chymotrypsin concentra-

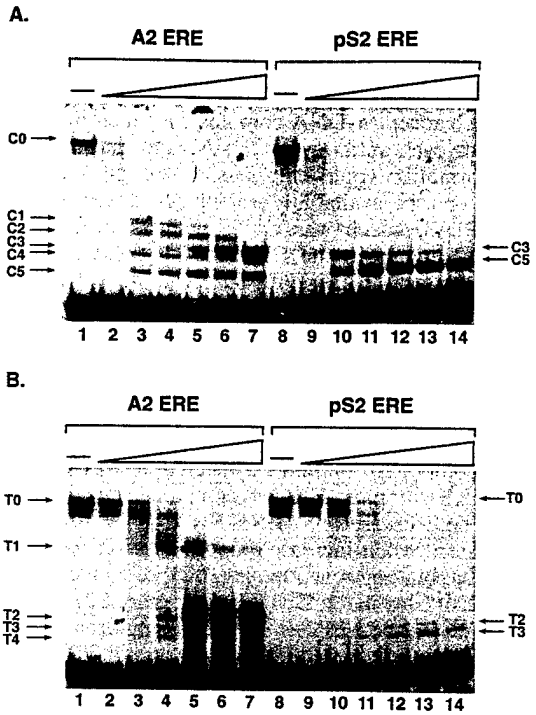

FIG. 7. Distinct protease digestion patterns of A2 and pS2 ERE-bound ER provide evidence for ERE-mediated differences in receptor conformation. (A) Partially purified, estrogen-occupied ER was combined with A2 or pS2 ERE-containing DNA fragments. After a short incubation, 0, 0.05, 0.5, 1.25, 2.5, 3.75, or 5 ng of chymotrypsin was added to the binding reaction. ER-DNA complexes and free DNA were fractionated on a nondenaturing acrylamide gel, and the gel was dried and subjected to autoradiography. The undigested ER-DNA complex (C0) and ER-DNA complexes formed with chymotrypsin-proteolyzed receptor (C1 to C5) are indicated. (B) Partially purified ER and A2 or pS2 ERE-containing DNA fragments were combined as for panel A except that 0, 0.05, 0.5, 1.25, 2.5, 3.75, or 5 ng of trypsin was added to the binding reactions. The undigested ER-DNA complex (T0) and ER-DNA complexes formed with trypsin-proteolyzed receptor (T1 to T4) are indicated.

tions. Since we have observed similar digestion patterns with partially purified yeast-expressed ER and ER-containing nuclear extracts from estrogen-treated CHO-ER cells, the difference in digestion patterns did not result from the association of different proteins with the ER (data not shown). Furthermore, the difference in digestion patterns was not due to dissociation of the ER from the pS2 ERE and enhanced proteolysis of the free receptor, since the amount of ER-DNA complex observed at the highest chymotrypsin concentration was similar to the amount of ER-DNA complex observed in the absence of protease (compare lanes 8 and 14). Finally, the higher mobility complexes (C1 to C5) produced by chymotrypsin cleavage were due to specific cleavage of the protein and not degradation of DNA since the free DNA was not degraded as chymotrypsin levels increased. Digestion of the A2 and pS2 ERE-bound ER was done in parallel, and the results were completely reproducible.

Trypsin digestion also resulted in distinctly different cleavage patterns of the A2 and pS2 ERE-bound ER (Fig. 7B). Digestion of the A2 ERE-bound ER with trypsin produced several products (T1 to T4), with complex T2 being most stable at high trypsin concentrations (Fig. 7B, lanes 1 to 7). In contrast, digestion of the pS2 ERE-bound ER produced fewer trypsin products, with complex T3 being the most stable (lanes 8 to 14). The pS2 ERE-bound ER appeared to be particularly susceptible to trypsin cleavage as evidenced by the loss of ER-DNA complex at higher trypsin concentrations. Therefore, we believe that the different digestion patterns that we observed with the A2 and pS2 ERE-bound ER resulted from differences in receptor conformation and that the conformation was dictated by the ERE sequence.

DISCUSSION

This study focused on the differential interaction of the ER DBD and the intact receptor with A2 and pS2 EREs. The A2 ERE (GGTCAnnnTGACC [16]) differs from the pS2 ERE (GGTCAnnnTGGCC [30]) by a single base pair (underlined) in the 3′ half site. Although the adenine residue in the 3′ A2 ERE half site can serve as a hydrogen bond donor and acceptor, the guanine residue residing in a comparable position in the pS2 ERE can function only as a hydrogen bond acceptor. From previous crystallographic studies of the vitellogenin A2 ERE (36) and B1 ERE2 (38), one would predict that substitution of a guanine for an adenine in the 3′ ERE half site would not only affect the hydrogen bond with the substituted nucleotide but also require the modification of a localized hydrogen bond network formed between the ERE and the DBD. We have previously demonstrated that binding of the ER DBD and the full-length ER to the ERE induces conformational changes in DNA structure (25, 26, 28, 29, 33). We now provide evidence that the DBD-DNA interaction is a dynamic process involving conformational changes in both the receptor and DNA.

Our DNase I footprinting studies revealed that 1.3 pmol of DBD was required to occupy 50% of the 5′ A2 ERE half site. In contrast, 6.5 pmol of DBD was required to occupy 50% of the 5′ pS2 ERE half site. Despite the fact that these 5′ ERE half sites have identical nucleotide sequences, the relative affinity of the DBD is ~5-fold lower for the 5′ pS2 ERE half site than for the 5′ A2 ERE half site (Fig. 3), suggesting that two adjacent consensus ERE half sites can act cooperatively to enhance DBD binding. When comparing the intact EREs, we found that the affinity of the DBD is more than sixfold greater for the two adjacent A2 ERE half sites than for the consensus and imperfect pS2 ERE half sites. We have previously demonstrated that the affinity of the intact ER is twofold lower for the pS2 ERE than for the A2 ERE (28). Thus, regions outside the DBD are important for enhancing binding of the intact receptor to the A2 ERE but may be even more important in enhancing binding of the receptor to imperfect ERE sequences.

We observed an apparent monomer-to-dimer transition as increasing concentrations of purified DBD were combined with the pS2 ERE. A similar monomer-to-dimer transition has been observed in experiments carried out with the ER DBD and the imperfect vitellogenin B1 ERE 2 (38), which differs from the consensus sequence by a single base pair in the 5′ half site (AGTCAnnnTGACC [50]). In contrast to the pS2 ERE and the B1 ERE2, we did not observe occupation of a single half site with the A2 ERE, implying that the DBD binds only as a dimer to the A2 ERE. Binding of the ER dimer to the A2 ERE has been a subject of substantial controversy. While NMR and crystal structure studies provide evidence for ER DBD dimer binding (36, 37), an antibody-based DNA binding assay (11) suggests that the ER may bind as a monomer to the A2 ERE. Taken together, our gel mobility, DNase I footprinting, and methylation interference assays examining the A2 and pS2 EREs in tandem provide compelling evidence that the DBD binds as a dimer to the A2 ERE and as a monomer and a dimer to the pS2 ERE.

Since we know that the DBD is a monomer in solution (27),

dimerization must occur upon binding of the DBD to the ERE. Dimerization could be fostered by simultaneous binding of two DBD monomers or binding of one DBD monomer and the subsequent recruitment of a second DBD monomer. In either case, protein-protein and protein-DNA interactions would help stabilize binding of the DBD dimer and discourage dissociation of one of the monomers from the A2 or pS2 ERE. Monomer binding to the pS2 ERE could result from the inability of the DBD monomer bound to the consensus half site to recruit a second DBD monomer to the imperfect 3′ half site or more rapid dissociation of the DBD from the imperfect 3′ ERE half site.

From our combined experiments, it is possible to compare binding of the ER DBD and the full-length ER to the A2 and pS2 EREs. The ER DBD bound to the pS2 ERE as a monomer at low DBD concentrations and then as a dimer at higher DBD concentrations. These findings are similar to those of studies examining binding of the full-length ER to the vitellogenin B1 ERE2 (22). In contrast to these results, the full-length ER used in our experiments bound only as a dimer to the A2 and pS2 ERE, as indicated by the migration of the ER-ERE complexes in gel mobility shift assays (Fig. 6 and 7). The exclusive binding of the ER dimer to the pS2 ERE emphasizes that the dimerization domain present in the ligand binding domain (8) plays an important role in ER stabilization. Methylation interference assays demonstrated that guanine residues in both A2 ERE half sites were important for ER DBD binding. Since the exact same guanine residues are involved in binding of the full-length ER to the A2 ERE (17), the ER DBD and the full-length ER must bind to the A2 ERE in a very similar fashion.

Protease sensitivity assays demonstrated that there were distinct differences in the digestion patterns of the A2 and pS2 ERE-bound receptor. What is uncertain at this point is the conformational state of the individual ER monomers. We anticipate that the two ER monomers bound to the A2 ERE would have the same conformation. However, it is not known whether both of the ER monomers bound to the pS2 ERE have the same conformation. One might argue that the monomer bound to the consensus pS2 ERE half site would have the same conformation as the monomers bound to the consensus A2 ERE half sites but that the conformation of the monomer bound to the imperfect pS2 half site would be different. Alternatively, it is possible that binding of the ER monomer to the imperfect ERE half site would induce the formation of an altered dimerization interface, which would in turn cause conformational changes in the adjacent ER monomer. Our data favor this latter model since we do not see two superimposed digestion patterns, one for each ER monomer, after partial digestion of the pS2 ERE-bound receptor.

Antibody supershift experiments demonstrated that several antibodies directed at different ER epitopes enhanced ER-ERE binding. The ability of ER-specific antibodies to enhance ER-DNA complex formation has been previously reported by Fawell et al. (7), who suggested that this enhanced binding is due to stabilization of the ER dimer. P1A3 had the most dramatic effect on ER-ERE complex formation. It significantly enhanced ER binding to the A2 ERE, decreased ER binding to the pS2 ERE, and yet failed to supershift either ER-ERE complex. These results suggest that ER binding to antibody and binding to DNA are mutually exclusive events. The inability of P1A3 to supershift the ERE-bound ER was not unexpected, since this antibody is directed against the ER DBD and binding of the DBD to the ERE could presumably occlude the antibody epitope. The ability of P1A3 to enhance ER binding to the A2 ERE yet inhibit binding to the pS2 ERE was somewhat perplexing. However, a similar phenomenon in which an antibody directed against the vitamin D3 receptor DBD enhanced binding of receptor to the osteopontin response element and inhibited binding of receptor to the osteocalcin response element, but did not supershift either complex, has been reported (40). Staal et al. (40) proposed that the presence of the additional immunoglobulin G protein may have simply increased the association of the receptor for its cognate response element and thereby enhanced binding. However, we find that inclusion of additional nonspecific protein in our binding reactions did not affect ER-DNA complex formation (data not shown). It seems more probable that P1A3 enhanced A2 ERE binding by promoting ER dimerization and that binding of the ER dimer to the A2 ERE dissociated the antibody. The inability of the receptor to interact with the pS2 ERE in the presence of P1A3 may be attributed to more efficient binding of the ER to antibody than to the ERE or to an unfavorable presentation of the antibody-stabilized ER dimer to the pS2 ERE.

A number of studies have demonstrated that the activity of many ERE-containing promoters is cell type specific (3, 23, 24, 46, 47). It is generally thought that these tissue-specific effects are brought about by restricting the expression of required regulatory cofactors to target cells. A more versatile way of differentially regulating gene expression would be to provide the receptor with a large repertoire of functional surfaces that can be formed and serve as contact points for other cellular proteins. The presentation of these functional surfaces and the selection of ER-associated proteins, which is dictated by the unique ERE sequence, would provide tremendous regulatory versatility to a single cell harboring multiple estrogen-responsive genes.

We propose that the conformation of nuclear hormone receptors is subject to two ligands—hormone and DNA—and that binding of either ligand can induce changes in receptor conformation. The ability of hormone to induce conformational changes in nuclear receptor ligand binding domains has been demonstrated (2, 5, 14, 34, 49). Our studies with the ER complement those carried out with glucocorticoid and the vitamin D receptors and suggest that DNA-induced conformational changes in the DBD can be transmitted to other regions of the receptor (19, 40, 41). Taken together, these studies provide evidence that conformational changes induced by DNA binding may serve as a common mechanism for regulating transcription of hormone-responsive genes.

ACKNOWLEDGMENTS

This research was supported by NIH grant R29 HD31299 (to A.M.N.) and USMRMC grant DAMD17-94-J4228 (to G.L.G.). Jennifer Wood was supported by NIH Reproductive Training Grant PHS 2T32 HD 0728-19.

We thank David Shapiro, Dean Edwards, and Robin Fuchs-Young for providing ER-specific antibodies and Varsha Likhite for additional protease sensitivity experiments. We are also grateful to David Shapiro for helpful comments during preparation of the manuscript.

REFERENCES

1. **Alber, T.** 1993. How GCN4 binds DNA. Curr. Biol. 3:182–184.
2. **Beekman, J. M., G. F. Allan, S. Y. Tsai, M.-J. Tsai, and B. O'Malley.** 1993. Transcriptional activation by the estrogen receptor requires a conformational change in the ligand binding domain. Mol. Endocrinol. 7:1266–1274.
3. **Berry, M., D. Metzger, and P. Chambon.** 1990. Role of the two activating domains of the oestrogen receptor in the cell-type and promoter-context dependent agonistic activity of the anti-oestrogen 4-hydroxytamoxifen. EMBO J. 9:2811–2818.
4. **Blaustein, J.** 1993. Estrogen receptor immunoreactivity in rat brain: rapid effects of estradiol injection. Endocrinology 132:1218–1224.
5. **Bourguet, W., M. Ruff, P. Chambon, H. Gronemeyer, and D. Moras.** 1995.

Crystal structural of the ligand-binding domain of the human nuclear receptor RXR-alpha. Nature **375**:377–382.
6. **Chang, T.-C., A. M. Nardulli, D. Lew, and D. J. Shapiro.** 1992. The role of estrogen response elements in expression of the *Xenopus laevis* vitellogenin B1 gene. Mol. Endocrinol. **6**:346–354.
7. **Fawell, S., R. White, S. Hoare, M. Sydenham, M. Page, and M. Parker.** 1990. Inhibition of estrogen receptor-DNA binding by the "pure" antiestrogen ICI 164,384 appears to be mediated by impaired receptor dimerization. Proc. Natl. Acad. Sci. USA **17**:6883–6887.
8. **Fawell, S. E., J. A. Lees, R. White, and M. G. Parker.** 1990. Characterization and colocalization of steroid binding and dimerization activities in the mouse estrogen receptor. Cell **60**:953–962.
9. **Frankel, A. D., and P. S. Kim.** 1991. Modular structure of transcription factors: implications for gene regulation. Cell **65**:717–719.
10. **Fujita, T., G. P. Nolan, S. Ghosh, and D. Baltimore.** 1992. Independent modes of transcriptional activation by the p50 and p65 subunits of NF-KB. Genes Dev. **6**:775–787.
11. **Furlow, J. D., F. E. Murdoch, and J. Gorski.** 1993. High affinity binding of the estrogen receptor to a DNA response element does not require homodimer formation or estrogen. J. Biol. Chem. **268**:12519–12525.
12. **Green, S., and P. Chambon.** 1987. Oestradiol induction of a glucocorticoid-responsive gene by a chimaeric receptor. Nature **325**:75–78.
13. **Greene, G., N. Sobel, W. King, and E. Jensen.** 1984. Immunochemical studies of estrogen receptors. J. Steroid Biochem. **20**:51–56.
14. **Hansen, J. C., and J. Gorski.** 1986. Conformational transitions of the estrogen receptor monomer. J. Biol. Chem. **261**:13990–13996.
15. **Hard, T., E. Kellenbach, R. Boelens, B. A. Naler, K. Dahlman, L. P. Freedman, J. Carlstedt-Duke, K. R. Yamamoto, J.-A. Gustafsson, and R. Kaptein.** 1990. Solution structure of the glucocorticoid receptor DNA-binding domain. Science **249**:157–160.
16. **Klein-Hitpass, L., G. U. Ryffel, E. Heitlinger, and A. C. B. Cato.** 1988. A 13 bp palindrome is a functional estrogen responsive element and interacts specifically with estrogen receptor. Nucleic Acids Res. **16**:647–663.
17. **Klein-Hitpass, L., S. Y. Tsai, G. L. Greene, J. H. Clark, M.-J. Tsai, and B. W. O'Malley.** 1989. Specific binding of estrogen receptor to the estrogen response element. Mol. Cell. Biol. **9**:43–49.
18. **Kuiper, G. G. J. M., E. Enmark, M. Pelto-Huikko, S. Nilsson, and J.-A. Gustafsson.** 1996. Cloning of a novel estrogen receptor expressed in rat prostate and ovary. Proc. Natl. Acad. Sci. USA **93**:5925–5930.
19. **Lefstin, J. A., J. R. Thomas, and K. R. Yamamoto.** 1994. Influence of a steroid receptor DNA-binding domain on transcriptional regulatory functions. Genes Dev. **8**:2842–2856.
20. **Littlewood, T. D., D. C. Hancock, P. S. Danielian, M. G. Parker, and G. I. Evan.** 1995. A modified oestrogen receptor ligand binding domain as an improved switch for the regulation of heterologous proteins. Nucleic Acids Res. **23**:1686–1690.
21. **Luisi, B. F., W. X. Xu, Z. Otwinowski, L. P. Freedman, K. R. Yamamoto, and P. B. Sigler.** 1991. Crystallographic analysis of the interaction of the glucocorticoid receptor with DNA. Nature **352**:497–505.
22. **Martinez, E., and W. Wahli.** 1989. Cooperative binding of estrogen receptor to imperfect estrogen-responsive DNA elements correlates with their synergistic hormone-dependent enhancer activity. EMBO J. **8**:3781–3791.
23. **Metzger, D., S. Ali, J.-M. Bornert, and P. Chambon.** 1995. Characterization of the amino-terminal transcriptional activation function of the human estrogen receptor in animal and yeast cells. J. Biol. Chem. **270**:9535–9542.
24. **Montano, M. M., K. Ekena, K. D. Krueger, A. L. Keller, and B. S. Katzenellenbogen.** 1996. Human estrogen receptor ligand activity inversion mutants: receptors that interpret antiestrogens as estrogens and estrogens as antiestrogens and discriminate among different antiestrogens. Mol. Endocrinol. **10**:230–242.
25. **Nardulli, A. M., G. L. Greene, and D. J. Shapiro.** 1993. Human estrogen receptor bound to an estrogen response element bends DNA. Mol. Endocrinol. **7**:331–340.
26. **Nardulli, A. M., C. Grobner, and D. Cotter.** 1995. Estrogen receptor-induced DNA bending: orientation of the bend and replacement of an estrogen response element with an intrinsic DNA bending sequence. Mol. Endocrinol. **9**:1064–1076.
27. **Nardulli, A. M., D. Lew, L. Erijman, and D. J. Shapiro.** 1991. Purified estrogen receptor DNA binding domain expressed in *Escherichia coli* activates transcription of an estrogen-responsive promoter in cultured cells. J. Biol. Chem. **266**:24070–24076.
28. **Nardulli, A. M., L. E. Romine, C. Carpo, G. L. Greene, and B. Rainish.** 1996. Estrogen receptor affinity and location of consensus and imperfect estrogen response elements influence transcription activation of simplified promoters. Mol. Endocrinol. **10**:694–704.
29. **Nardulli, A. M., and D. J. Shapiro.** 1992. Binding of the estrogen receptor DNA-binding domain to the estrogen response element induces DNA bending. Mol. Cell. Biol. **12**:2037–2042.
30. **Nunez, A.-M., M. Berry, J.-L. Imler, and P. Chambon.** 1989. The 5′ flanking region of the pS2 gene contains a complex enhancer region responsive to oestrogens, epidermal growth factor, a tumour promoter (TPA), the c-Ha-*ras* oncoprotein and the c-*jun* protein. EMBO J. **8**:823–829.
31. **Pabo, C. O., and R. T. Sauer.** 1992. Transcription factors: structural families and principles of DNA recognition. Annu. Rev. Biochem. **61**:1053–1095.
32. **Ponglikitmongkol, M., S. Green, and P. Chambon.** 1988. Genomic organization of the human oestrogen receptor gene. EMBO J. **7**:3385–3388.
33. **Potthoff, S. J., L. E. Romine, and A. M. Nardulli.** 1996. Effects of wild type and mutant estrogen receptors on DNA flexibility, DNA bending, and transcription activation. Mol. Endocrinol. **10**:1095–1106.
34. **Renaud, J.-P., N. Rochel, M. Ruff, V. Vivat, P. Chambon, H. Gronemeyer, and D. Moras.** 1995. Crystal structure of the RAR- gamma ligand-binding domain bound to all-trans retinoic acid. Nature **378**:681–689.
35. **Schreiber, E., P. Matthias, M. Müller, and W. Schaffner.** 1988. Identification of a novel lymphoid specific octamer binding protein (OTF-2B) by proteolytic clipping bandshift assay (PCBA). EMBO J. **7**:4221–4229.
36. **Schwabe, J. W. R., L. Chapman, J. T. Finch, and D. Rhodes.** 1993. The crystal structure of the estrogen receptor DNA-binding domain bound to DNA: how receptors discriminate between their response elements. Cell **75**: 567–578.
37. **Schwabe, J. W. R., L. Chapman, J. T. Finch, D. Rhodes, and D. Neuhaus.** 1993. DNA recognition by the oestrogen receptor: From solution to the crystal. Structure **1**:187–204.
38. **Schwabe, J. W. R., L. Chapman, and D. Rhodes.** 1995. The oestrogen receptor recognizes an imperfectly palindromic response element through an alternative side-chain conformation. Structure **3**:201–213.
39. **Spolar, R. S., and M. T. Record.** 1994. Coupling of local folding to site-specific binding of proteins to DNA. Science **263**:777–784.
40. **Staal, A., A. J. van Wijnen, J. C. Birkenhäger, H. A. P. Pols, J. Prahl, H. DeLuca, M.-P. Gaub, J. B. Lian, G. S. Stein, J. P. T. M. van Leeuwen, and J. L. Stein.** 1996. Distinct conformations of vitamin D receptor/retinoid X receptor-α heterodimers are specified by dinucleotide differences in the vitamin D-responsive elements of the osteocalcin and osteopontin genes. Mol. Endocrinol. **10**:1444–1456.
41. **Starr, D. B., W. Matsui, J. R. Thomas, and K. R. Yamamoto.** 1996. Intracellular receptors use a common mechanism to interpret signaling information at response elements. Genes Dev. **10**:1271–1283.
42. **Steitz, T. A.** 1990. Structural studies of protein-nucleic acid interaction: the sources of sequence-specific binding. Q. Rev. Biophys. **23**:205–280.
43. **Talanian, R. V., C. J. McKnight, and P. S. Kim.** 1990. Sequence-specific DNA binding by a short peptide dimer. Science **249**:769–771.
44. **Tan, S., and T. J. Richmond.** 1990. DNA binding-induced conformational change of the yeast transcriptional activator PRTF. Cell **62**:367–377.
45. **Tasset, D., L. Tora, C. Fromental, E. Scheer, and P. Chambon.** 1990. Distinct classes of transcriptional activating domains function by different mechanisms. Cell **62**:1177–1187.
46. **Tora, L., J. White, C. Brou, D. Tasset, N. Webster, E. Scheer, and P. Chambon.** 1989. The human estrogen receptor has two independent nonacidic transcriptional activation functions. Cell **59**:477–487.
47. **Tzukerman, M. T., A. Esty, D. Santiso-Mere, P. Danielian, M. G. Parker, R. B. Stein, J. W. Pike, and D. P. McDonnell.** 1994. Human estrogen receptor transactivational capacity is determined by both cellular and promoter context and mediated by two functionally distinct intramolecular regions. Mol. Endocrinol. **8**:21–30.
48. **von Hippel, P. H.** 1994. Protein-DNA recognition: new perspectives and underlying themes. Science **263**:769–770.
49. **Wagner, R., J. Apriletti, M. McGrath, B. West, J. Baxter, and R. Fletterick.** 1995. A structural role for hormone in the thyroid hormone receptor. Nature **378**:690–697.
50. **Walker, P., J.-E. Germond, M. Brown-Luedi, F. Givel, and W. Wahli.** 1984. Sequence homologies in the region preceding the transcription initiation site of the liver estrogen-responsive vitellogenin and apo-VLDLII genes. Nucleic Acids Res. **12**:8611–8626.
51. **Webster, N. J. G., S. Green, J. R. Jin, and P. Chambon.** 1988. The hormone-binding domains of the estrogen and glucocorticoid receptors contain an inducible transcription activation function. Cell **54**:199–207.

Molecular basis of agonism and antagonism in the oestrogen receptor

Andrzej M. Brzozowski, Ashley C. W. Pike, Zbigniew Dauter, Roderick E. Hubbard, Tomas Bonn, Owe Engström, Lars Öhman, Geoffrey L. Greene, Jan-Åke Gustafsson & Mats Carlquist

Reprinted from Nature, Vol. 389, October 16, 1997 Issue

Molecular basis of agonism and antagonism in the oestrogen receptor

Andrzej M. Brzozowski*‖, Ashley C. W. Pike*‖, Zbigniew Dauter*, Roderick E. Hubbard*, Tomas Bonn†, Owe Engström†, Lars Öhman†, Geoffrey L. Greene‡, Jan-Åke Gustafsson§ & Mats Carlquist†

* *Protein Structure Group, Chemistry Department, University of York, York YO1 5DD, UK*
† *Karo Bio AB, NOVUM, S-141 57 Huddinge, Sweden*
‡ *The Ben May Institute for Cancer Research, The University of Chicago, 5841 S. Maryland Ave, Chicago, Illinois 60637, USA*
§ *Karolinska Institute, S-141 86 Huddinge, Sweden*
‖ *These authors contributed equally to this work.*

Oestrogens are involved in the growth, development and homeostasis of a number of tissues[1]. The physiological effects of these steroids are mediated by a ligand-inducible nuclear transcription factor, the oestrogen receptor (ER)[2]. Hormone binding to the ligand-binding domain (LBD) of the ER initiates a series of molecular events culminating in the activation or repression of

target genes. Transcriptional regulation arises from the direct interaction of the ER with components of the cellular transcription machinery[3,4]. Here we report the crystal structures of the LBD of ER in complex with the endogenous oestrogen, 17β-oestradiol, and the selective antagonist raloxifene[5], at resolutions of 3.1 and 2.6 Å, respectively. The structures provide a molecular basis for the distinctive pharmacophore of the ER and its catholic binding properties. Agonist and antagonist bind at the same site within the core of the LBD but demonstrate different binding modes. In addition, each class of ligand induces a distinct conformation in the transactivation domain of the LBD, providing structural evidence of the mechanism of antagonism.

The structure of the complex between ER's LBD and the antagonist raloxifene (RAL) was determined by conventional multiple isomorphous replacement in combination with multicrystal averaging, and was subsequently used as a phasing model in molecular replacement to solve the structure of the complex of the LBD with 17β-oestradiol (E_2) (see Methods and Table 1). The overall architecture of the ER LBD (helices H3–H12) is similar to that seen in the crystal structures of other nuclear receptor LBDs[6–8], and emphasizes the universal nature of this fold within this receptor superfamily[9]. The LBD is folded into a three-layered antiparallel α-helical sandwich comprising a central core layer of three helices (H5/6, H9 and H10) sandwiched between two additional layers of helices (H1–4 and H7, H8, H11). This helical arrangement creates a 'wedge-shaped' molecular scaffold that maintains a sizeable ligand-binding cavity at the narrower end of the domain. The remaining secondary structural elements, a small two-stranded antiparallel β-sheet (S1 and S2) and H12, are located at this ligand-binding portion of the molecule, and flank the main three-layered motif (Fig. 1a).

The ER LBDs are arranged as non-crystallographic dimers within both the E_2 and RAL complex crystals in a manner consistent with both the oligomeric state of liganded ER in solution[10] and previous

Table 1 Data collection, phase determination and refinement statistics

			ER RAL derivatives		
	ER RAL	ER E_2	PCMBS-1 (4 mM, 5 day)	PCMBS-2 (4 mM, 14 day)	$KAu(CN)_2$ (4 mM, 2 day)
Resolution (Å)	25–2.6	20–3.1	20–3	20–3	20–3.6
Unique reflections	15,433	33,981	10,335	9,316	5,835
Completeness (%)	95.7	99.1	97.6	89.0	94.2
Multiplicity	4.5	2.5	4	3.1	2.5
R_{sym} (I)*	8.0	10.0	8.1	9.2	7.0
R_{iso}†			16.9	20.7	13.7
Phasing power (centric/acentric)‡			1.22/1.88	1.23/2.02	0.71/0.94
R_{Cullis} (centric/acentric)§			0.75/0.68	0.76/0.66	0.90/0.85
Refinement					
Reflections used (R_{free} set)	13,868 (1,565)	30,583 (3,398)			
R_{cryst} (R_{free})‖	21.9 (29.9)	21.8 (25.1)			
Protein (solvent) atoms	3,633 (100)	11,382 (114)			
% A,B,L (a,b,l,p)¶	94.2 (5.8)	94.2 (5.8)			
R.m.s.d. bond lengths/angles (Å)#	0.016/0.035	0.011/0.039			
R.m.s.d. n.c.s. protein (Å)*	0.66	0.07			
R.m.s.d. n.c.s. B (Å^2)**	7.9	1.15			

*$R_{sym}(I) = 100 \times \Sigma_h \Sigma_i |I_{h,i} - \langle I_h \rangle| / \Sigma_h \Sigma_i I_{h,i}$, where I is the observed intensity. $\langle I \rangle$ is the average intensity of multiple observations of symmetry-related reflections.
†$R_{iso} = \Sigma||F_{PH}| - |F_P|| / \Sigma|F_P|$, where $|F_P|$ is the protein structure factor amplitude and $|F_{PH}|$ is the heavy-atom derivative structure factor amplitude.
‡Phasing power for centric and acentric reflections = r.m.s. ($|F_H|/E$), where F_H is the heavy atom structure factor amplitude and E is the residual lack of closure error.
§$R_{Cullis} = \Sigma|E| / \Sigma||F_{PH}| - |F_P||$ for centric and acentric reflections. Figure of merit was 0.48 for acentric reflections and 0.67 for centric reflections (20–3 Å).
‖$R_{cryst} = 100 \times \Sigma||F_o| - |F_c|| / \Sigma|F_o|$; R_{free} is the same as R_{cryst} but was calculated using a separate validation set of reflections that was excluded from the refinement process.
¶Percentage of residues located in most favoured (additional) regions of the Ramachandran plot as determined by PROCHECK[29].
#R.m.s. deviation in bond length and angle distances from Engh and Huber ideal values.
*Root mean squared distance between all non-crystallographic symmetry (n.c.s.) related protein atom positions.
**R.m.s. difference between all n.c.s.-related atomic temperature factors.

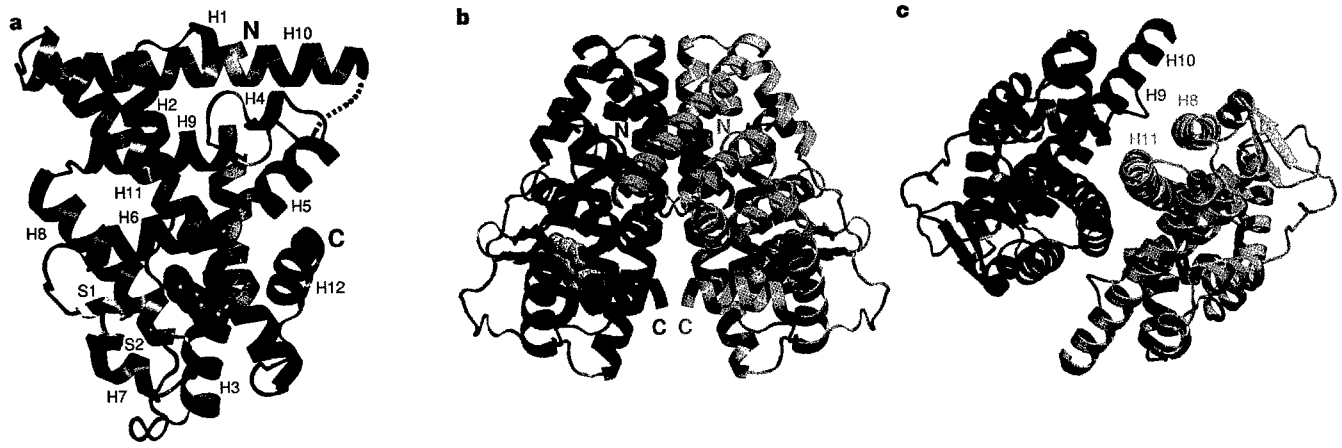

Figure 1 Ribbon representations of the ER-α LBD. **a**, The ER-α LBD indicating the locations of the secondary structural elements. α and 3_{10} helices (H) are coloured red, extended regions (S) are yellow, and coil regions are blue. All secondary structural elements have been numbered in keeping with the nomenclature that has been established for other nuclear receptor LBDs. The monomer is displayed looking onto the dimerization face. The dotted line indicates the unmodelled region between H9 and H10. **b**, ER-α LBD homodimer viewed perpendicular to the dimer axis. **c**, ER-α LBD homodimer viewed down the dimer axis. The component monomers are drawn in red and green. The N and C termini and the helices that are involved in the dimer interface are labelled. E_2 is coloured blue and depicted in space-filling form.

mutagenesis studies[11]. All crystal forms of the liganded ER LBD obtained so far contain identical non-crystallographic dimers (data not shown). The overall homodimeric arrangement is the same in both the E_2 and RAL complexes, and is reminiscent of the crystallographic apo-retinoid-X receptor homodimer[8]. The dimer axis roughly coincides with the longest dimension of the LBD with each molecule tilted approximately 10° away from the two-fold axis. This symmetric 'head-to-head' arrangement locates the chain termini of each monomer on opposite sides of the dimer with the carboxy termini projecting towards the two-fold axis (Fig. 1b). The H8/H11 face of the monomers line up to form an extensive dimerization interface that encompasses about 15% (1,703 Å^2) of each monomer's surface area. Contacts between the two molecules are made primarily through the H11 helices, which intertwine to form a rigid backbone, but also involve H8 from one monomer and parts of H9 and H10 from the neighbouring monomer (Fig. 1c).

The E_2 binding cavity is completely partitioned from the external environment and occupies a relatively large portion of the ER LBD's hydrophobic core (Fig. 1a). It is located at one end of the molecule and is formed by parts of H3 (Met 342 to Leu 354), H6 (Trp 383 to Arg 394), H8 and the preceding loop (Val 418 to Leu 428), H11 (Met 517 to Met 528), H12 (Leu 539 to His 547) and the S1/S2 hairpin (Leu 402 to Leu 410). Hormone recognition is achieved through a combination of specific hydrogen bonds and the complementarity of the binding cavity to E_2's non-polar character (Fig. 2a,c). E_2 binds diagonally across the cavity between H11, H3 and H6 and adopts a low-energy conformation. The phenolic hydroxyl of the A-ring (O3; see Fig. 2c for atom numbering) nestles between H3 and H6 and makes direct hydrogen bonds to the carboxylate of Glu 353, the guanidinium group of Arg 394, and a water molecule. The 17-β hydroxyl (O17) of the D-ring makes a single hydrogen bond with His 524 in H11. The remainder of the molecule participates in a number of hydrophobic

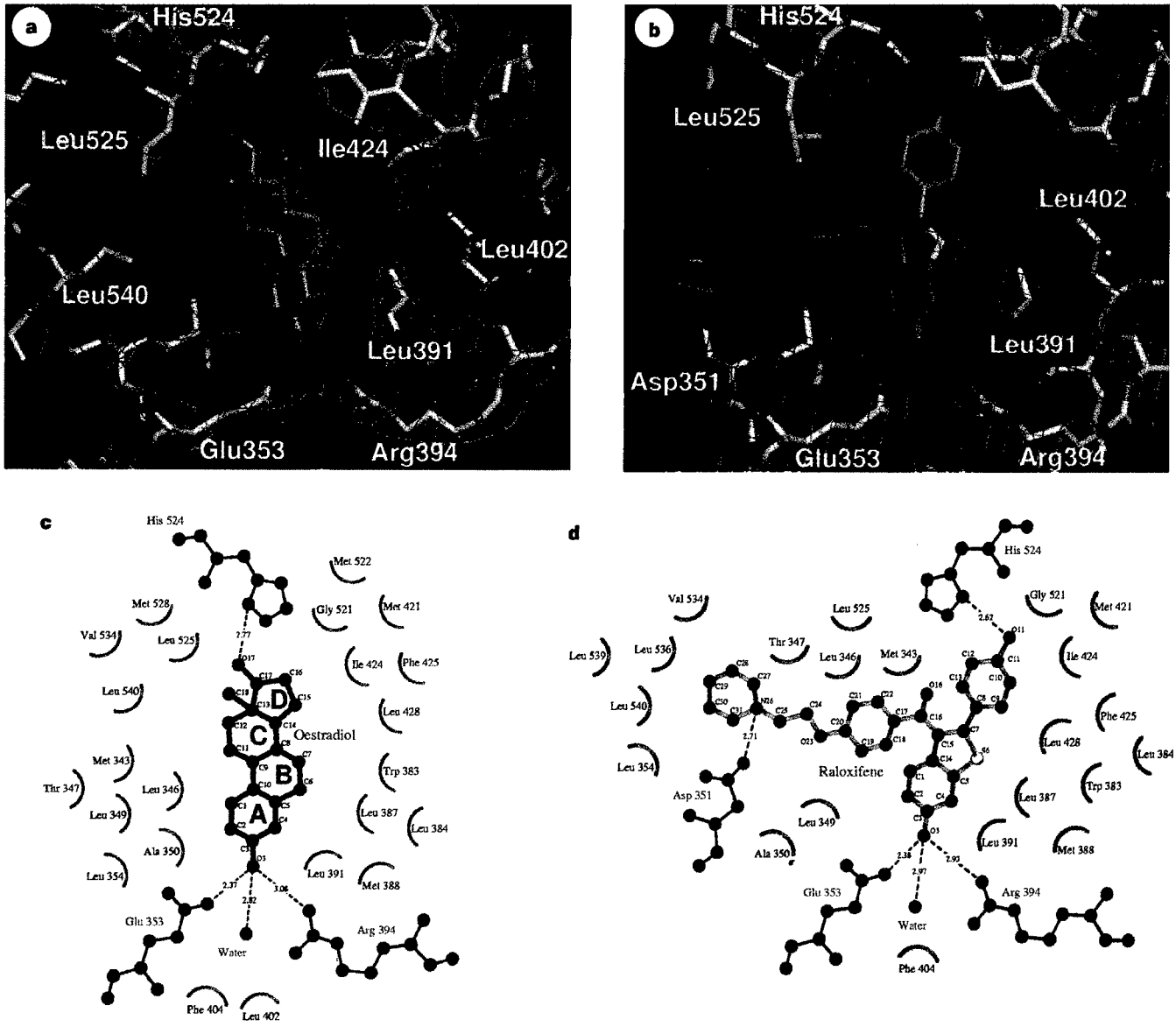

Figure 2 Agonist and antagonist binding modes. **a**, The 3.1-Å resolution, six-fold averaged electron-density map (using model phases) for the ER LBD-E_2 complex. **b**, The experimental, 2.6-Å resolution electron-density map for the ER LBD-RAL complex after DMMULTI multicrystal averaging. In both cases, the map is contoured at 1σ and overlaid on the final refined models. **c**, **d**, Schematic representation of the interactions made by E_2 (**c**) and RAL (**d**) within the binding cavity. Residues that interact with ligand and/or line the cavity are shown in their approximate positions. Those that make direct hydrogen bonds are depicted in ball-and-stick style with broken lines between the interacting atoms. The hydrogen-bond distances shown are averaged between the six (E_2) or two (RAL) monomers. The atom names and ring nomenclature of E_2 are also given.

contacts that are concentrated over the A, A/B interface and D-rings. The A-ring, as well as the planar A/B-ring interface, is sandwiched between the side chains of Ala 350 and Leu 387 on its β face and Phe 404 on its α face. At the other end of the binding cavity, the D-ring makes non-polar contacts with Ile 424, Gly 521 and Leu 525. Although the cavity itself appears to be devoid of ordered water molecules, an extensive solvent channel runs from the A-ring hydroxyl's water ligand to the exterior of the LBD between H3 and H5/6. The combination of the specific polar and non-polar interactions account for the ability of ER to selectively recognize and bind E_2 with subnanomolar affinity over the large and varied range of endogenous steroids.

Extensive binding studies of E_2 analogues have provided a detailed description of the pharmacophore of ER[12]. The ER is unique among the steroid receptors in its ability to embrace a wide variety of non-steroidal compounds. Although the 'pincer-like' arrangement around the A-ring imposes an absolute requirement on effective ligands to contain an aromatic ring, the remainder of the binding pocket can accept a number of different hydrophobic groups[12,13]. This overall promiscuity can be attributed to the size of the cavity, which has a probe accessible volume (450 Å^3) nearly twice that of E_2's molecular volume (245 Å^3). The length and breadth of the E_2 skeleton is well matched by the receptor, but there are large unoccupied cavities opposite the α face of the B-ring and the β face of the C-ring (Fig. 2a). The positions of these preformed cavities are similar to those predicted from binding studies[12].

This structure is the first example of an LBD from the steroid class of nuclear receptors, and provides an instructive model for members of this family. A similar overall hormone-binding mode is anticipated with the A-ring probably bound between H3 and H6 by an arginine (homologue of Arg 394) and a glutamine (homologue of Glu 353). This exclusive replacement of the Glu 353 of ER by a glutamine fulfils the hydrogen-bonding requirements of the 3-keto steroids. The model proposed for the ligand binding mode of dexamethasone in the human glucocorticoid receptor[9], in which the D-ring binds between H3 and H6, should therefore be re-examined in the light of our observations.

RAL is a clinically relevant selective antagonist that specifically counters the mitogenic effects of E_2 in the reproductive tissues, while maintaining beneficial oestrogenic effects in other tissues[5,14].

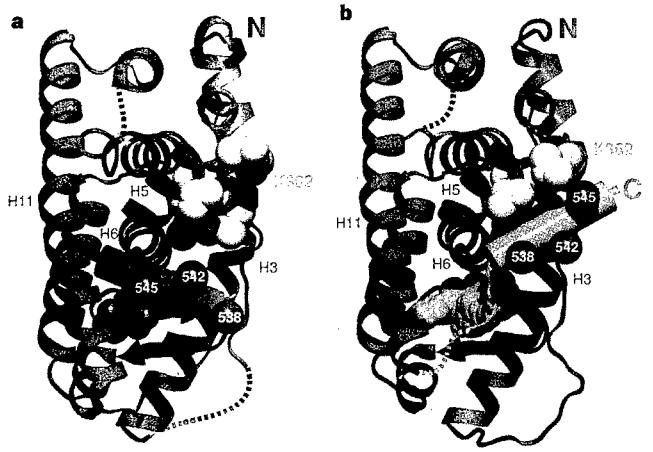

Figure 3 Positioning of helix H12. Position is shown in **a**, the ER LBD-E_2 complex; and **b**, the ER LBD-RAL complex. H12 is drawn as a cylinder and coloured blue (E_2 complex) or green (RAL complex). The remainder of the ER LBD is shown in red. Dotted lines indicate unmodelled regions of the structures. Hydrophobic residues located in the groove between H3 and H5 (yellow) and Lys 362 (K362, pink) are depicted in space-filling form. The locations of Asp 538, Glu 542 and Asp 545 are highlighted (brown spheres) along with the helices that interact with H12 in the two complexes.

RAL binds at the same site as E_2 within the LBD (Fig. 2b,d), with the hydroxyl group of the benzothiophene moiety (O3; see Fig. 2d for atom numbering) mimicking the A-ring phenolic hydroxyl of E_2 by binding in the polar pocket between H3 and H6. In contrast, the binding mode of RAL at the 'D-ring end' of the cavity, between H8 and H11, is markedly different from that of E_2. Although the phenolic hydroxyl (O11) hydrogen bonds with His 524, it is displaced 5.1 Å from the position occupied by the 17β-OH in the E_2 complex. Consequently, the imidazole ring of His 524 rotates in the RAL complex to compensate for the change in oxygen position and to maintain a favourable hydrogen-bonding position. The remainder of the core is involved in non-polar contacts similar to those seen for E_2. The side chain of RAL makes extensive hydrophobic contacts with H3 and H5/6, H11 and the loop between H11 and H12. It is anchored to the protein by a direct hydrogen bond between Asp 351 and the piperazine ring nitrogen (N26). However, at over 11 Å in length, the side chain is too long to be contained within the confines of the binding cavity, and instead it displaces H12 and protrudes from the pocket between H3 and H11. This helix displacement is anticipated to be a general feature of both steroidal and non-steroidal anti-oestrogens that possess a bulky side-chain substitutent. The importance of the narrow cleft at the A-ring end of the cavity in determining the overall ligand-binding mode is highlighted by the observation that RAL's benzothiophene moiety occupies the same spatial position as the A and B rings of E_2. The alternate D-ring binding mode of RAL presumably arises as a result of both the inflexibility of the arylbenzothiophene core and the limited scope for positioning the side chain. The orientation of E_2 and RAL should allow the accurate positioning of most of ER's ligands, but further structural studies will be required to understand both the cavity's plasticity and the reported range of different binding modes[15].

The LBD's transcriptional activation function (AF-2) can interact with a number of putative transcriptional coactivators in a ligand-dependent manner[4,16–18]. Helix 12 is essential for such transactivation as both loss or mutation in this region results in a receptor that is unresponsive to ligand[19]. Mutational analyses in both ER and other nuclear receptors[20,21] have identified several additional residues that influence the function of AF-2, suggesting that the LBD's coactivator recruitment surface, although centred on H12, probably also encompasses parts of the surrounding helices H3, H5/6 and H11.

In the E_2-liganded complex, H12 sits snugly over the ligand-binding cavity and is packed against H3, H5/6 and H11. Although it makes no direct contact with E_2, it forms the 'lid' of the binding cavity and projects its inner hydrophobic surface towards the bound hormone. Its charged surface, comprising Asp 538, Asp 545 and the highly conserved Glu 542, is directed away from the body of the LBD on the side of the molecule lying perpendicular to the dimerization interface (Fig. 3a). This precise positioning of H12, which is observed in all known structures of the liganded forms of the LBD[6,7], seems to be a prerequisite for transcriptional activation as, by sealing the ligand-binding cavity, it generates a competent AF-2 that is capable of interacting with coactivators. In contrast, the alignment of H12 over the cavity is prevented by RAL, and instead the helix lies in a groove formed by H5 and the carboxy-terminal end of H3. This antagonist-induced repositioning of H12 involves a rotation of 130° combined with a 10-Å rigid-body shift towards the amino terminus of the LBD compared with the agonist-induced conformation (Fig. 3b). The complementarity of this hydrophobic groove to the inner surface of H12 suggests that its positioning in the RAL complex represents a real conformation rather than an artefact produced by the crystal lattice. A highly conserved lysine residue (Lys 362), which is required for efficient E_2-dependent recruitment of certain coactivators[21], is located at one end of this hydrophobic groove, and is partly buried by the reoriented helix. Taken together, these observations provide compelling evidence

that the antagonistic properties of RAL are based on its ability to prevent the formation of a transcriptionally competent AF-2 conformation. The movement of H12 clearly disrupts the overall surface topography of AF-2, but it is feasible that the tissue selectivity of RAL may reside in its ability to occlude particular coactivator recruitment sites on the surface of the ER LBD.

Selective antagonism of the kind exhibited by RAL is a complicated phenomenon that arises through the interplay of a number of factors, such as differential ligand effects on the transactivation functionalities of the ER, the type of coactivator recruited, and the cell and promoter context[3,4,22,23]. Nevertheless, our data on these structures give valuable insights into the binding of ligands to this receptor, and provide the basis for the structure-based design of improved agonists and antagonists for the treatment of oestrogen-related diseases. □

Methods

Protein purification and crystallization. The LBD of human ER-α (residues Ser 301 to Thr 553) was expressed, purified and carboxymethylated as described[24]. ER LBD–E_2 and LBD–RAL complexes were prepared by including 75 μM of the respective ligand in the column elution buffer. The ER LBD is particularly refractive to crystallization, and carboxymethylation of the free thiol groups was essential for growing crystals suitable for diffraction studies. Examination of the electron-density maps shows that Cys 381 is uniformly modified and the remaining three cysteines are either unmodified (Cys 447) or in flexible regions of the structure. The ER LBD–RAL and LBD–E_2 complexes were crystallized using the hanging-drop technique at 18 °C. For the RAL complex, the reservoir solution contained 12% (w/v) PEG 4000, 0.2 M magnesium chloride, 50 mM L-lysine, 0.1 M sucrose and 5% 1,4-dioxane in 0.1 M Tris-HCl, pH 8.5. Hanging drops were composed of equal volumes of protein (7.2 mg ml^{-1}) and reservoir solutions. Monoclinic crystals, belonging to the space group $C2$ with unit cell dimensions $a = 104.53$ Å, $b = 53.68$ Å, $c = 102.71$ Å, $\beta = 116.79°$ and containing one ER LBD dimer per asymmetric unit, appeared within 2–4 weeks. Two other crystal forms were grown by subtle manipulation of the crystallization conditions ($C2$, $a = 89.91$ Å, $b = 75.09$ Å, $c = 87.50$ Å, $\beta = 103.01°$; $C222_1$, $a = 65.47$ Å, $b = 95.99$ Å, $c = 168.14$ Å). For the E_2 complex, drops containing equal volumes of protein (7–13 mg ml^{-1}) and reservoir solution were equilibrated against 0.1 M Tris-HCl, pH 8.1, 2.4 M ammonium formate and 8% dimethylsulphoxide. The E_2 complex crystals belong to the space group $P2_1$, with unit cell dimensions $a = 61.48$ Å, $b = 115.16$ Å, $c = 137.38$ Å, $\beta = 98.8°$, and contain three ER LBD dimers per asymmetric unit.

Data collection, phasing and refinement. For the ER LBD–RAL complex, native diffraction data were collected from a single frozen crystal (120 K) on beamline X11 at EMBL (DESY, Hamburg). Heavy-atom derivatives were collected in-house from flash-frozen crystals. Data were integrated and reduced using the programs DENZO and SCALEPACK[25]. MIR analysis was performed using the CCP4 suite of programs[26]. Diffraction data for the alternate $C2$ (York) and $C222_1$ (DESY, Hamburg) crystal forms were collected to resolutions of 3.0 and 3.1 Å, respectively. Initial phases were calculated to 3 Å using MLPHARE[26] and subsequent two-fold averaging, non-crystallographic matrix refinement and phase extension were carried out using DM[26]. An initial polyalanine trace was used to generate a dimeric search model which was correctly positioned in the alternate $C2$ and $C222_1$ crystal forms using molecular replacement (AMoRe[26]). Twenty cycles of cross-averaging between all three crystal forms were carried out with DMMULTI[26], using only the MIR phase information. The resultant electron-density map showed no bias towards the input model and enabled the unambiguous tracing of the remainder of the molecule and the assignment of most of the amino-acid sequence. Refinement was performed with REFMAC[27] using bulk solvent corrections and anisotropic scaling. All data between 25 and 2.6 Å were included with no sigma cut-offs. Tight non-crystallographic restraints were maintained during the initial cycles but were loosened in the final stages of refinement. Phases from multicrystal averaging were included at all stages and individual atomic temperature factors were refined isotropically. The final model comprises residues 307–459, 470–528 and 535–547. The missing regions correspond to flexible loops between helices H9 and H10 (460–469) and H11 and H12 (529–534) and the chain termini. Residues Tyr 331(A), Asp 332(A), His 377(B), Glu 397(AB), Lys 416(AB), Glu 419(AB), Glu 423(B), Leu 469(B), Glu 470(AB), Glu 471(AB), Lys 472(AB), Arg 477(AB), Lys 492(A), Glu 542(A), Arg 548(B) and Leu 549(B) were poorly resolved in the electron-density maps and not fully modelled.

For the ER LBD–E_2 complex, diffraction data were collected at room temperature from a single ER LBD–E_2 crystal on beamline X11 at EMBL (DESY, Hamburg). Initial phase estimates were obtained with AMoRe using the refined ER LBD–RAL dimer as a search model. The correct solution, corresponding to three ER LBD dimers, had a correlation coefficient of 69.8 and an R-factor of 40.6 after AMoRe rigid-body refinement. Six-fold averaging was performed using DM and the structure was refined with REFMAC using tight non-crystallographic restraints, averaged phases from DM, bulk solvent corrections and anisotropic scaling. All data between 20 and 3.1 Å were included with no sigma cut-offs. A single, overall B-value was applied in the early stages of refinement until the R_{free} converged. Subsequent cycles used tightly constrained, full isotropic B-value refinement. The final model for each monomer comprises residues 305–548 but includes two unmodelled loops between residues 331–336 and 462–464. The first four (301–304) and last five (549–553) residues are disordered. The side chains of Leu 306, Leu 466, Leu 469, Lys 492, Lys 531 and Leu 536 were poorly resolved in the electron-density maps and not modelled beyond their Cβ atoms. All model building was carried out using the graphics package QUANTA (Molecular Simulations Inc., San Diego).

Illustrations. Figures 1, 2a,b, 3 were prepared with QUANTA (Molecular Simulations Inc., San Diego); Fig. 2c, d was prepared with LIGPLOT[28].

Received 9 June; accepted 8 September 1997.

1. Ciocca, D. R. & Roig, L. M. V. Estrogen-receptors in human nontarget tissues—Biological and clinical implications. *Endocr. Rev.* **16,** 35–62 (1995).
2. Tsai, M.-J. & O'Malley, B. W. Molecular mechanisms of action of steroid/thyroid receptor superfamily members. *Annu. Rev. Biochem.* **63,** 451–486 (1994).
3. Katzenellenbogen, J. A., O'Malley, B. W. & Katzenellenbogen, B. S. Tripartite steroid hormone receptor pharmacology: Interaction with multiple effector sites as a basis for the cell- and promoter-specific action of these hormones. *Mol. Endocrinol.* **10,** 119–131 (1996).
4. Beato, M. & Sánchez-Pacheco, A. Interaction of steroid hormone receptors with the transcription initiation complex. *Endocr. Rev.* **17,** 587–609 (1996).
5. Grese, T. A. *et al.* Structure-activity relationships of selective estrogen receptor modulators: Modifications to the 2-arylbenzothiophene core of raloxifene. *J. Med. Chem.* **40,** 146–167 (1997).
6. Wagner, R. L. *et al.* A structural role for hormone in the thyroid hormone receptor. *Nature* **378,** 690–697 (1995).
7. Renaud, J.-P. *et al.* Crystal structure of the RAR-γ ligand-binding domain bound to all-*trans* retinoic acid. *Nature* **378,** 681–689 (1995).
8. Bourguet, W., Ruff, M., Chambon, P., Gronemeyer, H. & Moras, D. Crystal structure of the ligand-binding domain of the human nuclear receptor RXR-α. *Nature* **375,** 377–382 (1995).
9. Wurtz, J.-M. *et al.* A canonical structure for the ligand-binding domain of nuclear receptors. *Nature Struct. Biol.* **3,** 87–94 (1996).
10. Kumar, V. & Chambon, P. The estrogen receptor binds tightly to its responsive element as a ligand-induced homodimer. *Cell* **55,** 145–156 (1988).
11. Fawell, S. E., Lees, J. A., White, R. & Parker, M. G. Characterisation and colocalization of steroid binding and dimerization activities in the mouse estrogen receptor. *Cell* **60,** 953–962 (1990).
12. Anstead, G. M., Carlson, K. E. & Katzenellenbogen, J. A. The estradiol pharmacophore: Ligand structure–estrogen receptor binding affinity relationships and a model for the receptor binding site. *Steroids* **62,** 268–303 (1997).
13. Katzellenbogen, B. S. *et al.* Antiestrogens: Mechanisms and actions in target cells. *J. Steroid Biochem. Mol. Biol.* **53,** 387–393 (1995).
14. Draper, M. W. *et al.* A controlled trial of raloxifene (LY139481) HCl: Impact on bone turnover and serum lipid profile in healthy postmenopausal women. *J. Bone Miner. Res.* **11,** 835–842 (1996).
15. Ekena, K., Weis, K. E., Katzenellenbogen, J. A. & Katzenellenbogen, B. S. Different residues of the human estrogen receptor are involved in the recognition of structurally diverse estrogens and antiestrogens. *J. Biol. Chem.* **272,** 5069–5075 (1997).
16. Cavaillès, V., Dauvois, S., Danielian, P. S. & Parker, M. G. Interaction of proteins with transcriptionally active estrogen receptors. *Proc. Natl Acad. Sci. USA* **91,** 10009–10013 (1994).
17. L'Horset, F., Dauvois, S., Heery, D. M., Cavaillès, V. & Parker, M. G. RIP-140 interacts with multiple nuclear receptors by means of two distinct sites. *Mol. Cell. Biol.* **16,** 6029–6036 (1996).
18. vom Baur, E. *et al.* Differential ligand-dependent interactions between the AF-2 activating domain of nuclear receptors and the putative transcriptional intermediary factors mSUG1 and TIF1. *EMBO J.* **15,** 110–124 (1996).
19. Danielian, P. S., White, R., Lees, J. A. & Parker, M. G. Identification of a conserved region required for hormone dependent transcriptional activation by steroid hormone receptors. *EMBO J.* **11,** 1025–1033 (1992).
20. Pakdel, F., Reese, J. C. & Katzenellenbogen, B. S. Identification of charged residues in an N-terminal portion of the hormone-binding domain of the human estrogen receptor important in transcriptional activity of the receptor. *Mol. Endocrinol.* **7,** 1408–1417 (1993).
21. Henttu, P. M. A., Kalkhoven, E. & Parker, M. G. AF-2 activity and recruitment of steroid receptor coactivator 1 to the estrogen receptor depend on a lysine residue conserved in nuclear receptors. *Mol. Cell. Biol.* **17,** 1832–1839 (1997).
22. McInerney, E. M. & Katzenellenbogen, B. S. Different regions in activation function-1 of the human estrogen receptor required for antiestrogen- and estradiol-dependent transcriptional activation. *J. Biol. Chem.* **271,** 24172–24178 (1996).
23. McInerney, E. M., Tsai, M.-J., O'Malley, B. W. & Katzenellenbogen, B. S. Analysis of estrogen receptor transcriptional enhancement by a nuclear hormone receptor coactivator. *Proc. Natl Acad. Sci. USA* **93,** 10069–10073 (1996).
24. Hegy, G. B. *et al.* Carboxymethylation of the human estrogen receptor ligand-binding domain-

estradiol complex: HPLC/ESMS peptide mapping shows that cysteine 447 does not react with iodoacetic acid. *Steroids* **61,** 367–373 (1996).
25. Otwinowski, Z. & Minor, W. Processing X-ray diffraction data collected in oscillation mode. *Methods Enzymol.* **276,** 307–326 (1997).
26. Collaborative Computational Project No. 4. The CCP4 suite: programs for protein crystallography. *Acta Crystallogr. D* **50,** 760–763 (1994).
27. Murshudov, G. N., Vagin, A. A. & Dodson, E. J. Refinement of macromolecular structures by the maximum-likelihood method. *Acta Crystallogr. D* **53,** 240–255 (1997).
28. Wallace, A. C., Laskowski, R. A. & Thornton, J. M. LIGPLOT—A program to generate schematic diagrams of protein ligand interactions. *Prot. Eng.* **8,** 127–134 (1995).
29. Laskowski, R. A., MacArthur, M. W., Moss, D. S. & Thornton, J. M. PROCHECK: a programme to check the stereochemical quality of protein structure coordinates. *J. Appl. Crystallogr. A* **42,** 140–149 (1993).

Acknowledgements. We thank G. Murshudov for discussions on refinement strategy and J. Baxter, R. Fletterick, S. Nilsson and K. Koehler for comments on the manuscript. The Protein Structure Group at York is supported by the BBSRC. We thank the European Union for support of the work at EMBL DESY/ Hamburg through the HCMP access to large installations project.

Correspondence and requests for materials should be addressed to R.E.H. (e-mail: rod@yorvic.york.ac.uk). Coordinates have been deposited at the Brookhaven Protein Data Bank, accession codes 1ERE for the oestradiol-liganded structure and 1ERR for the raloxifene-liganded structure.